Engineering periodontal tissue interfaces using multiphasic scaffolds and membranes for guided bone and tissue regeneration

Ozgü Ozkendir [1, #], Ilayda Karaca [1, #], Selin Cullu [1, #], Oğul Can Erdoğan [2, #], Hüsniye Nur Yaşar [2, #], Serkan Dikici [1], Robert Owen [3], Betül Aldemir Dikici [1,*]

[1]Department of Bioengineering, Izmir Institute of Technology, Urla, Izmir, 35433, Turkey
[2]Department of Molecular Biology and Genetics, Izmir Institute of Technology, Urla, Izmir, 35433, Turkey
[3]School of Pharmacy, University of Nottingham Biodiscovery Institute, University of Nottingham, Nottingham, NG7 2RD, United Kingdom

[#] OO, IK, SC, OCE, and HNY contributed equally to this work as co-first authors. As equally contributing authors, they are allowed to re-order their names on their portfolios.

**** Correspondance:***
betulaldemir@iyte.edu.tr
Tel 1: 00 90 232 750 69 61
Tel 2: 00 90 506 476 21 90
Fax: 00 90 232 750 65 05

Abstract

Periodontal diseases are one of the greatest healthcare burdens worldwide. The periodontal tissue compartment is an anatomical tissue interface formed from the periodontal ligament, gingiva, cementum, and bone. This multifaceted composition makes tissue engineering strategies challenging to develop due to the interface of hard and soft tissues requiring multiphase scaffolds to recreate the native tissue architecture. Multilayer constructs can better mimic tissue interfaces due to the individually tuneable layers. They have different characteristics in each layer, with modulation of mechanical properties, material type, porosity, pore size, morphology, degradation properties, and drug-releasing profile all possible. The greatest challenge of multilayer constructs is to mechanically integrate consecutive layers to avoid delamination, especially when using multiple manufacturing processes. Here, we review the development of multilayer scaffolds that aim to recapitulate native periodontal tissue interfaces in terms of physical, chemical, and biological characteristics. Important properties of multiphasic biodegradable scaffolds are highlighted and summarised, with design requirements, biomaterials, and fabrication methods, as well as post-treatment and drug/growth factor incorporation discussed.

Keywords: *biomaterials, tissue engineering, periodontitis, guided bone regeneration, GBR, GTR*

1. Introduction

Periodontal diseases are one of the greatest global healthcare challenges, affecting 19% of the global adult population and accounting for nearly one-third of the approximately 3.5 billion oral disease cases worldwide [1]. With more than 1 billion instances of periodontitis globally in 2019, the burden is increasing, with the prevalence rate increasing by almost 8.5% since 1990 [2].

Periodontium, where soft tissues are in direct contact with calcified tissues, contains four distinct tissues: gingiva (the gums), cementum (a calcified material that covers the tooth), the periodontal ligament (PDL, which supports the teeth) and alveolar bone [3,4] (Figure 1A). Periodontal diseases refer to a broad range of chronic inflammatory conditions affecting the gingiva, alveolar bone, and PDL. Gingivitis, a local inflammation of the gingiva caused by bacteria in dental plaque, causes the gum to swell, redden, and bleed. Untreated, it leads to the separation of the gum from the tooth, and chronic periodontitis develops (Figure 1B). Eventually, it may result in the formation of deep periodontal pockets and tooth loss (Figure 1C).

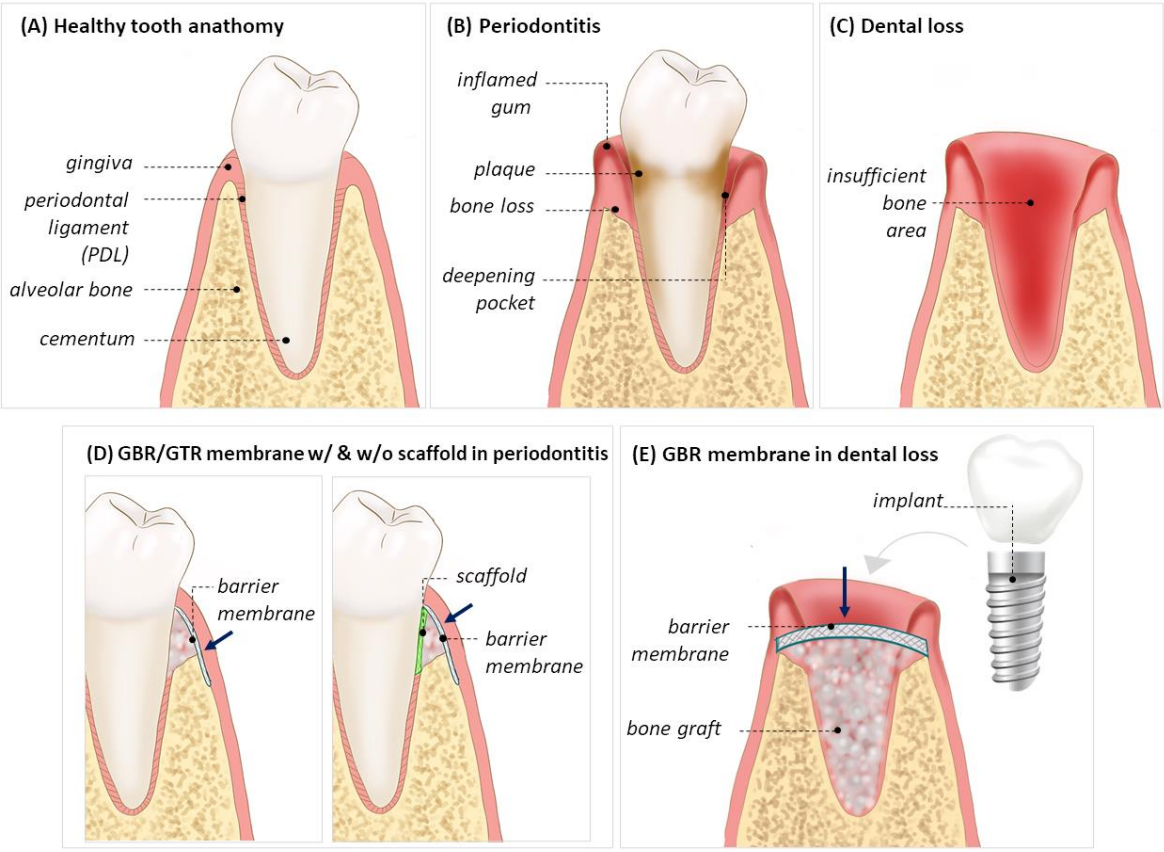

Figure 1: *(A) Healthy tooth anatomy. Periodontal pathologies; (B) periodontitis; and (C) dental loss. And treatments; (D) GBR/GTR membrane use in periodontitis with or without scaffold; (E) GBR membrane in dental loss before implant placement. Navy blue arrows show the soft tissue whose infiltration is intended to be limited using dental membranes.*

Due to their ability to spatially direct regeneration, guided tissue regeneration/guided bone regeneration membranes (GTR/GBR) are of note when treating pathological periodontitis. These membranes act as a barrier between the epithelial tissue and bone/bone graft, inhibiting migration of fast-proliferating fibroblasts and epithelial cells into the defect site (Figure 1D, E), allowing space and time for bone cells to infiltrate into the defect site and regenerate the dental tissue [5,6] (Figure 2A-C). When tooth loss has occurred, there is not sufficient alveolar bone remaining for implant placement, necessitating a bone graft. Whilst these membranes can be used in isolation as a barrier, they can also be combined with tissue engineering scaffolds that facilitate regeneration of the alveolar bone and PDL (Figure 1D) for the treatment of periodontitis. Long-term follow-up studies (5-12 years) showed that the survival rate of the implants placed simultaneously with the GBR membrane was higher than 90%, demonstrating the capability of this approach [7–9].

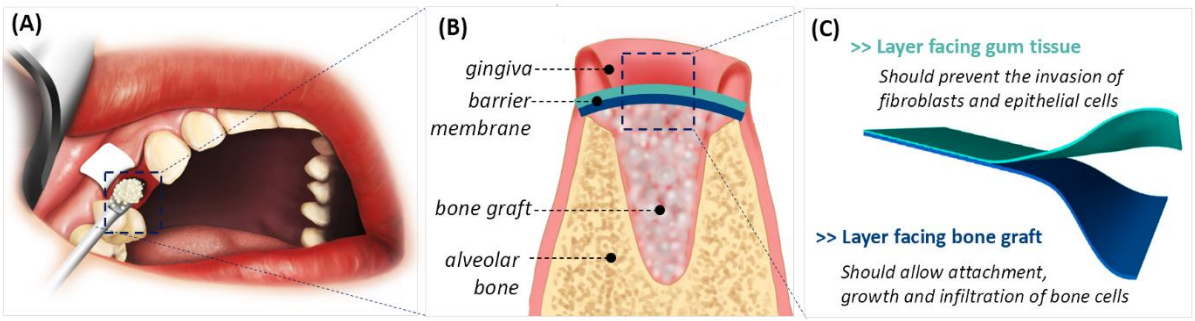

Figure 2: *(A) GBR membrane implantation procedure [10], (B) multi-layer GBR membrane placement in dental loss before implant placement, (C) role of each layer of multi-layer GBR constructs.*

Membranes for GTR/GBR applications can be non-resorbable or bioresorbable [11]. Non-resorbable membranes are made from synthetic materials, e.g. Cytoplast® TXT-200 (polytetrafluoroethylene (PTFE)), Cytoplast® Ti-250 (titanium-reinforced PTFE), and Gore-Tex (expanded PTFE). Whilst their inability to degrade necessitates a second surgery for removal, PTFE-based membranes are widely preferred due to their open microstructure and biocompatibility [12]. Bioresorbable GBR/GTR membranes do not require secondary surgical operations as they degrade within the body and can be formed from natural or synthetic materials. Bioresorbable collagen membranes are mainly composed of collagen type I and III isolated from swine, bovine, and human sources [13]. Collagen is a structural protein that makes up most of the connective tissue and demonstrates great biocompatibility in tissue engineering applications [14]. However, its antigenicity must be removed chemically to avoid an immune response. Furthermore, whilst biodegradation is desirable to minimise surgical interventions, minimally processed collagen degrades rapidly, meaning various crosslinking agents such as glutaraldehyde, formaldehyde, or enzymes are often used to prevent their fast deterioration rate [15,16]. Alternatively, biodegradable synthetic polymers such as poly(lactic acid) (PLA), polycaprolactone

(PCL), poly(glycolic acid) (PGA), poly(hydroxyl butyric acid) (PHB), poly(hydroxyl valeric acid), and their copolymers are also used clinically [17–19]. Whilst the mechanical properties of synthetic polymers are superior to their native counterparts, their interaction with the biological tissue is limited. Therefore, it is common to dope synthetic membranes with bioactive natural polymers to enhance cellular responses [20].

2. Design considerations for multiphase constructs for periodontal tissue interfaces

Regeneration of the complex, hierarchical nature of periodontal tissues requires the design of multiphase GBR/GTR constructs where the composition and structure of each layer recapitulates the native tissue architecture [21]. Although the barrier component between the gingiva and alveolar bone is referred to as 'membrane' and the regeneration component that restores the cementum, PDL and alveolar bone is referred to as 'scaffold' here, it should be noted the terms 'scaffold' and 'membrane' are often used interchangeably in periodontal literature (Figure 1D). Each phase of the scaffolds and membranes needs different chemical, physical, and biological properties to meet the unique design requirements of periodontal tissues (Figure 3). The different approaches taken to achieve these ranges of chemical and physical properties using different biomaterial compositions and fabrication techniques are reviewed herein.

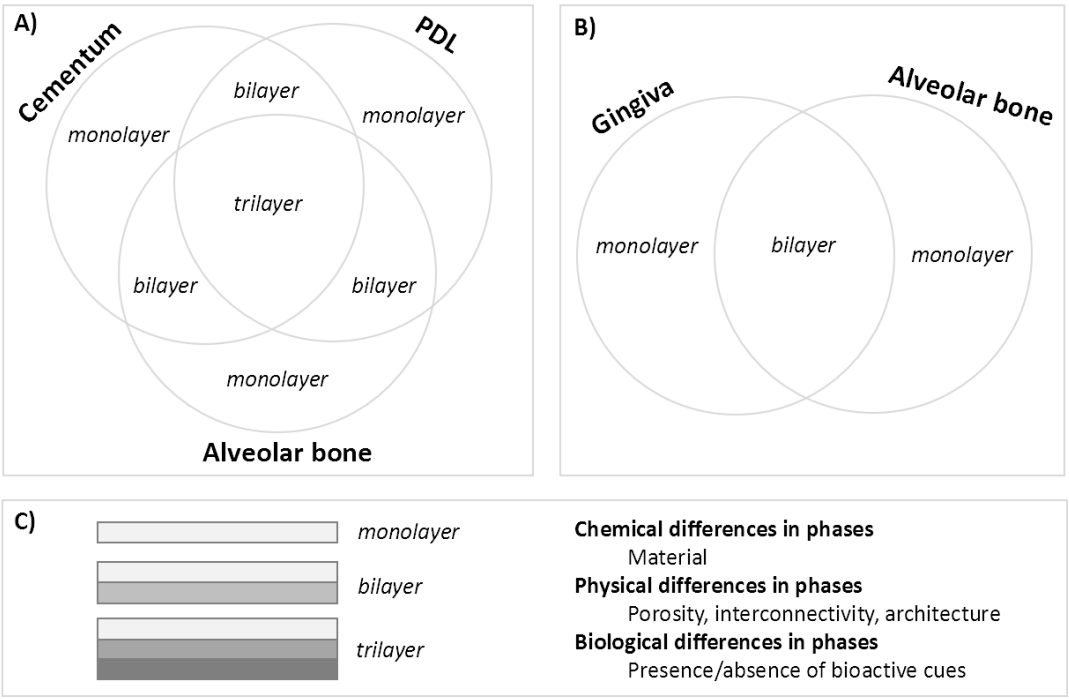

Figure 3: *A) Periodontal scaffolds can be designed to mimic cementum, PDL, and alveolar bone and their combinations – in the form of monolayer, bilayer and trilayer scaffolds. B) In GBR membrane design, mostly bilayer membranes are designed to be implanted between the gingiva and alveolar bone.*

The physical, mechanical, chemical, and biological properties of the membrane play a crucial role in the proliferation, adhesion, differentiation, and migration of cells and the regeneration of the defect site. These properties can be reduced into key characteristics that should be considered in the design of an ideal dental membrane/scaffold (Figure 4), namely: biocompatibility, biodegradability, porosity, mechanical strength, surface roughness, handleability, hydrophilicity, occlusiveness (barrier effectiveness), space maintenance, and swelling.

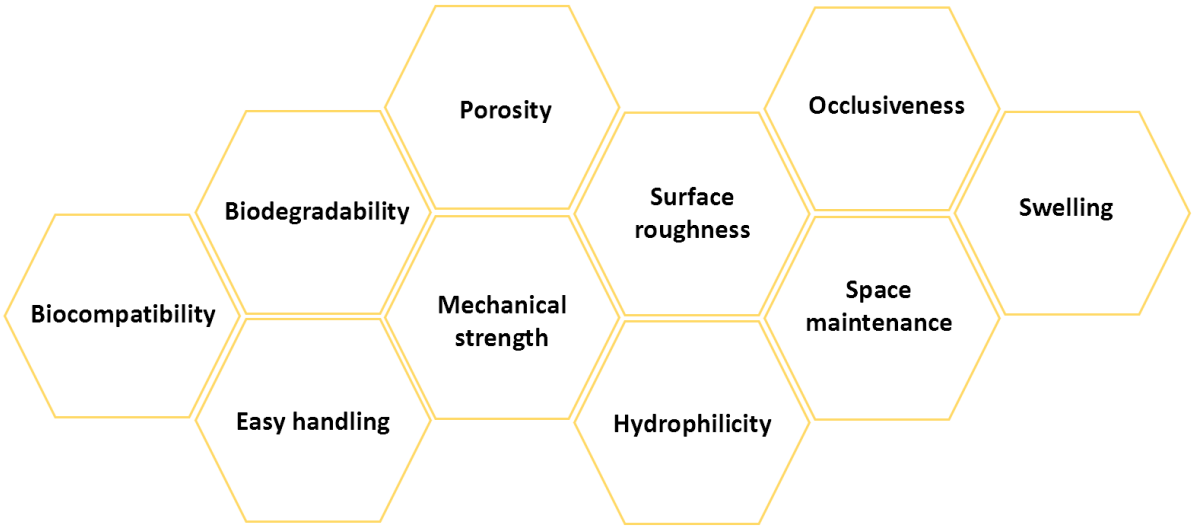

Figure 4: *Ideal design considerations for periodontal GBR/GTR membranes.*

Mechanically, the membrane should be elastic and flexible, rather than hard and brittle, with good fatigue and tensile strength to improve processability and durability post-implantation so it is not deformed by repetitive chewing forces [22,23]. Regardless of the material and cell type, surface topography and micrometre to sub-micrometre scale surface roughness are also other design considerations that directly affect cell proliferation, morphology, migration, and phenotypic expression of the cell *in vivo* and *in vitro* [24–27].

Swelling/water uptake is a crucial parameter for wound healing as it affects the release of biologically active substances in the wound area and ensures the absorption of exudate [22]. An ideal scaffold should encourage cell adhesion, which is principally modulated by material hydrophilicity; more hydrophobic materials may reduce biological interaction [28]. An additional consideration is the degradation rate, which should not be faster than the remodelling and maturation of the neo-tissue [29].

Cell morphology is directly affected by pore geometry and scaffold stiffness. Pore size and interconnectivity must permit cell infiltration through the scaffold, with higher porosity also facilitating efficient nutrient transport and timely vascularisation by new blood vessels, which are essential for successful regeneration [30,22,31,32]. Since wound healing begins with hemostasis, it is

important periodontal scaffold materials are hemocompatible by avoiding damaging the erythrocytes [22]. Additionally, ideally, the scaffold would also resist the accumulation of bacterial plaque to minimise infection risk due to the high probability of bacterial contamination in the mouth [22]. Some of the critical design parameters, such as morphological properties, mechanical properties, and the degradation rate of the periodontal constructs, will be reviewed in the following section.

2.1.1. Morphological properties

Porosity is a material-independent morphological feature that is defined as the percentage of empty space in a solid [33, 34]. Materials with high porosity facilitate the efficient release of biological factors, serve as excellent substrates for nutrition transfer, and permit the ingrowth of more cells and neo-vasculature. Consequently, various porosity-related elements such as pore distribution, pore geometry, pore size, total porosity, and pore interconnectivity must be considered when manufacturing scaffolds for tissue engineering [35]. They modulate tissue regeneration by affecting the mechanical properties, topography, degradation rate, surface-specific area, and roughness of the scaffold, which consequently affect cell penetration, cell distribution, cell migration, cell-to-cell interaction, fluid diffusion, extracellular matrix (ECM) deposition, angiogenesis, and initial adsorption of proteins [36].

Although high porosity is desirable from the biological point of view, this must be balanced with the corresponding reduction in mechanical properties so that the structural integrity of the biomaterial is not compromised [37]. Greater fluid entry into the scaffold and a larger surface area with increased porosity will also accelerate degradation [38]. Consequently, there is a limit to the degree of porosity that may be included in a scaffold without significantly impairing its degradation rate and mechanical strength [36]. Wall thickness and density of the scaffolds are also related to mechanical performance, directly contributing to compressive strength [39]. The use of materials with high innate mechanical strength may provide a solution to these problems that arise with greater porosity [40].

Another critical morphological parameter in membrane design is pore size [41], as it affects cell morphology, differentiation, and gene expression [42,43]. Pore diameter has been shown to be an effective modulator of bone marrow-derived stem/stromal cell differentiation into osteogenic, chondrogenic and myogenic lineages and adipose-derived stem cells into chondrogenic and hepatic lineages [44]. Due to the multiscale nature of biological tissues, it has also been shown that a hierarchy of pore sizes is beneficial to recreate the different native length scales. For example, membrane nanoporosity improves the deposition of collagen fibres and ECM, while membrane macroporosity modulates cell attachment, distribution, migration, and subsequent angiogenesis *in vivo* [45].

Pore morphology also affects the physical and biological properties of the scaffold. As the complexity of the pore structure increases, so does the compressive strength of the scaffold [46]. Pore curvature, e.g., concave or convex, can also be used to modulate cell behaviour [47]. Nonetheless, the complexity of pore morphology should not impede normal cellular functions. Optimising pore morphology must establish a balance that maximises mechanical performance whilst preserving or promoting desirable cellular behaviour [35].

Interconnected and open pore networks govern the permeability of the scaffold via regulating fluid circulation [35] and are required for cell proliferation, migration, and nutrition for tissue vascularisation and the development of neo-tissues [37,48,49]. Specific surface area is the relative scaffold volume accessible for cell attachment and is inversely proportional to the average pore size [50]. Consequently, a scaffold with larger pores gives a smaller specific surface area for cell attachment, while a scaffold with smaller pores has a larger specific surface area that promotes greater initial cell adhesion [51]. However, very strong initial cell attachment may lead to cellular overcrowding and the creation of a compact cellular capsule at the exterior of the scaffold, which inhibits appropriate cell movement and restricts diffusion [34,52].

Ensuring the continued survival of new tissue and cells at the site healing requires neo- vascularisation. Porosity and permeability significantly impact the degree of vascularisation and viability of the regenerating tissue inside the scaffold [35]. Different pore sizes are suggested for optimal vascularisation and angiogenesis within a scaffold. The proposed minimal pore size for penetration of endothelial cells is 30–40 µm [53], yet alternative larger size ranges, such as 160–270 µm [54] and 300 µm [55], are also commonly suggested.

Vaquette et al. fabricated a biphasic scaffold that is in contact with the PDL and bone tissue using solution and melt electrospinning, respectively. The bone compartment of the structure showed a three-dimensional (3D), highly porous, highly interconnected morphology with low stiffness and an average macroscopic pore size of 220 ± 141 µm. On the other side, the periodontal portion is comprised of a flexible membrane with comparably smaller pore-sizes (10-20 µm range), which is capable of mechanically assisting the cell sheet and offering initial tissue occlusion. After up to 10 weeks in an ovine periodontal defect model, the histological investigation revealed the membrane was completely infiltrated by cells and ECM, confirming excellent integration of the construct with the surrounding tissues. As shown by oblique attachment in bone and cementum and the existence of a vascularised PDL, the regenerated periodontium exhibited a striking similarity to the natural, healthy periodontium [56].

192 Zhang et al. fabricated sandwich-like multifunctional scaffolds composed of chitosan/gelatin/PCL
193 using lyophilisation and electrospinning techniques. Fabricated scaffolds had an average pore size of
194 10 µm and porosity of less than 50%. These composite scaffolds had blood-clotting capability, with
195 the porosity and swelling properties of the scaffolds improving hemostatic effectiveness. Blood cells
196 adhered to the surfaces of the scaffolds, and the hierarchical pore structure and morphology of the
197 sandwich-like scaffolds resulted in high liquid absorbability for hemostasis control. Therefore, small
198 pore-size composite scaffolds may serve as useful barrier membranes by restricting cell infiltration
199 and enhancing blood clotting [57].

200 **2.1.2. Mechanical properties**

201 Mechanical characteristics are one of the most important considerations for periodontal scaffolds.
202 They must retain their integrity peri-transplantation and survive the constant dynamic mechanical
203 environment of the jaw post-implantation. Ideally, scaffold mechanical properties would closely
204 match those of the tissues where the scaffold is transplanted to avoid adverse effects arising from
205 stress-shielding [58–60]. Table 1 shows the mechanical properties of periodontal tissues.

206 ***Table 1:*** *Young's modulus and tensile strength for dental structures* [61, 62, 63, 64].

Structure	Young's modulus (MPa)	Tensile strength (MPa)
Alveolar bone	1.38×10^4	121
Gingiva	3-37.36	3.81
Cementum	1.8×10^4	-
PDL	6.9	-

207

208 Biomaterials made from synthetic and natural biodegradable polymers have shown significant
209 potential for regenerative medicine [65]. Among natural polymers, collagen and chitosan are the most
210 used for periodontal regeneration [66–68]. Natural polymers mimic the ECM, have good biocompatibility,
211 and in the case of chitosan, antimicrobial capabilities; however, they often have poor mechanical
212 properties [69,70]. Natural polymers can be combined with synthetic polymers or can be cross-linked with
213 various chemicals such as genipin or N-(3-Dimethylaminopropyl)-N'-ethyl carbodiimide hydrochloride
214 (EDC) to improve mechanical performance [71].

215 Varoni et al. developed a tri-layered porous periodontal scaffold using chitosan with different
216 molecular weights and genipin-mediated crosslinking to improve mechanical performance. For
217 gingiva, bone and PDL, low molecular weight (LMW) chitosan, medium molecular weight (MMW)
218 chitosan, and MMW-chitosan with microchannels were used, respectively. The MMW-chitosan layer
219 had more than 2-fold higher compressive modulus (18 ± 6 KPa and 7.7 ± 0.8 KPa, respectively) and
220 degraded more slowly than the LMW-chitosan layer [72].

Rather than genipin crosslinking, Tai et al. modulated the mechanical performance of their biphasic chitosan scaffold through the incorporation of calcium phosphate (Ca) particles and PHB to make it suitable for bone regeneration. The elastic modulus of separate chitosan and PHB layers were 10.7 ± 0.6 MPa and 554 ± 25 MPa, respectively. It was 467 ± 22 MPa in combination, and CaP incorporation further increased this to 524 ± 20 MPa [73].

Among synthetic polymers, PCL [74,75], PGA [76], PLA [77], and polylactide-co-glycolide (PLGA) [76,78] are the most used materials for dental regeneration. Although those synthetic polymers have superior mechanical properties to natural materials, they are poor in bioactivity [69,70]. Therefore, in periodontal membrane applications, they are often combined with natural biomaterials and nanoparticles to boost biological performance whilst retaining good mechanical strength.

Puppi et al. created a biphasic scaffold by combining a wet-spun PCL fibre construct (with and without hydroxyapatite (HA)) and a chitosan/poly(γ-glutamic acid) hydrogel. The pure PCL layer had the highest Young's Modulus; HA doping reduced it from 1.3401 ± 0.1923 MPa to 1.2375 ± 0.2282 MPa. The Young's modulus of the bilayer scaffold with and without HA doping to the PCL layer were 0.0348 ± 0.0114 MPa and 0.1472 ± 0.0808 MPa, respectively. Both HA incorporation and inclusion of the chitosan layer reduced the mechanical properties of the PCL-based membrane [79].

Li et al. prepared a bilayer scaffold composed of PLGA and PLGA/micro-nano bioactive glass (MNBG) by solvent casting and electrospinning, respectively. MNBG is used to enhance PLGA bioactivity in the layer that will be in contact with bone tissue. Three different osteogenic layers with concentrations of 0%, 20%, and 40% MNBG were prepared to observe the impact on the mechanical properties of the scaffolds. 40% MNBG incorporation reduced Young's modulus of the PLGA electrospun layer from 14.5 MPa to 10 MPa. Moreover, in this study, it is observed that the fabrication method, which directly affects the morphology, also influences mechanical properties. While the dense layer, which is obtained with the solvent casting method, has Young's modulus of 20.90 MPa, the electrospun PLGA layer has 14.5 MPa [80].

2.1.3. Degradation rate

A key tenet of tissue engineering is that implanted materials resorb at a rate that matches new tissue formation, ultimately leaving no traces behind. Scaffolds should direct cell attachment and proliferation on the surface whilst simultaneously degrading and being resorbed by the body. As non-degradable periodontal membranes have the disadvantage of requiring a second surgery for removal after they have fulfilled their purpose, biodegradable alternatives are preferred where possible [78,81].

Natural biocompatible and biodegradable polymers such as collagen are widely used in GBR applications [82,83]. Synthetic biocompatible and biodegradable polymers such as PLA, PGA and PCL are also widely used; however, they have the disadvantage of releasing lactic acid or glycolic acid into the environment, which lowers the pH of the site during degradation and eventually triggers an inflammatory response. Although PCL also releases various acids upon degradation, it doesn't trigger an inflammatory response to the same extent as PGA and PLA, as it is released at a slower rate, making it a preferable choice [84]. Furthermore, ε-caprolactone is water-soluble, making it easier to distribute throughout the body, minimising local inflammatory effects, and is also easier to excrete via urination, making the product quick to eliminate and relatively non-toxic [85]. This, in combination with PCL's high mechanical stability, makes it a robust material choice, with the main shortcoming being its relatively long (up to 3–4 years) degradation time, which can be undesirable for some tissues [86,87].

Multiphase, composite membranes and scaffolds allow fine tuning of degradation properties to achieve the desired material profile, which in the case of successful regeneration of periodontal tissues should be 4-6 weeks [84]. Imazato et al. developed a poly(l-lactic acid/caprolactone) (PLCL) bilayer GBR membrane and investigated degradation in phosphate buffer saline (PBS) at 37°C for 2 - 52 weeks. By week 26, only half of the PLCL scaffold weight was lost, with PCL copolymerisation enhancing the durability of the membrane. Although longer than the timeframe outlined by Kiremitçi, it may bring the advantage of slower accumulation of acidic degradation byproducts in the host tissue, reducing inflammation [81]. Faster degradation within bilayer membranes has been achieved using a PLGA-based approach where one phase is grafted with hyaluronic acid, observing 40% degradation of hyaluronic acid-grafted PLGA/PLGA membranes within 8 weeks [6]. Apart from polymer type, molecular weight and degree of crystallinity are other critical parameters that have a direct impact on the degradation rate and should also be taken into consideration in the engineering process of the degradation rate of a scaffold.

2.2. Fabrication routes

2.2.1. Electrospinning

Electrospinning uses electrostatic force to produce fibres with a pore size between 5 µm and 150 µm [88] using solutions of natural or synthetic polymers [80,89]. It has found application in a wide range of fields, including catalysis, filtration, protective clothing production, and the food industry, but most importantly, here, within healthcare, it has been investigated for drug, cell and gene delivery, biosensing, wound healing and tissue engineering [90].

The electrospinning apparatus consists of four main components: a syringe pump, a high-voltage power supply, a spinneret, and a conductor collector (Figure 5A) [91]. The polymer solution is held at the

end of the capillary tube by surface tension, and the electric field is applied until the electric force overcomes this. The jet of the charged solution is sprayed from the tip of the Taylor cone, and a spiral-like structure is formed between the capillary tip and the collector. Meanwhile, the solvent evaporates, leaving a solid polymer. Since the jet is stable only at the tip of the nozzle, fibre formation is achieved [92].

Electrospinning can provide aligned or random fibres with a radius as low as 100–1100 nm that mimics the ECM structure [93–95]. However, a critical disadvantage of the technique is its reliance on the use of toxic organic solvents to create polymer solutions, necessitating thorough post-processing for use in medical applications. Recently, green solvents have been investigated to minimise associated toxicity [96]. Whilst the effect of various parameters, such as polymer concentration, needle-to-collector distance, and needle diameters on fibre morphology, is known, optimisation of the process to achieve the desired morphology takes time and needs experience and is best performed under tightly controlled environmental conditions (temperature, humidity, etc.) to improve reproducibility [97]. Despite this, electrospinning is the most widely used technique for the fabrication of GBR/GTR membranes [22,56,98–102] .

The tissue-specific performance of electrospun scaffolds can be improved by doping the polymer solution with appropriate compounds. Zhong et al. developed a bi-layered PLGA electrospun membrane that used different pore sizes to achieve occlusive and osteogenic properties and nano-HA (nHA) particles in the bone-adjacent phase [103]. Barrier properties were attained with 4-7 µm pores and 200-300 nm fibres, and osteogenic properties with 20-28 µm pores and 1000-1800 nm fibres. Achieving different fibre and pore morphology and inclusion of additives requires different electrospinning parameters that must be optimised for each condition. For GBR membrane applications, processing parameters for core polymers of PLGA, PCL and polyethylene oxide (PEO) have been investigated with nHA [103], MNBG [80], calcium carbonate [104], and silicon-doped nHA [105] as additives to improve performance. These changes in material and desired morphology all require careful fine-tuning of voltage, flow rate, polymer/plasticizer ratio, syringe diameter, and solvent ratio.

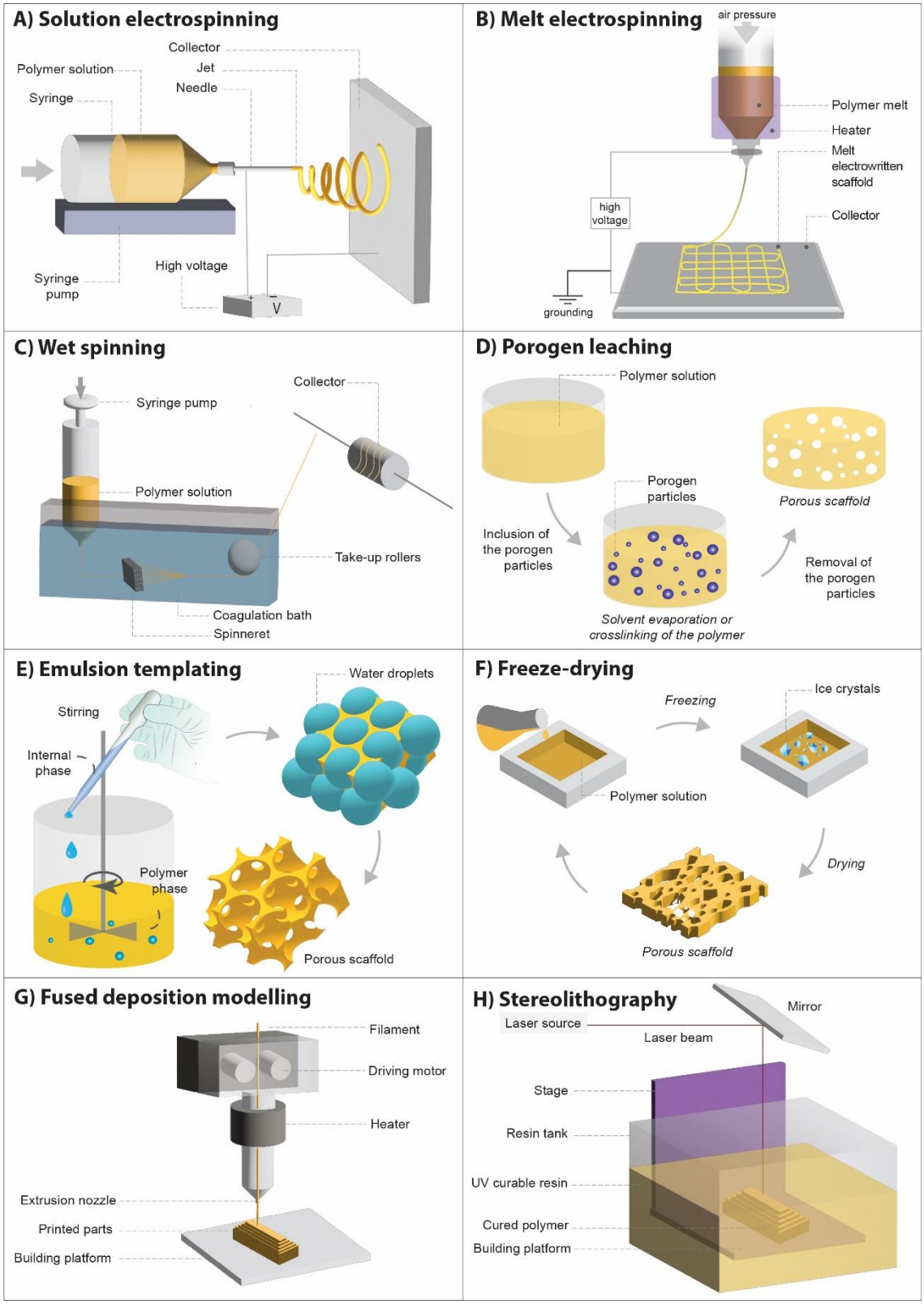

Figure 5: *Schematic diagrams showing the setups of the most common scaffold fabrication techniques (A) solution electrospinning, (B) melt electrospinning, (C) wet spinning, (D) porogen leaching, (E) emulsion templating, (F) freeze-drying, (G) fused deposition modelling, (H) stereolithography.*

315 **2.2.2. Melt electrospinning**

316 Melt electrospinning, also known as melt electrowriting, uses heat rather than solvents to create a
317 polymer solution that can then be deposited via ionisation using an electric field and spraying onto a
318 collector (Figure 5B) [106]. In comparison to traditional electrospinning, molten polymers are more
319 viscous than dissolved polymers, and solid fibres are formed via cooling rather than evaporation.
320 Whilst this eliminates the solvent toxicity risk, it cannot form fibres with diameters as low as traditional
321 electrospinning as the solvent evaporation process helps thin the fibres [107,108]. Melt
322 electrospinning/writing can be considered a form of extrusion 3D printing and can be combined with
323 other manufacturing techniques to create multiphase scaffolds [109]. S. Ivanovski et al. developed a
324 biphasic membrane where melt electrospinning was used to fabricate the bone compartment. Here,
325 an extraskeletal ovine calvarial model revealed the PCL-based bone compartment with 400 µm pore
326 size mimicked native cancellous bone and encouraged bone formation [110].

327 **2.2.3. Wet spinning**

328 Wet spinning requires a polymer solution, a spinneret, and a coagulation bath (Figure 5C). The polymer
329 solution is extruded into the coagulation bath with the help of a hollow wire-like structure resembling
330 a very thin tunnel that the polymer passes through. As the polymer indirectly interacts with the
331 coagulation bath, it solidifies, creating polymer fibres. In the final step, traces of the coagulation bath
332 are removed by chemical reaction or diffusion. For molecular alignment and orientation, fibres may
333 go through several mechanical changes, such as applying tension or drawing. Dry-jet wet spinning is a
334 modified version of wet spinning where the polymer is extruded into an air gap rather than directly
335 onto the coagulation bath. This results in the opportunity to obtain greater molecular alignment [111].

336 The main advantages of wet spinning over traditional and melt electrospinning are that thick fibres
337 with high mechanical strength can be obtained with no thermal degradation [109]. However, the process
338 is slow and requires additional steps to remove the impurities [112].

339 As with other spinning techniques, wet spinning can be combined with other manufacturing
340 techniques to create multiphase scaffolds. Gomes et al. developed a double-layer membrane by
341 combining wet-spinning and solvent-casting [113,114]. The wet spun layer was fabricated by dissolving
342 starch and PCL in chloroform and injecting it through the coagulation bath. Two different fibre types
343 were created by varying the solution in the coagulation bath from methanol to calcium silicate
344 solution. Whilst diameters remained similar (192 µm vs. 195 µm, respectively), the surface of the
345 calcium silicate group was smoother than the methanol group. Post-functionalisation with silanol
346 groups showed increased expression of osteocalcin in canine adipose-derived stem cells over a 28-day
347 period [113].

2.2.4. Solvent casting and particulate leaching

The process of solvent casting and particulate leaching (SCPL) requires dissolving a polymer in an organic solvent, supplementing the solution with particles insoluble in the selected solvent (porogen), and casting it in a mould to create a scaffold or a membrane (Figure 5D). The polymer and porogens combine to form a composite material structure as the solvent evaporates. Particles are then dissolved, leaving a porous structure behind. Porogens can have different sizes, shapes, and proportions [115]; paraffin beads, salt, and sugar are some of the most frequently utilized porogens. A high porogen ratio is needed to obtain scaffolds with high interconnectivity [116]; however, it is challenging to achieve an even dispersal of porogen in the polymer solution. As such, the degree of direct contact between particles is not well regulated, which can lead to uneven pore distribution [117]. Furthermore, as porogens are entirely encased by the polymer solution, it is difficult to fully remove these even with a porogenic solvent due to the physical polymer barrier around them. As a result, the thickness of most porous materials created using the SCPL process is 4 mm or less to improve this process, and the necessity of cytotoxic solvents is a further drawback to this technique [118,119].

Jamuna-Thevi et al. developed a triple-layered PLGA/nano apatite/lauric acid-graded composite membrane for periodontal-guided bone regeneration by combining solvent casting and phase separation techniques in the same step with dimethyl sulfoxide (DMSO) as the solvent for PLGA. Instead of employing the traditional solvent evaporation procedure, PLGA solutions were frozen at - 18 °C, and the solidified DMSO was removed by immersion in cold water at 4 °C, which significantly decreased membrane toxicity. The pore sizes of all three layers were larger than 100 µm and asymmetric columnar in shape, with the PGA and nano apatite ratio having a significant impact on the morphology of the membrane [120].

Gümüşderelioğlu et al. developed a chitosan and PCL-based bilayer barrier membrane, with the chitosan-based layer created by SCPL. Here, chitosan was dissolved in aqueous acetic acid and silica particles were included as a porogen. The solvent was evaporated at room temperature before submerging in 80 °C aqueous 5% (w/v) sodium hydroxide (NaOH) to dissolve the silica particles and obtain a porous membrane. The resulting chitosan membrane had an interconnected and homogenous morphology with an average pore size of 170 ± 79 µm. However, the surface that was in contact with the glass petri dish was comparably less porous with small pores [84].

2.2.5. Emulsion templating

Emulsion templating is based on creating a stable emulsion by mixing two immiscible liquids in the presence of a surfactant or Pickering particles and then polymerising the continuous phase [121]. Emulsion droplets (internal phase) act as a pore template during polymerisation and, when removed

afterwards, leave porous matrices (Figure 5E). When the internal phase volume (total droplet volume) of the emulsion is greater than 74%, it is defined as a High Internal Phase Emulsion (HIPE) [122]. Emulsion-templated matrices have been used in various fields, such as catalysis, separation columns, heavy metal removal, solid-phase synthesis, and substrates for electrodes [123].

Recently, emulsion templating has also gained attention as a tissue engineering scaffold fabrication technique [10,121,123–134] as it provides (i) high porosity (up to 99% [135]), (ii) high interconnectivity, (iii) high tunability [121,123,136–141], and (iv) can be combined with other fabrication techniques (such as 3D printing [121,130,142] and electrospinning [143]) for the fabrication of more complex structures. Although emulsion-templated matrices have been widely used for soft [133,134,144–146] and hard [121,132,147–152] tissue engineering applications, there is only a limited number of studies on the use of emulsion-templated matrices in the fabrication of GBR membranes.

Aldemir Dikici et al. recently investigated the potential use of photocurable PCL-based polymerised HIPE (PolyHIPE) scaffolds for guided bone regeneration. 90% of the pores of PCL PolyHIPEs have pore sizes between the 20–75 µm range and window sizes distributed between the 2–13 µm range (Figure 7F). They showed that PolyHIPE morphology supported attachment, proliferation, and infiltration of murine long bone post-osteoblasts/pre-osteocytes (MLO-A5s) up to 400 µm. The suitability of the morphology of the pores for blood vessel ingrowth has also been shown using the chick chorioallantoic membrane (CAM) assay [10], which is an alternative *in vivo* model to assess the angiogenic potential of biomaterials, cells, and drugs [121,153–156]. The CAM of the chick embryo is an extraembryonic membrane that functions as an organ for gas exchange between the chick embryo and the environment. Working on the membrane without direct contact with the experimental animal and before nerve tissue development makes the CAM model a more ethical alternative to studying angiogenesis on more developmentally advanced animals.

2.2.6. Freeze-drying

Freeze-drying (lyophilisation) is based on the dehydration of polymeric solutions and has traditionally been employed in the field of tissue engineering for manufacturing 3D porous biomaterials, where the resulting overall morphology of the biomaterial solution is defined by the shape of the mould [157]. Lyophilization is an attractive fabrication method as (i) high temperatures are not applied, (ii) there is no need for separate leaching, and (iii) varied sizes of scaffolds can be fabricated with (iv) high porosity (over 90% can be achieved) [158,159].

The first step is freezing (liquid nitrogen or mechanical refrigeration), where the obtained polymer solutions are inserted into the desired mould and cooled to a temperature that is below the solvent's triple point, ensuring sublimation will occur in the subsequent drying step. The last step is split into

414 two parts: primary and secondary drying. In primary drying, the sublimation process takes place,
415 extracting approximately 95% of the water (Figure 5F). In secondary drying, evaporation removes
416 residual unfrozen solvent molecules [160].

417 Parivatphun et al. developed a biphasic scaffold with a freeze-dried and micro-bubbled layer for the
418 regeneration of the oral maxillofacial area. The micro-bubble technique is used to obtain the main
419 pores of the scaffold (~400 µm), and freeze-drying is secondarily applied to form the sub-pores
420 (~100 µm) of the scaffold for better mimicry of natural trabecular bone. Desired pore dimensions were
421 achieved with homogenous distribution [161].

422 Tamburaci et al. fabricated a bilayer membrane by lyophilization with phases designed to be in contact
423 with soft and hard tissues. Si-doped nHA particle (Si-nHAp) incorporated chitosan fabricated with
424 lyophilization of both LMW and MMW chitosan formed the soft tissue phase, whilst chitosan/PEO
425 formed the hard tissue phase. Molecular weight significantly influenced membrane morphology, with
426 greater molecular weight increasing pore size (LMW: 174-191 µm, MMW: 252-306 µm) [105].

427 **2.2.7. Cryo-gelation**

428 Cryo-gelation has gained popularity recently due to its ability to provide both macroporous
429 morphology and outstanding swellability [162]. To produce a cryogel, the cross-linkable polymer is
430 dissolved in water, poured into a mould, and then immediately frozen. Ice crystals start to form and
431 result in phase separation between the crystals and solutes (macromonomers, initiators).
432 Concurrently, the polymer in the liquid phase starts to cross-link (cryo-polymerization). Once
433 crosslinked, cryo-gels can be thawed at room temperature to dissolve ice crystals, revealing a
434 macroporous structure [163,164.]

435 Huang et al. fabricated a biphasic scaffold by cryo-gelation to enhance periodontal regeneration at
436 the soft and hard tissue interface. The first layer, designed to be in contact with soft tissue, was
437 composed of gelatin; the other layer, designed for bone tissue, was made of β-TCP/HA particles
438 incorporated in gelatin. The soft tissue layer had a pore size and porosity of 406 ± 76 µm and 95.5 ±
439 0.2%, respectively, and the addition of ceramic particles to the gelatin increased the pore size to 431
440 ± 61 µm, reducing the porosity to 81.7 ± 1.2%. *In vivo*, the scaffold preserved its structural integrity
441 and permitted rapid hemostasis and early vascularisation, increasing early bone deposition [165].

442 **2.2.8. 3D printing**

443 3D printing (3DP), also known as additive manufacturing (AM), rapid prototyping (RP), and solid free-
444 form fabrication (SFF), has enabled the production of scaffolds with complex morphologies that could
445 not be achieved with traditional manufacturing techniques [166,167]. The most common 3DP techniques

are extrusion-based (e.g., fused deposition modelling (FDM), Figure 5G)), light-based (e.g., stereolithography (SLA, Figure 5H) multi-photon lithography/two-photon polymerisation (MPL/2PP), computed axial lithography (CAL)/volumetric additive manufacture (VAM), and selective laser sintering (SLS)), and inkjet-based printing. System choice depends on the properties of the biomaterials and the design requirements [168,169].

First, a 3D model is designed in computer-aided design (CAD) software and exported into a file format that defines the surface mesh in 3D space, such as .stl [170]. Another application converts this model into print instructions relevant to the printing technique, e.g., for SLA, a 'slicer' would be used to create a cross-section of each printed layer. Algorithms may be used to determine optimal fill patterns for each layer, and parameters such as exposure time, layer thickness, laser power, light intensity, and printhead speed can also be fine-tuned to achieve precise replication of the original 3D model [171,172].

The advantages of 3DP are reproducibility, enabling tight control of pore morphology, connectivity, and spatial distribution with otherwise unachievable complex designs, high resolution (nm to mm resolution across available technologies), rapid prototyping, comparably fast fabrication, cost-effectiveness, and being environmentally friendly by reducing waste material, especially when compared with subtractive manufacturing technologies [172, 173, 174]. Depending on the printing method, cells may be incorporated directly into scaffold material at high densities, allowing spatial distribution of multiple cell types within a single construct. Multiple materials can be printed concurrently, bioactive compounds can be printed without loss of function, and gradients of mechanical, chemical, and geometric properties can be achieved throughout a single scaffold [167]. It is worth noting that for biological applications, the choice of materials available is currently limited as non-biological 3DP materials are often cytotoxic, but this is an active area of research and development. Furthermore, initial equipment setup costs may be expensive [175,173,176].

Lee et al. developed an HA-doped PCL-based trilayer scaffold with gradient microchannels using FDM for periodontal applications. The cementum-dentin interface, the PDL compartment, and the alveolar bone section were designed to have channels with 100 µm, 600 µm and 300 µm, respectively. *In vivo,* testing with an immunodeficient mouse model that scaffolds with bioactive agents and dental stem/progenitor cells promoted the regeneration of multiphasic tissue when implanted in the dorsum [177].

Park et al. designed and fabricated 3D-printed wax moulds, which were then cast with PGA and PCL for PDL and bone regions of the scaffold, respectively. Acid-treated human tooth dentin slices were integrated into designed bilayer scaffolds to better mimic the periodontal environment. Subcutaneous examination *in vivo* showed fibrous tissue on PGA constructs with oblique or perpendicular

479 alignments to dentin and mineral tissue formed in the dentin interface and bone construct, suggesting
480 the regeneration of bone and cementum tissue. Periodontal ligament-bone tissues were generated
481 with distinct compartmentalisation and highly controlled organisation, with the most significant
482 finding being that the structural/geometric cues precisely influence the orientation of connective
483 tissue in the 250-300 µm interfaces. In addition to the alignment of fibrous tissue, the restricted
484 infiltration of newly formed bone into the PDL structure improved the spatial-temporal tissue
485 organisation [178].

486 **2.2.9. Alternative strategies**

487 In addition to conventional scaffold fabrication techniques, there are alternative tissue engineering
488 approaches such as cell sheet technology and decellularisation. Cell sheet technology enables the
489 fabrication of 3D constructs without the use of any tissue engineering scaffold. Using a temperature-
490 responsive polymer-grafted (poly(N-isopropyl acrylamide) (PIPAAm)) cell culture surface, confluent
491 cultivated cells may be retrieved as an entire cell sheet. PIPAAm provides non-invasive regulation of
492 cell attachment and detachment by reducing the temperature to 32 °C without any protease
493 treatments. The ECM, cell surface proteins, and cell-cell junctions are preserved, allowing many cell
494 sheets to be layered to readily create functional 3D tissue that can be directly implanted without the
495 need for scaffolds [179]. Cell sheet technology is widely used in periodontal tissue engineering, e.g.,
496 through the generation of intact periodontal cell sheets with a robust ECM due to the presence of
497 ascorbic acid during culture. The ECM contains many proteins, including fibronectin, which serves as
498 a natural adhesive to bind cell sheets to other surfaces [180].

499 Dan H. et al. developed a cell sheet-supported CaP-coated PCL (CaP-PCL) scaffold from harvested PDL,
500 alveolar bone and gingival margin-derived human cells (hGMC). Following primary cell culture and *in*
501 *vitro* characterisation, a cell sheet was prepared and combined with CaP-coated melt electrospun PCL
502 (CaP-PCL) and transplanted into a rat periodontal defect model for *in vivo* evaluation. After 4 weeks,
503 the CaP-PCL scaffold without cell sheet-support had encouraged alveolar bone formation. Although
504 hGMC-based cell sheets did not support regeneration, bone and PDL-derived sheets significantly
505 promoted periodontal attachment, showing that the source of the cell sheet has a significant impact
506 on the biological performance of the scaffolds [181]. Other research groups have also utilised cell sheets
507 with reinforcing carriers (e.g., hyaluronic acid [182]) or without the use of any supporting scaffold [180] for
508 periodontal regeneration.

509 Another alternative strategy, decellularisation, involves removing DNA and other cellular components
510 from the tissue whilst retaining the native ECM structure and regulatory proteins via a combination of
511 chemical, enzymatic, and physical methods [121,183,184]. The removal of genetic material to avoid

512 immuno-rejection of the construct, the preservation of ECM and the retention of mechanical
513 properties define the quality of the decellularisation process [185]. To be considered effective,
514 decellularised ECM must have no visible nuclear material by 4',6-diamidino-2-phenylindole (DAPI)
515 staining, fewer than 50 ng double-stranded DNA (dsDNA) per mg ECM dry weight, and less than 200
516 bp DNA fragment lengths [186].

517 Son et al. investigated the regeneration potential of decellularised human tooth slices as periodontal
518 scaffolds, assessing two different decellularisation protocols: (1) 2% TritonX-100 and 0.1% ammonium
519 hydroxide (NH_4OH) for 72 hours or (2) three cycles of 1% sodium dodecyl sulfate (SDS) for 24 hours
520 and 1% TritonX-100 for 24 hours. Total DNA quantification showed that protocol 2 was almost twice
521 as effective as protocol 1, removing 62.32% of DNA. Tissue type and decellularisation procedure
522 influence the effectiveness of the process, and incomplete decellularization could result in an
523 immunological response that has a detrimental impact on the course of treatment [187,188]. Here,
524 collagen I was preserved after decellularisation, the scaffolds maintained their structural integrity, and
525 they supported the repopulation and differentiation of PDL cells [188].

526 **2.2.10. Challenges in the fabrication of multiphasic constructs**

527 In multilayer GBR/GTR membranes, the occlusive layer should limit the infiltration of the soft tissue,
528 whilst the other layer should facilitate bone infiltration and regeneration. Accordingly, the occlusive
529 soft tissue layer is fabricated with a smaller pore size than the bone regeneration phase. Each of the
530 common fabrication modalities reviewed here has distinct advantages and disadvantages with regard
531 to creating the unique morphologies required in each layer of these multiphase constructs (Table 2).
532 Whilst these are general to the technique, there is an opportunity within each manufacturing method
533 to fine-tune the structures created through modulation of the parameters and materials used,
534 allowing a construct with morphologically distinct layers to be created with the same manufacturing
535 technique. Alternatively, this can be achieved through hybrid manufacturing, combining different
536 techniques.

537 Regardless of which approach is selected, the main challenge to overcome is the integration of
538 consecutive layers into each other to avoid delamination and maintain mechanical integrity during
539 surgical implantation and subsequent tissue regeneration. The most common way this is achieved is
540 by fabricating the first layer via one of the aforementioned fabrication techniques (3D printing (Figure
541 6B, 6F), emulsion templating (Figure 6C), electrospinning (Figure 6G), freeze-drying (Figure 6H),
542 solvent casting (Figure 6J)), then constructing the second layer directly on the top via electrospinning
543 [189, 10, 190, 102, 105, 80]. Hutmacher et al. used an alternative approach where they developed a bilayer
544 membrane with a PCL and β-tricalcium phosphate (β-TCP)-based bone phase fabricated by FDM and

545 a PCL periodontal phase created by melt electrospinning. For the latter, random-oriented PCL fibres
546 were achieved with diameters of 10-15 µm and pore sizes ranging from 100 µm to 400 µm. In this
547 study, layers were integrated into each other by heating and press-fitting (Figure 6A, Figure 7A) [191].

548 ***Table 2:*** *Advantages and disadvantages of various scaffold fabrication techniques widely used in the*
549 *development of multiphasic periodontal constructs.*

	Advantages	Disadvantages	REF
Melt Electrospinning	+ Solvent free (environment friendly) + Diameter is controllable with the mass flow rate + Low production cost due to the absence of the solvent + High fibre consistency and quality	- Viscosity can interfere with the process - Thermal stability of polymers is required - Low fibre diameter can be difficult to obtain	107
Wet Spinning	+ Can provide large fibres with maximum strength + Low cost + Large-scale production	- Solvent and chemical recovery - Non-aligned fibres - Can produce only microfibers	192
Electrospinning	+ Can produce uniform and/or aligned fibres + High interconnectivity + High porosity + Scaffold architecture similar to natural ECM + Comparably facile fabrication	- Use of cytotoxic organic solvents - Limited control on pore morphology	193
Emulsion templating	+ High porosity (up to 99%) + High interconnectivity + Precise tunability of the morphology + Can be combined with other fabrication techniques for the fabrication of more complex structures	- Surfactant removal may be needed (except Pickering PolyHIPEs)	123
Porogen leaching	+ No extra specific equipment needs + Can provide high porosity	- Residual solvent and porogen materials - Time-consuming - Poor interconnectivity	194,195,196
Freeze -drying	+ No need for separate leaching + High porosity (over 90% can be achieved) + High temperatures are not applied	- Slow - Expensive - High energy consumption	158,159 197–199
Cryo-gelation	+ Macroporous morphology + Outstanding swellability + Flexibility	- Low surface area - Low adsorption capacity	163,165,200, 201,202
3D Printing	+ Customised design and production + Control on outer architecture + Cost effective + Environment friendly	- Specific equipment needs - Clinical impacts and potential risks are poorly understood - Extrusion techniques have low resolution - May have insufficient mechanical properties	173, 203,204,205, 172

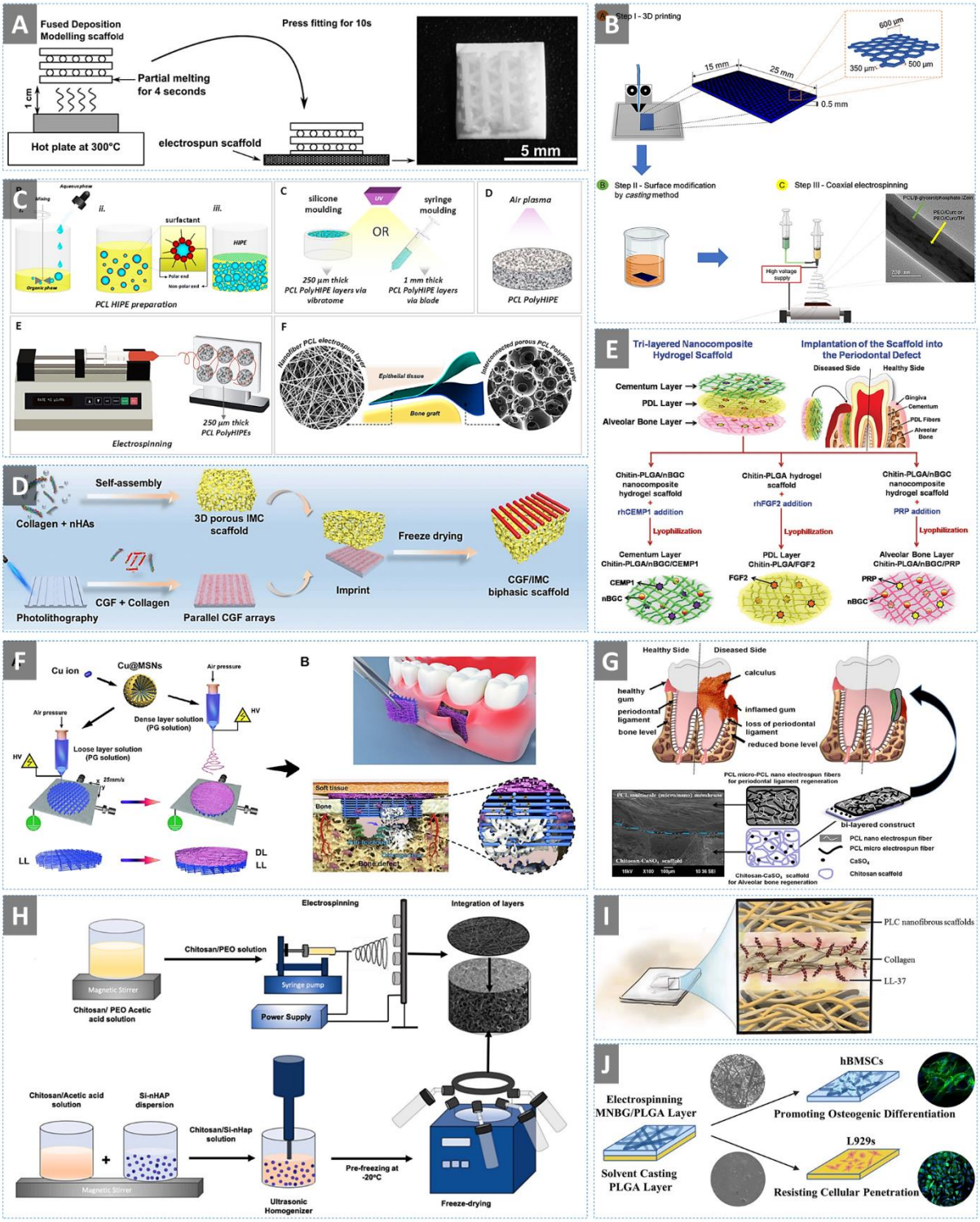

Figure 6: *Multiphasic scaffold fabrication schemes combining various porous material production routes (A) FDM deposition and electrospinning [206], (B) 3D printing and coaxial electrospinning [189], (C) emulsion templating and electrospinning [10], (D) self-assembly and microstamping [207], (E) hydrogels [208], (F) solution electrospinning writing and solution electrospinning [190], (G) electrospinning [102], (H) electrospinning and freeze-drying [105], (I) electrospinning [209], (J) electrospinning and solvent casting [80].*

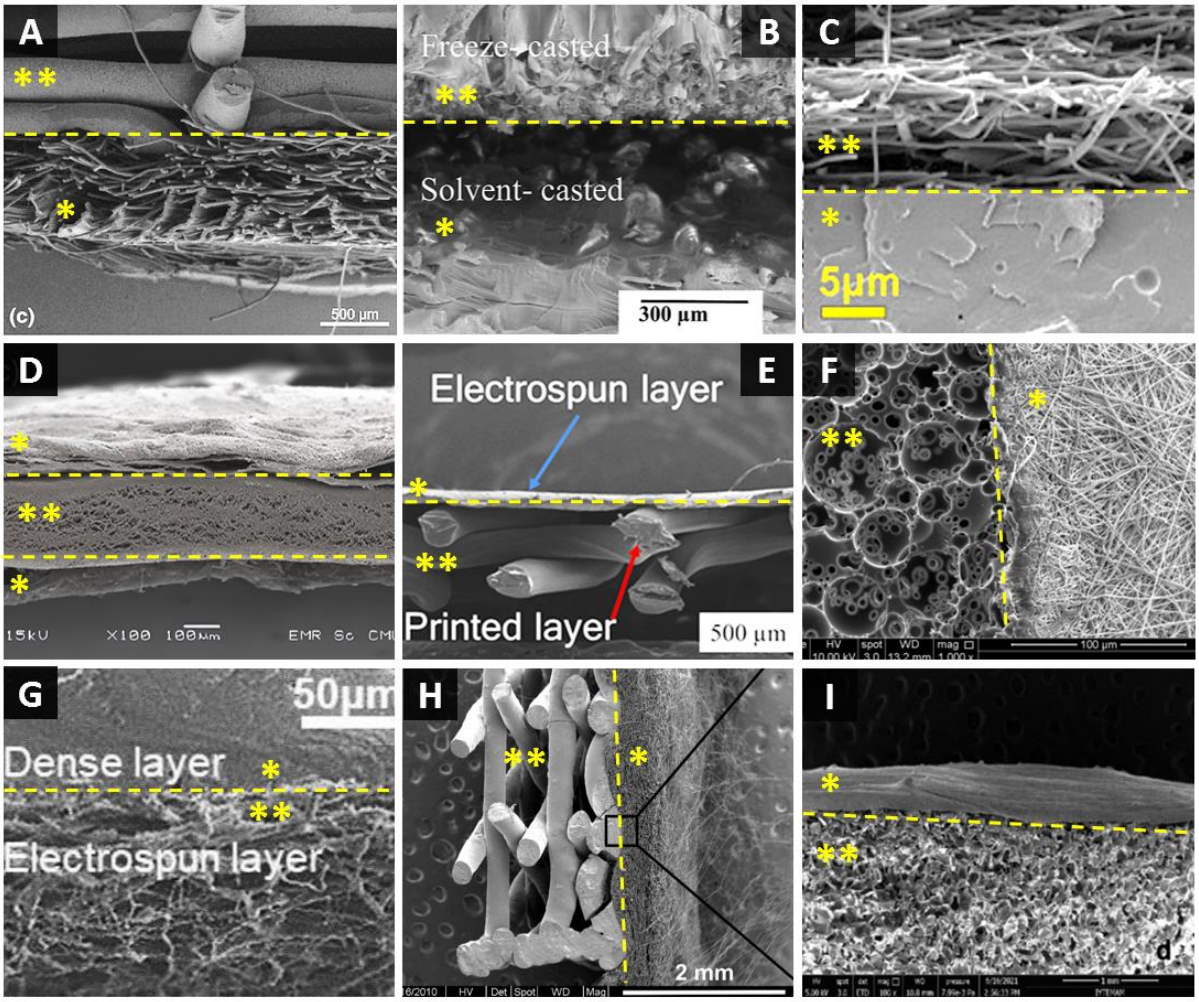

Figure 7: *SEM images of the multilayer membrane designs. (**: bone compartment, *: barrier layer). (A) *: melt electrospun PCL, **: FDM fabricated PCL and β-TCP [191], (B) *: solvent-cast chitosan and gelatin, **: freeze-cast chitosan and gelatin [210], (C) *: solvent-cast PLGA and wool keratin, **: electrospun PLGA and wool keratin [211], (D) *: poly(L-lactide-co-ε-caprolactone) (PLC) electrospun, **: commercially available collagen type I scaffold [209], (E) *: coaxial electrospinning of poly(ethylene oxide) (PEO)/curcumin/tetracycline hydrochloride as the core and zein/PCL/β-glycerolphosphate (β-GP) as the sheath, **: 3D printed honeycomb PLA/zein/Curcumin [189], (F) *: PCL electrospun, **: emulsion templated photocurable PCL [10], (G) *: Solvent-cast PLGA, **: micro-nano bioactive glass and PLGA-based electrospun [80], (H) *: PCL electrospun, **: FDM fabricated PCL and β-TCP [206], (I) *: chitosan and PEO electrospun, **: freeze-dried chitosan and Si-doped nHA [105].*

2.3. Biomaterials used in the fabrication of periodontal tissue engineering scaffolds

2.3.1. Synthetic polymers

The physical and chemical properties of biomaterials affect tissue regeneration by mediating cell adhesion, proliferation, and differentiation [205]. Consequently, the selection of a biomaterial for the regeneration of a specific target tissue requires an understanding of how these properties affect said tissue. Synthetic polymers, natural polymers, and ceramics are the most commonly used biomaterials in periodontal tissue engineering, with each having advantages and disadvantages (Table 3).

576 ***Table 3:*** *Advantages and disadvantages of various biomaterial types widely used in the development of*
577 *multiphasic periodontal constructs.*

	Advantages	Disadvantages	Refs
Synthetic Polymers **Polycaprolactone (PCL)** **poly(lactic acid) (PLA)** **poly(glycolic acid) (PGA)** **polylactide-co-glycolide (PLGA)** **polyvinyl alcohol (PVA)**	+ Controllable mechanical strength + Controllable degradation rate + Highly processable	- Lower cell attachment - Slow degradation rate (PCL) - Hydrophobicity (PCL)	212
Natural Polymers **Collagen** **Chitin/chitosan** **Gelatin** **Silk**	+ Hydrophilicity + Chemically modifiable	- Rapid degradation rate - Low mechanical strength - Batch-to-batch variation	213,214,215
Ceramics **Biphasic calcium phosphate (BCP)** **Tricalcium phosphates (TCPs)** **Hydroxyapatite (HA)** **Bioglass**	+ Bioactivity + Hydrophilicity + Availability + Resemblance to bone + Osteoconductivity	- Brittle - Not easy to process	216,191

578

579 Most natural polymers have the advantage of being biocompatible and hydrophilic, which facilitates
580 cell attachment. However, they typically undergo rapid degradation and have low mechanical
581 strength, which may hinder the process of tissue regeneration [213]. Synthetic polymers generally have
582 superior and controllable degradation and mechanical strength, and [220] can be mass-produced[217].
583 However, they typically are more hydrophobic, resulting in lower cell attachment unless overcome
584 through post-treatment. Furthermore, whilst degradation is controllable, it is still slower than natural
585 polymers [253,212]. Some of the widely used synthetic polymers in periodontal tissue engineering are PCL,
586 PLA, PGA, polyvinyl alcohol (PVA) and their copolymers [218,217,252].

587 ***2.3.1.1. PCL***

588 PCL is a semi-crystalline, aliphatic polymer with high thermal stability (melting point ~ 60°C, glass
589 transition temperature ~-60°C) [219]. It degrades more slowly than most other synthetic polymers, which
590 can reduce the inflammatory effect of acidic degradation products that can occur with faster
591 degrading synthetic materials [219,220]. As the Food and Drug Administration (FDA) has already approved
592 the use of several PCL-based products, including surgical sutures in clinics [221], this polymer is an
593 attractive choice for biomedical applications. In addition to the more common linear, high molecular
594 weight, thermoplastic PCL, thermoset, photocurable, *in-house* synthesised PCL that has functional
595 groups and can create polymer networks, is increasingly used as a biomaterial in the development of
596 GBR membranes [10].

597 Türkkan et al. designed a bilayer membrane that combines a nano-CaP-incorporated silk fibroin-PCL-
598 PEG-PCL (SPCA) layer with a PCL layer fabricated using electrospinning. PEG was used to enhance the
599 hydrophilicity, biocompatibility, and biodegradability of PCL, whilst CaP nanoparticles were
600 incorporated with the PCL-PEG-PCL layer to boost osteoconductivity. *In vitro* confirmation of cell

601 adhesion, proliferation, and differentiation through calcium deposition and alkaline phosphatase
602 (ALP) activity of human dental pulp stem cells suggest its suitability for periodontal regeneration
603 applications [222].

604 Gürbüz et al. developed a trilayer membrane using electrospinning and solvent casting/particulate
605 leaching techniques, with layers composed from (1) PCL/collagen-bone morphogenetic protein-7
606 (BMP-7), (2) PCL-nHA, and (3) PCL/collagen, finding that the BMP-7 incorporated multilayer
607 membrane supported cell proliferation and osteogenic differentiation [223].

608 ***2.3.1.2. PLA, PGA, and PLGA***

609 PLA is an aliphatic thermoplastic, biodegradable, and biocompatible polymer with linear polymeric
610 chains [224,225]. During the hydrolytic degradation of PLA, lactic acid - a natural intermediary in the
611 metabolism of carbohydrates, is produced [226]. With a melting temperature of ~180°C and a
612 crystallization temperature of ~130°C, it can easily be thermally extrusion printed (FDM) [227]. Although
613 PGA has a chemically similar structure to PLA, it provides very different properties, with much faster
614 degradation and a melting and crystallisation temperature ~50°C higher than PLA [228]. PLGA is the
615 copolymer of PGA and PLA. The lactic acid: glycolic acid (LA:GA) ratio has a critical impact on the
616 properties of PLGA scaffolds, and through modulation of this copolymerisation, the final properties
617 (glass transition temperature, degradation rate, mechanical strength) of the material can be tuned [229
618 230]. As PLGA has low osteoconductivity, it is often used with other biomaterials in bone and periodontal
619 applications to augment this [231].

620 Sowmya et al. manufactured a tri-layered scaffold for the treatment of periodontitis. The PLGA/chitin-
621 based scaffold was designed to mimic cementum, PDL and alveolar bone. Accordingly, they
622 incorporated nano bioglass ceramics (nBGC) into the chitin/PLGA matrix for cementum and bone
623 layers to increase the bioactivity of the scaffold. Chitin was selected due to its similarity with natural
624 ECM, and PLGA was incorporated to overcome the limitations of rapid degradation and negate the
625 mechanical instability of natural polymers. Cementum, PDL and alveolar bone layers were enriched
626 with cementum protein 1 (CEMP1), fibroblast growth factor 2 (FGF-2) and platelet-rich plasma-derived
627 growth factor (PRP), respectively. Lyophilised scaffolds were implanted into rabbit maxillary
628 periodontal defects, achieving complete regeneration of the periodontal defect according to results
629 of micro-computed tomography (micro-CT) and histological analyses [208].

630 Similarly, in a study conducted by Zhong et al., an electrospun PLGA-based bilayer membrane was
631 developed with different pore and fibre sizes in each layer, aiming to achieve occlusive and osteogenic
632 properties. PLGA was chosen as a biomaterial because of its controllable degradation rate, good
633 biocompatibility, and appropriate mechanical properties (e.g., surviving stresses exerted from

634 chewing). To provide osteoconductivity, nHA was incorporated into the bone layer. *In vitro*
635 degradation rates were appropriate for use on periodontal tissue engineering, losing 40% of their
636 weight within 9 weeks [103].

637 ***2.3.1.3. PVA***

638 PVA is formed from the polymerisation of vinyl acetate [232]. Due to it being a non-toxic [232,233], highly
639 hydrophilic [234], and biocompatible [233,235] polymer, with good chemical resistance and physical
640 properties [234], it is used in a wide range of industrial applications [236]. It can be electrospun [233] and has
641 been used in several FDA-approved pharmaceuticals for a range of medical conditions [237].

642 Shoba et al. designed a two-layer membrane composed of a freeze-dried collagen and sericin phase
643 and an electrospun PVA phase enriched with bromelain-conjugated magnesium-doped HA
644 nanoparticles. The PVA provides mechanical and structural stability by increasing the tensile strength
645 of the scaffold, whilst the use of collagen and sericin improved the biocompatibility and regeneration
646 capacity by modifying the surface chemistry. Contact angle measurements of the collagen/sericin
647 layer, the nanoparticle encapsulated PVA layer, and the bromelain-conjugated magnesium-doped HA
648 nanoparticle doped PVA coated collagen/sericin construct were 40 ± 3.2 °C, 78 ± 1.2 °C, and 60 ± 1.6
649 °C, respectively [22], demonstrating how this property and subsequently the hydrophilicity, water
650 absorption, degradation rate and the release of the bioactive agents can be tuned for the specific need
651 and application.

652 **2.3.2. Natural polymers**

653 The definition of a tissue engineering scaffold has evolved since the field's inception, moving from a
654 substance that serves as an inert provision of surface area to support cell attachment to one that
655 provides a more complex, dynamic, instructive environment for tissue formation [238]. With few
656 exceptions, natural polymers are biocompatible, biodegradable, inexpensive at small scales, easily
657 accessible, and chemically modifiable [214,215]. They can be included in oral treatment or bolus matrix
658 delivery systems since they are often non-toxic, even at high doses [239]. However, there are questions
659 about whether it would be possible to locate significant quantities of these natural polymers for
660 therapeutic uses in a commercially viable manner, as well as concerns over their comparatively poor
661 mechanical qualities and the certainty of pathogen elimination. The immune system can identify some
662 regions of these molecules as unfamiliar, which might result in material rejection [240]. Despite this,
663 naturally derived polymers are the most frequently used materials for bioengineered resorbable
664 periodontal membranes. They are generally not used alone as they are insufficient in terms of
665 mechanical and mineralisation properties; instead, they are often produced as composites with
666 synthetic polymers or ceramics [241].

667 ***2.3.2.1. Collagen***

668 Collagen is an abundant structural protein in animals and the most frequent component of ECM in
669 humans, making up one-third of the total protein and three-quarters of the dry weight of skin ECM. In
670 vertebrates, 28 different forms of collagen are made up of at least 46 different polypeptide chains,
671 and many additional proteins have collagenous domains [242–244]. As a biomaterial, its key advantages
672 derive from its excellent biocompatibility, resorbability and remodellability by the body, with minimal
673 antigenicity [245]. For GTR applications, there are products based on natural polymers available on the
674 market, such as ParoGuide®, which contains a combination of collagen and chondroitin sulfate [246], and
675 BioMend®, which consists of cross-linked bovine type I collagen [247]. These products are simple to use,
676 which reduces intervention time and patient discomfort. However, they are not perfect solutions due
677 to their erratic rate of resorption, degree of breakdown and low mechanical strength [248].

678 Zhou et al. developed a bilayer GBR membrane where layers were composed of fish collagen and PVA.
679 The layers were well-integrated, and both layers exhibited hydrophilic characteristics. Degradation
680 studies showed that the remaining weights of collagen/PVA bilayer membrane and PVA membrane
681 were around 58-67% and 80-86%, respectively, after 17 days of incubation in PBS, with the PVA layer
682 improving the durability and degradation time of the collagen/PVA-based bilayer membrane [249].

683 Tang et al. developed a nanofiber electrospun membrane with core and shell structures using coaxial
684 electrospinning to promote bone growth, drug release, and occlusiveness for periodontal
685 regeneration. The core and shell of the fibres were composed of PLGA/HA and collagen/amoxicillin
686 (AMX), respectively. Collagen concentration was shown to have a direct impact on the fibre
687 morphology and drug release rate, likely due to the degradation rate of collagen [250].

688 Li et al. tested the *in vivo* performance of bi-layered electrospun fish collagen/PLGA and FDM printed
689 nHA/PLGA scaffolds with/without injectable platelet-rich fibrin (I-PRF) in a New Zealand White Rabbit
690 model. I-PRF is a flowable fibrin extracted from blood that sets in 15 minutes to a hydrogel. It is rich
691 in platelets, leukocytes, and growth factors and is used in tissue engineering to enhance angiogenesis,
692 mechanical strength, degradation time of the scaffolds and tissue regeneration. Results showed that
693 I-PRF incorporation reduced inflammatory reactions and provided a higher degree of angiogenesis,
694 with micro-CT showing bone volume fraction was higher in scaffold alone and scaffold+ I-PRF groups
695 compared to control (no scaffold). However, I-PRF inclusion provided a higher degree of bone
696 regeneration [251].

697 ***2.3.2.2. Chitin/chitosan***

698 Chitin is one of the most abundant biopolymers in nature, and it is found in the exoskeletons of
699 shellfish, insects, and the cell walls of fungi. It is a polymer of β-(1→4)- linked N-acetyl-glucosamine

700 monomers, whilst chitosan is the deacetylated form of chitin. These materials are widely used in tissue
701 engineering applications due to being non-toxic, biodegradable, biocompatible, having antimicrobial
702 properties, their amenability to drug release applications, and being easily brought into gel form [252].
703 In periodontal and bone tissue engineering applications, they are mostly used as a composite with
704 other materials [253].[254–256].

705 Gorgieva et al. developed a bi-layer GBR membrane made of chitosan and gelatin in both layers, with
706 the soft tissue layer made by solvent casting and the bone tissue layer made by freeze casting.
707 Chitosan was selected due to its film and membrane-forming ability and similarity to periodontal ECM
708 properties [210]. In addition to chitosan composites being made with natural polymers[257,258], synthetic
709 polymers and ceramics have also been used to enhance the overall properties of the membranes [208].

710 Rehman et al. developed a freeze-dried, functionally graded, trilayer scaffold manufactured by
711 changing concentrations of chitosan, hydroxypropyl methylcellulose (HPMC), Pluronic F127, and
712 bioglass nanoparticles. They tested the *in vivo* performance of these scaffolds in 8 weeks old adult
713 Wistar rats. Histological analysis on day 21 and day 35 showed no bacterial accumulation on the
714 wound, and there was no difference in the presence of the inflammatory cells in the test group
715 compared to the control group. Also, a layer of connective tissue was observed at the tissue-implant
716 interface, indicating good tissue-material interaction [259].

717 ***2.3.2.3. Gelatin***

718 Gelatin is a natural biopolymer that is obtained from the tendons, skin, and bones of animals by partial
719 acid (type A) or alkaline hydrolysis (type B) [260]. As gelatin is structurally similar to the collagen from
720 which it is ultimately derived, it is often used *in lieu* [261,262]. However, whereas native collagen can form
721 a polymerised network through physical crosslinking [263], pure gelatin gels are highly unstable and weak
722 at physiological conditions and, therefore, need to be chemically crosslinked. This can be done using
723 a crosslinker such as 1-ethyl-3-(3-dimethylaminopropyl) carbodiimide (EDC) or genipin [264] , or through
724 a photochemical reaction by the addition of reactive side groups. The most common of these is gelatin
725 methacryloyl (GelMA), which is a gelatin derivative that contains mostly methacrylamide groups and
726 a few methacrylate groups [265]. Alternatives, such as gelatin-norbonene (GelNB) that undergoes thiol-
727 mediated crosslinking are increasingly common due to improved cytocompatibility in comparison to
728 GelMA [266], and both can be photopolymerised and 3D printed [267,268]. As a result, GelMA and GelNB are
729 widely used in wound healing and other tissue engineering applications [269–272]. In alveolar bone
730 regeneration, GelMA is preferred as an injectable biomaterial due to its ability to fill the defect site
731 [273].

732 Huang et al. fabricated a gelatin-based bilayer membrane using the cryogel technique, with a pure
733 gelatin PDL phase and a gelatin/ β-TCP/HA bone phase. Bioactive cues, enamel matrix derivatives and
734 bone morphogenetic protein-2 (BMP-2) were incorporated into the membrane with gelatin, providing
735 high cell affinity and sustained release of the biomolecules [165].

736 Wang et al. designed a bilayer scaffold using electrospinning and photo-crosslinking for GBR
737 applications made of GelMA and GelMA/poly (ethylene glycol) diacrylate (PEGDA) to be in contact
738 with soft and bone tissues, respectively. The incorporation of PEGDA into the composition improved
739 the mechanical properties of the scaffold significantly, suggesting this composite fibrous membrane
740 is a new promising and tunable material to be used in GBR applications [274].

741 ***2.3.2.4. Silk***

742 Silk is a natural protein-based polymer produced from the larvae of animals such as spider mites, flies,
743 and silkworms, and it is widely used in tissue engineering applications [275,276,277]. Silk fibres are mainly
744 composed of two proteins: sericin and fibroin. Silk fibroin is commonly used in tissue engineering due
745 to being biocompatible, biodegradable, bioabsorbable, having low immunogenicity, and controllable
746 mechanical properties [278–281]. Silk fibroin (SF) is used in periodontal treatment for buccal healing,
747 mineralised tissue formation, and implant treatment [282]. Silk sericin provides mechanical strength; in
748 nature sericin filaments ensure the integrity of the cocoon [283]. In bone regeneration applications, it
749 supports bone-like HA nucleation [284], which would typically occur on collagen.

750 Guo et al. designed a bilayer GTR membrane, with one layer consisting of SF cast over an
751 electrospunSF/PCL mat and the other composed of freeze-dried SF/nHA. Although silk fibroin is a
752 favourable material due to the aforementioned advantages, it has low mechanical strength.
753 Accordingly, casting SF into an SF/PCL electrospun mat improved the mechanical characteristics of the
754 scaffolds significantly, with HA addition (up to 30%) further enhancing the compressive strength and
755 modulus of the scaffolds [285]. Freeze-dried sericin was also used as a GBR material in combination with
756 collagen, with the sericin/collagen ratio influencing pore morphology where greater sericin presence
757 resulted in larger, more homogenous pores [22].

758 **2.3.3. Ceramics**

759 Bioceramics, such as CaP ceramics and bioactive calcium glasses, are inorganic biomaterials [286].
760 Calcium phosphate bioceramics are composed of TCP (α-TCP and β-TCP), HA, and a combination of
761 these as a biphasic calcium phosphate (BCP) [287]. Due to their bioactivity, hydrophilicity,
762 biocompatibility, availability, resemblance to inorganic components of natural bone,
763 osteoconductivity [60], and potential osteoinductivity [288], bioceramics are widely used for bone and
764 periodontal regeneration [216,191].

765 Even though bioceramics possess advantageous characteristics, they are highly brittle, and it is hard
766 to shape them because of their rigidity, limited flexibility, and poor mouldability [289]. Due to their weak
767 fracture toughness [290] and poor mechanical strength [291], their use in load-bearing applications is
768 limited. However, their combination with mechanically strong biomaterials, such as synthetic
769 polymers or metals, overcomes this by reducing brittleness, difficulty in shaping, and weak mechanical
770 strength [292].

771 As 60-70% of the bone inorganic matrix is composed of HA, it is the most studied CaP ceramic in bone
772 tissue engineering research. HA favourably promotes the proliferation and adhesion of osteoblasts [293].
773 Despite these advantages, crystalline HA takes a long time to break down *in vivo*, allowing the residual
774 particles to inhibit full bone formation and raise the risk of infection and exposure in the maxillofacial
775 and oral areas [294]. As a result, crystalline HA is replaced by amorphous HA, which exhibits a faster
776 degradation rate [295]. The degradation rate of HA may also be altered by combining it with other fast-
777 degrading biomaterials [296].

778 Kutikov et al. reported the fabrication of 3D printed, biodegradable, amphiphilic poly (D, L-lactic acid)-
779 poly (ethylene glycol)-poly (D, L-lactic acid) (PLA-PEG-PLA) (PELA) triblock co-polymer microporous
780 composite scaffolds both with HA (HA-PELA – bone phase) and without HA (PELA – soft tissue phase)
781 for use in GBR applications. Changes in hydrophilicity and mechanical properties of the materials were
782 dependent on the dry or wet state of the material, which may be beneficial for the self-fixation of the
783 scaffold during surgery. The degree of swelling and increase in the stiffness of the scaffolds were
784 measured as 55% and 44%, 1.38-fold and 4-fold, for HA-PELA and PELA scaffolds, respectively. HA
785 inclusion increased both hydrophilicity and the stiffness of the scaffolds, and the presence/absence of
786 HA in each phase resulted in differing responses of NIH-3T3 fibroblasts and mesenchymal
787 stem/stromal cells (MSCs), with HA-PELA supporting *in vitro* MSC osteogenic differentiation [297].

788 Shoba et al. designed a biphasic membrane based on freeze-dried collagen/sericin and bromelain-
789 conjugated, magnesium-doped HA nanoparticle incorporated electrospun PVA. In addition to *in vitro*
790 characterisation and *in vivo* testing in a Wistar rat model, they also conducted a CAM assay to
791 investigate the angiogenic potential of the scaffolds. They had four groups: (1) collagen/sericin layer,
792 (2) bromelain-conjugated magnesium-doped HA nanoparticle/PVA electrospun coated collagen
793 sericin, (3) positive control [20 ng/ml VEGF], and (4) negative control [200 µg/mL thalidomide]. The
794 number of blood vessels found was higher in group 2 compared to group 1, likely due to bromelain
795 released from magnesium-doped HA nanoparticles encouraging vascularisation [22].

796 β-TCP is another extensively researched CaP ceramic due to its capacity to produce a robust bond
797 between bone and CaP [216] and its rapid degradation rate [298]. Combining TCP and HA to produce BCP

[299] provides considerable benefits over alternative CaP ceramics in terms of stability, regulated bioactivity, and controllable degradation rate [300], with BCP having a faster degradation rate than HA but slower than β-TCP [301].

Vaquette et al. fabricated a biphasic scaffold where the bone phase was composed of FDM printed, β-TCP incorporated PCL, and the other layer was electrospun PCL combined with three layers of PDL cell sheets. The bone compartment promoted cell proliferation and ECM mineralization *in vitro*, whilst the electrospun layer enhanced the stability of the cell sheet layer. *In vivo* analysis where the scaffold was mounted to a dentin slice and inserted subcutaneously indicated that the integration of PDL cell sheets with a biphasic scaffold enables the supply of the cells required for the *in vivo* regeneration of periodontal tissues [206].

Bioactive glass (BG), which is calcium-substituted silicon oxide, is yet another biomaterial studied in bone tissue engineering [302,303]. As BG is exposed to body fluids, a coating of CaP develops on its surface that chemically integrates it into the bone [304]. BGs are also incorporated into natural and synthetic polymers to enhance their hydrophilicity, bioactivity, and regeneration potential of the hard tissues [208].

2.4. Post treatments

As cell attachment, proliferation, and differentiation on 3D constructs are crucial for tissue regeneration, it is important to understand the cell activity and response on the surface of the scaffold material in the process of developing effective bioactive 3D structures [41]. Surface topography, chemistry [305], microstructure [253,306], and mechanical properties [307] of 3D constructs are some of the critical characteristics that influence cellular behaviour. Adjusting these features for a specific tissue type can be quite challenging, and, in some cases, cell attachment and migration can be limited due to the properties or morphology of the biomaterials [308]. Post-treatments such as surface modification/functionalisation routes have been used widely to overcome such problems and enhance the characteristics of the 3D constructs and, consequently, the biological activity of the cells on designed scaffolds (Table 4) [308–310].

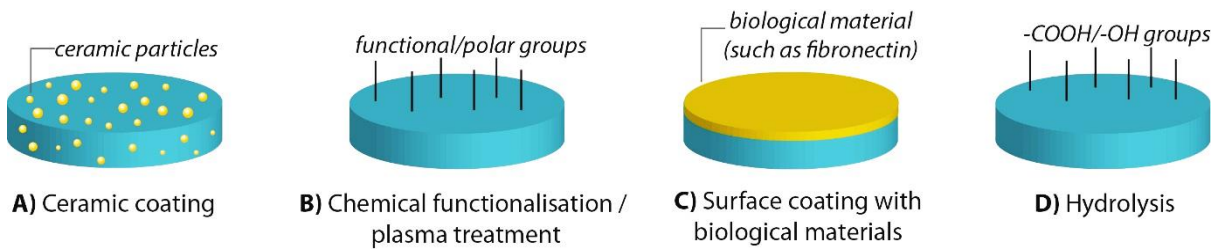

Figure 8: *(A-D) Commonly used surface functionalisation techniques/post-treatments to increase the scaffolds' hydrophilicity and/or biological activity.*

827 Post-treatments to enhance cell-material interaction include physical modification to create surface
828 topography (e.g., through surface alkali hydrolysis [311] or physical interpenetrating techniques [312]),
829 chemical modification to manipulate surface chemistry (e.g. plasma treatment [313] and photo-grafting
830 [314]) and biological modifications that tether biomolecules to the surface to harness their activity
831 (Figure 8) [315].

832 Although PCL is a widely used material in tissue engineering, cell attachment on native PCL-based
833 surfaces is challenging due to the hydrophobic nature of the material. Park et al. developed a PCL-
834 based scaffold that is oxygen plasma treated and then coated with graphene oxide (GO) to overcome
835 this. Water contact angle values were measured as 73.14°, 74.94°, 40.52° and 27.8° for PCL, PCL-
836 plasma, PCL-GO, and PCL-plasma-GO, respectively. *In vitro,* periodontal ligament stem cells (PDLSCs)
837 culture characterisation results showed that plasma treatment and GO coating increase cell
838 proliferation and osteogenic differentiation compared with the non-treated group [316].

839 Pilipchuk et al. developed 3D-printed and micropatterned PCL scaffolds for periodontal regeneration
840 and tested various surface modification techniques such as amination, hydrolysis, fibronectin coating,
841 and hydrolysis+fibronectin coating to improve their biological performance. Human PDL cells were
842 seeded on test groups, and cell seeding efficiency analysis showed that hydrolysis, fibronectin, and a
843 combination of them showed better cell adherence than both aminated and non-treated PCL (control)
844 [317].

845 Coating the scaffold with CaP is another surface modification method to support the integration of
846 the 3D constructs and enhance bone formation [191,210]. Costa et al. designed a bi-phasic scaffold
847 composed of FDM fabricated β-TCP incorporated medical-grade PCL and electrospun medical-grade
848 PCL. The bone compartment of the bi-phasic scaffold was coated with CaP to improve
849 osteoconductivity. *In vitro* osteoblast culture showed increased ALP activity and improved
850 mineralisation in comparison to non-coated controls [191].

851 ***Table 4:*** *Surface functionalisation routes used for multiphasic GBP membranes in the literature.*

Modification	Material (monomer/macromer)	*In vitro/ In vivo*	Result	Ref
Air plasma treatment	PCL	*in vitro*	- hydrophilicity ↑ - cell attachment ↑ - cell infiltration ↑	10
Air plasma treatment	PCL PCL/calcium carbonate	*in vitro*	- hydrophilicity ↑	104
Calcium phosphate (CaP) coating	PCL/β-TCP	*in vitro* *in vivo*	- osteoconductivity ↑ - ALP activity ↑ - deposition of mineralised ECM - mineralisation (micro-CT)↑	191
Calcium phosphate (CaP) coating	Chitosan/gelatin	*n/a*	- formation of osseointegrative interface	210

Chemical vapour deposition (CVD)	PLGA/PCL PCL	*in vitro* *in vivo*	- enables immobilisation of gene therapy vector	318
Silanol group functionalisation	Starch/PCL	*in vitro*	- cell metabolic activity ↑ - osteogenic differentiation↑	114
Oxygen plasma treatment & graphene oxide coating	PCL	*in vitro*	- hydrophilicity ↑ - cell proliferation ↑ - osteogenic differentiation↑	316
Hydrolysis	PCL	*in vitro*	- cell adhesion ↑	317
Fibronectin coating	PCL		- cell adhesion ↑	
Hydrolysis & fibronectin coating	PCL		- cell adhesion ↑	

2.5. Bioactive cue-releasing scaffolds

In drug delivery systems, the delivery of the therapeutic agents is targeted to a specific organ, tissue, or cell [319]. Drugs can be incorporated into the scaffolds by one of the following routes; - physical entrapment (blend loading), where the polymer solution and the drug are mixed pre-fabrication and then the scaffold is fabricated, - physical adsorption (soak loading), where the scaffold is soaked into the drug solution/suspension post-fabrication,- covalent immobilisation or drug-polymer conjugation, where the drugs can be immobilised/conjugated into specific groups on scaffold surface post-fabrication, and finally, - using microparticles, where the drug solution is loaded into microparticles, and these particles are incorporated into the scaffold [320,321,322].

The drug release profile from the scaffold depends on various parameters, such as the fabrication technique, the material type, degradation rate, drug loading route, and the morphology of the scaffold, alongside the drug type and concentration [323]. There are two different types of release in controlled drug released systems. In a sustained release, the drug spreads to the living tissue for a prolonged period of time, while in burst release, a high fraction of the drug is released in a short time [324]. Drug delivery systems that include (i) antimicrobial, (ii) anti-inflammatory drugs (Table 5), and (iii) growth factors (Table 6) are widely used in the systems in periodontal regeneration [325], and these drug-loaded multiphasic periodontal scaffolds will be reviewed herein.

Through an immunopathogenic mechanism, bacteria play a major role in the start and evolution of periodontitis, resulting in the creation of the periodontal pocket, connective tissue degradation, and alveolar bone loss [326]. Thus, antibacterial agents are widely used for long or short periods of time in damaged areas for periodontal infections [327]. Antimicrobial drug-loaded scaffolds could be utilised to avoid post-surgical infections and other disorders over a longer period than traditional administration methods [328] and would provide a healing environment that promotes regeneration by preventing the reoccurrence of bacterial infection [329]. The most used antibacterial drugs in polymer membranes include tetracycline hydrochloride, metronidazole (MET), and AMX [330,249]. Although the origin of periodontitis is bacterial, the resulting inflammation and excessive host immune response are key drivers of the disease progression, and these can be targeted independently of the pathogens [331].

880 Following scaffold implantation, inflammation may ensue if good and adequate care is not provided
881 [3,332,333]. To overcome this problem, anti-inflammatory steroids such as dexamethasone (DEX) and non-
882 steroidal anti-inflammatory drugs such as ibuprofen, diclofenac, and rolipram can be incorporated
883 into periodontal scaffolds [334–338].

884 Lian et al. reported the development of an anti-inflammatory and antimicrobial drug-incorporated
885 biphasic scaffold where one layer was composed of DEX-loaded mesoporous silica nanoparticle
886 incorporated (DEX@MSNs) PLGA/gelatine nanofibers and the other layer of the broad-spectrum
887 antibiotic doxycycline hyclate (DCH) loaded PLGA electrospun nanofibers. *In vitro* analysis showed
888 sustained release of DEX, with the total released from DEX@MSNs and DEX@MSNs/PLGA/Gel-PLGA
889 bi-layered membranes being 57.6% and 38.8% after 21 days, respectively. DCH initially underwent
890 burst release and then subsequent persistent release. Bacterial inhibition experiments showed that
891 DCH has an antimicrobial effect on both *E. coli* (gram-negative) and *S. aureus* (gram-positive). As well
892 as being an anti-inflammatory, DEX is also used to induce osteogenic differentiation of MSCs by acting
893 as a *Runx2* promoter [339]. Here, it was observed that DEX incorporation increased ALP activity and
894 calcium deposition and upregulated osteocalcin (OCN) expression of rat bone marrow stem cells
895 (BMSCs) *in vitro* [340].

896 Santos et al. developed a biphasic membrane loaded with curcumin as a natural anti-inflammatory
897 agent and tetracycline hydrochloride (TH) as a broad-spectrum antibiotic against periodontitis. One
898 phase was made of 3D printed zein/curcumin doped PLA, and the other layer was created using coaxial
899 electrospinning, where fibres were composed of PEO/curcumin/TH and zein/PCL/β-glycerolphosphate
900 (β-GP) at the core and sheath of the scaffolds, respectively (Figure 7E). They showed the
901 cytocompatibility of the scaffolds using human oral keratinocytes, demonstrating sustained release of
902 the active agents for up to 8 days. The antibacterial activity of the scaffolds was demonstrated against
903 the bacteria *Porphyromonas gingivalis* and *Treponema denticola,* common instigators of periodontitis
904 [189].

905 An important part of ensuring the regeneration of the periodontal structure is creating an
906 environment that supports the differentiation of progenitor cells. Growth factors [341–345], and cytokines
907 [346] are some of the molecules that facilitate periodontal regeneration (maxillary/mandibular bone,
908 salivary glands, dentin-pulp). These signalling molecules stimulate cells throughout development, and
909 controlling the delivery of those factors can promote cell proliferation, differentiation, and tissue
910 regeneration [347,328,348]. Platelet-derived growth factor (PDGF), insulin-like growth factor (IGF), FGF-2,
911 transforming growth factor beta (TGF-β) [207,349], bone morphogenetic proteins (BMPs), and vascular

912 endothelial growth factor (VEGF) [347] have been some of the most researched growth factors for
913 periodontal regeneration [350].

914 BMPs have a role predominantly in bone and cartilage development and are widely used in bone tissue
915 engineering applications due to osteoinductive properties. There are many members of the BMP
916 family, from BMP-2 to BMP-18 [351,352]. BMP-2 is one of the most widely used growth factors in bone
917 and periodontal tissue engineering [353,165,177] and provides bone formation [354] by differentiation and
918 migration of osteoblasts [347]. There are also clinical and pre-clinical studies showing the potential of
919 BMP-7 [178,318,355], BMP-12 [350] and BMP-6 [84] in periodontal regeneration.

920 Tevlek et al. fabricated a bilayer scaffold made of a β-TCP and poly(glycerol-sebacate) (PGS) phase,
921 and a ceramic phase was doped with BMP-2 and/or TGF-β1. MC3T3-E1 cells cultured on BMP-2 doped
922 scaffolds resulted in higher proliferation and exhibited a more osteoblastic phenotype than cells
923 cultured on TGF-β1 doped scaffolds. The use of both growth factors showed better performance in
924 terms of bone cell morphology and bone ECM production when compared to the use of BMP-2 or TGF-
925 β1 alone [353].

926 Lee et al. fabricated triphasic 3D-printed PCL/HA-based scaffolds with varying microchannel sizes,
927 where each phase was doped with different bioactive cues. Cementum, PDL, and alveolar bone
928 mimicking layers were enriched with recombinant human amelogenin, the protein that contributes to
929 the formation of mineralised dentin or cement structure [356], connective tissue growth factor, and
930 BMP-2, respectively. Agents were incorporated into PLGA microspheres and delivered to the
931 microchannels of the scaffold. Through this work, they proposed a system that enables the release of
932 multiple drugs from the same system to stimulate the differentiation of dental stem/progenitor cells
933 [177].

934 Whilst the efficiencies of the antimicrobial agents are tested using zone inhibition tests and diffusion
935 assays, as most of the incorporated growth factors are bone-related factors, their efficiency is
936 assessed by quantifying osteogenic differentiation markers, bone ECM deposition, and osteogenesis-
937 related gene expression in drug-releasing constructs. However, some of the studies incorporated
938 drugs as model agents to test the suitability of their system as a drug-releasing system, and they did
939 not test the performance and the efficiency of the final intended drug. More detailed analyses are
940 needed to test the performance of these systems as drug-releasing scaffolds.

941 ***Table 5:*** *Antimicrobial and anti-inflammatory drugs used in multiphasic constructs developed for periodontal tissue engineering.*

Category	Material	Fabrication route	Agent	Incorporation route	Results	Ref
Antimicrobial	PLA/gelatin	Electrospinning	Metronidazole (MET)	Mixing with polymer solution before fabrication	Experiment N/A to show the antimicrobial activity.	357
	Collagen	Coaxial electrospinning	Amoxicillin (AMX)	Mixing with polymer solution before fabrication	Experiment N/A to show the antimicrobial activity.	250
	PLGA	Electrospinning	Doxycycline Hyclate (DCH)	Mixing with polymer solution before fabrication	Antimicrobial activity was observed against both E. coli (gram-negative) and S. aureus (gram-positive) in the zone inhibition test.	340204
	PEO/curcumin	Coaxial electrospinning	Tetracycline hydrochloride (TH)	Mixing with polymer solution before fabrication	Antibacterial activity was observed in disc diffusion assay (against bacterial strains isolated from periodontal subgingival plaques of human patients suffering from chronic periodontitis).	189
	PLGA/HA	Solvent casting & solvent leaching	Lauric Acid	Mixing with polymer solution before fabrication	Experiment N/A to show the antimicrobial activity.	120
	Mg-doped HA/PVA	Electrospinning	Bromelain	Conjugation to Mg-doped HA and mixing with polymer solution before fabrication	Antibacterial activity was observed in the disc diffusion assay (against S. aureus).	22
	Collagen type I	Commercial scaffold (Collatape®)	Antimicrobial peptide (LL-37)	Absorbed into the scaffold	Experiment N/A to show the antimicrobial activity.	209
	PHB/β-TCP/vitamin D3	Electrospinning	Ciprofloxacin	Mixing with polymer solution before fabrication	Experiment N/A to show the antimicrobial activity.	358
Anti-inflammatory	PEO/TH and PLA/zein/curcumin	Coaxial electrospinning and 3D printing	Curcumin	Incorporation Into the Composition	Experiment N/A to show the anti-inflammatory activity.	189

942

943

944

945

946 ***Table 6:*** *Growth factors used in multiphasic constructs developed for periodontal tissue engineering.*

947

Material	Fabrication route	Agent	Incorporation route	Results	Ref
Type-1 Collagen	Freeze-drying	Concentrated growth factor (CGF)	Mixing with polymer solution before fabrication	Transforming growth factor-beta 1 (TGF-β1) and vascular endothelial growth factor (VEGF) release from CGF-incorporated scaffolds. Expression of genes responsible for osteogenesis and angiogenesis.	207
PGS/β-TCP	Casting and crosslinking	BMP-2 and TGF-β1	Delivery of the drug solution on the ceramic surface and drying	Closer osteoblast morphology and more bone extracellular matrix deposition compared to the control.	353
PCL/HA	3D printing	Connective tissue growth factor (CTGF)	Encapsulated in PLGA microspheres	Provided a stimulus for periodontal ligament formation.	177
PCL/HA	3D printing	BMP-2	Encapsulated in PLGA microspheres	Enabled the differentiation of dental pulp stem/progenitor cells (DPSCs) and supported the formation of mineralized tissue.	177
PCL/HA	3D printing	Recombinant human amelogenin	Encapsulated in PLGA microspheres	Supported the formation of mineralized tissue by stimulation of DPSCs.	177
Gelatin and	Freeze-drying	BMP-2	Infused into the scaffold	Promotion of osteogenesis *in vivo.*	165
PCL/collagen	Electrospinning	BMP-7	Mixing with polymer solution before fabrication	Enhanced osteogenic differentiation.	223
PCL/HA	Selective laser sintering	Recombinant Human Platelet-Derived Growth Factor BB (rhPDGF-BB)	Immersion in rhPDGF-BB solution for 15 minutes	Control scaffold group without rhPDGF-BB n/a.	359
Chitin/PLGA/nano bioactive glass-ceramic	Freeze-drying	Recombinant human cementum protein 1 (rhCEMP1)	Loading after scaffold fabrication and lyophilisation	Provided cementogenic differentiation.	208
Chitin/PLGA	Freeze-drying	Recombinant human fibroblast growth factor 2 (rhFGF2)	Loading after scaffold fabrication and lyophilisation	Provided fibrogenic differentiation/fibrogenesis.	208
Chitin/PLGA/nBGC	Freeze-drying	Platelet-rich Plasma (PRP)	Loading after scaffold fabrication and lyophilisation	Provided osteogenic differentiation.	208
CaP coated chitosan	Solvent casting-particulate leaching	BMP-6	BMP-6 solution was pipetted onto the scaffold	Enhanced the formation of ECM of MC3T3-E1 cells.	84
PCL	Fused deposition modelling and melt electrospinning	BMP-2	Encapsulated into three thiolated hyaluronic acid-heparin, thiolated gelatine and polyethyleneglycol diacrylate hydrogel and injected into the biphasic scaffold	Increase in the expression of osteogenesis-related genes.	360
PCL	Fused deposition modelling and melt electrospinning	BMP-2	Encapsulated into heparinized hyaluronic acid/gelatin hydrogel and injected into the biphasic scaffold	Enhanced bone regeneration *in vivo*.	110

3. Conclusions

Interface tissue engineering concentrates on regenerating the anatomical interface between different types of tissues and has the potential to develop integrated scaffolds that will accelerate the adoption of tissue-engineered technologies in clinical settings. Multi-layer scaffolds are promising constructs for this application that better mimic interface tissue due to the individually tuneable layers. These types of scaffolds can have different characteristics in each layer, with modulation of mechanical properties, material type, porosity, pore size, morphological properties, degradation properties, and drug-releasing profiles possible. However, it is imperative that good integration between layers is achieved to avoid delamination during and post-implantation.

In this review, we discussed the major actors in the design of multiphasic constructs: biomaterials, the types of fabrication methods, the use of drugs/growth factors, and post-treatment processes, summarising the current status of multiphasic constructs for dental interface tissue. Most of the studies discussed in this review concluded that according to material characterisation and the *in vitro*/*in vivo* results, multilayer designs not only more closely mimic the native periodontal interface, but they also provide better and faster regeneration of both hard and soft tissues. Following more detailed characterisations of the developed membranes in comparison with the commercial counterparts, more in-depth *in vivo* tests are needed to have a better understanding of cell differentiation, *in vivo* degradation, new tissue formation, and vascularisation for the clinical translation of these designs.

4. Acknowledgements

Authors acknowledge the Department of Scientific Research Projects of Izmir Institute of Technology (IZTECH-BAP, 2021-IYTE-1-0110 and 2022-IYTE-2-0025); Health Institutes of Turkey (TUSEB-2022B02-22517). The authors thank Zeynep Güner for her contributions to the writing process at BaldemirLab Summer Writing Club 22'. RO acknowledges funding from the Engineering and Physical Sciences Research Council (EPSRC) programme grant 'Dialling up performance for on demand manufacturing' (EP/W017032/1) and would like to thank the University of Nottingham for his Nottingham Research Fellowship.

5. Author Contribution

All the authors contributed to preparing this manuscript regarding literature review and writing-up. BAD contributed to the conceptualisation and design of the study, writing specific sections of the manuscript and supervising the team. BAD, SD, and RO contributed to revising the manuscript critically

for important intellectual content. All authors read and have given final approval of the final manuscript.

6. Competing interests

The authors declare that they have no competing interests.

7. References

(1) WHO. *https://www.who.int/news-room/fact-sheets/detail/oral-health*.

(2) Chen, M. X.; Zhong, Y. J.; Dong, Q. Q.; Wong, H. M.; Wen, Y. F. Global, Regional, and National Burden of Severe Periodontitis, 1990–2019: An Analysis of the Global Burden of Disease Study 2019. *J Clin Periodontol* **2021**, *48* (9). https://doi.org/10.1111/jcpe.13506.

(3) Liang, Y.; Luan, X.; Liu, X. Recent Advances in Periodontal Regeneration: A Biomaterial Perspective. *Bioact Mater* **2020**, *5* (2), 297–308. https://doi.org/10.1016/j.bioactmat.2020.02.012.

(4) Iranmanesh, P.; Ehsani, A.; Khademi, A.; Asefnejad, A.; Shahriari, S.; Soleimani, M.; Ghadiri Nejad, M.; Saber-Samandari, S.; Khandan, A. Application of 3D Bioprinters for Dental Pulp Regeneration and Tissue Engineering (Porous Architecture). *Transp Porous Media* **2022**, *142* (1–2). https://doi.org/10.1007/s11242-021-01618-x.

(5) Zhang, B.; Zhang, X. J.; Bao, C. Y.; Wang, Q.; Yao, J. F.; Fan, H. S.; Xiong, C. D.; Zhang, X. D. Repairing Periodontal Bone Defect with In Vivo Tissue Engineering Bone. *Key Eng Mater* **2007**, *330–332*, 1121–1124. https://doi.org/10.4028/www.scientific.net/KEM.330-332.1121.

(6) Park, J. K.; Yeom, J.; Oh, E. J.; Reddy, M.; Kim, J. Y.; Cho, D.-W.; Lim, H. P.; Kim, N. S.; Park, S. W.; Shin, H.-I.; Yang, D. J.; Park, K. B.; Hahn, S. K. Guided Bone Regeneration by Poly(Lactic-Co-Glycolic Acid) Grafted Hyaluronic Acid Bi-Layer Films for Periodontal Barrier Applications. *Acta Biomater* **2009**, *5* (9), 3394–3403. https://doi.org/10.1016/j.actbio.2009.05.019.

(7) Kim, O.; Choi, J.; Kim, B.; Seo, D. Long-term Success Rates of Implants with Guided Bone Regeneration or Bone Grafting. *Clin Oral Implants Res* **2020**, *31* (S20), 230–230. https://doi.org/10.1111/clr.171_13644.

(8) Hong, J.-Y.; Shin, E.-Y.; Herr, Y.; Chung, J.-H.; Lim, H.-C.; Shin, S.-I. Implant Survival and Risk Factor Analysis in Regenerated Bone: Results from a 5-Year Retrospective Study. *J Periodontal Implant Sci* **2020**, *50* (6). https://doi.org/10.5051/jpis.2002140107.

(9) Jung, R. E.; Fenner, N.; Hämmerle, C. H. F.; Zitzmann, N. U. Long-Term Outcome of Implants Placed with Guided Bone Regeneration (GBR) Using Resorbable and Non-Resorbable Membranes after 12-14 Years. *Clin Oral Implants Res* **2013**, *24* (10). https://doi.org/10.1111/j.1600-0501.2012.02522.x.

(10) Aldemir Dikici, B.; Dikici, S.; Reilly, G. C.; MacNeil, S.; Claeyssens, F. A Novel Bilayer Polycaprolactone Membrane for Guided Bone Regeneration: Combining Electrospinning and Emulsion Templating. *Materials* **2019**, *12* (16), 2643. https://doi.org/10.3390/ma12162643.

1015 (11) Wang, J.; Wang, L.; Zhou, Z.; Lai, H.; Xu, P.; Liao, L.; Wei, J. Biodegradable Polymer
1016 Membranes Applied in Guided Bone/Tissue Regeneration: A Review. *Polymers*. MDPI AG
1017 2016. https://doi.org/10.3390/polym8040115.

1018 (12) Gentile, P.; Chiono, V.; Tonda-Turo, C.; Ferreira, A. M.; Ciardelli, G. Polymeric Membranes for
1019 Guided Bone Regeneration. *Biotechnol J* **2011**, *6* (10), 1187–1197.
1020 https://doi.org/10.1002/BIOT.201100294.

1021 (13) Parrish, L. C.; Miyamoto, T.; Fong, N.; Mattson, J. S.; Cerutis, D. R. Non-Bioabsorbable vs.
1022 Bioabsorbable Membrane: Assessment of Their Clinical Efficacy in Guided Tissue
1023 Regeneration Technique. A Systematic Review. *J Oral Sci* **2009**, *51* (3), 383–400.
1024 https://doi.org/10.2334/JOSNUSD.51.383.

1025 (14) Chattopadhyay, S.; Raines, R. T. Review Collagen-Based Biomaterials for Wound Healing.
1026 *Biopolymers* **2014**, *101* (8), 821–833. https://doi.org/10.1002/BIP.22486.

1027 (15) Veríssimo, D. M.; Leitão, R. F. C.; Ribeiro, R. A.; Figueiró, S. D.; Sombra, A. S. B.; Góes, J. C.;
1028 Brito, G. A. C. Polyanionic Collagen Membranes for Guided Tissue Regeneration: Effect of
1029 Progressive Glutaraldehyde Cross-Linking on Biocompatibility and Degradation. *Acta*
1030 *Biomater* **2010**, *6* (10), 4011–4018. https://doi.org/10.1016/J.ACTBIO.2010.04.012.

1031 (16) Rothamel, D.; Schwarz, F.; Sager, M.; Herten, M.; Sculean, A.; Becker, J. Biodegradation of
1032 Differently Cross-Linked Collagen Membranes: An Experimental Study in the Rat. *Clin Oral*
1033 *Implants Res* **2005**, *16* (3), 369–378. https://doi.org/10.1111/J.1600-0501.2005.01108.X.

1034 (17) Donos, N.; Kostopoulos, L.; Karring, T. Alveolar Ridge Augmentation Using a Resorbable
1035 Copolymer Membrane and Autogenous Bone Grafts. *Clin Oral Implants Res* **2002**, *13* (2), 203–
1036 213. https://doi.org/10.1034/j.1600-0501.2002.130211.x.

1037 (18) Coonts, B. A.; Whitman, S. L.; O'Donnell, M.; Polson, A. M.; Bogle, G.; Garrett, S.; Swanbom,
1038 D. D.; Fulfs, J. C.; Rodgers, P. W.; Southard, G. L.; Dunn, R. L. Biodegradation and
1039 Biocompatibility of a Guided Tissue Regeneration Barrier Membrane Formed from a Liquid
1040 Polymer Material. *J Biomed Mater Res* **1998**, *42* (2), 303–311.
1041 https://doi.org/10.1002/(SICI)1097-4636(199811)42:2<303::AID-JBM16>3.0.CO;2-J.

1042 (19) Hou, L.-T.; Yan, J.-J.; Tsai, A. Yi.-M.; Lao, Chia.-S.; Lin, Shih.-J.; Liu, C.-M. Polymer-Assisted
1043 Regeneration Therapy with AtrisorbR Barriers in Human Periodontal Intrabony Defects. *J Clin*
1044 *Periodontol* **2004**, *31* (1), 68–74. https://doi.org/10.1111/j.0303-6979.2004.00436.x.

1045 (20) Zhuang, Y.; Lin, K.; Yu, H. Advance of Nano-Composite Electrospun Fibers in Periodontal
1046 Regeneration. *Frontiers in Chemistry*. Frontiers Media S.A. July 10, 2019.
1047 https://doi.org/10.3389/fchem.2019.00495.

1048 (21) Wang, C. Y.; Chiu, Y. C.; Lee, A. K. X.; Lin, Y. A.; Lin, P. Y.; Shie, M. Y. Biofabrication of Gingival
1049 Fibroblast Cell-Laden Collagen/Strontium-Doped Calcium Silicate 3D-Printed Bi-Layered
1050 Scaffold for Osteoporotic Periodontal Regeneration. *Biomedicines* **2021**, *9* (4).
1051 https://doi.org/10.3390/BIOMEDICINES9040431.

1052 (22) Shoba, E.; Lakra, R.; Kiran, M. S.; Korrapati, P. S. 3 D Nano Bilayered Spatially and Functionally
1053 Graded Scaffold Impregnated Bromelain Conjugated Magnesium Doped Hydroxyapatite
1054 Nanoparticle for Periodontal Regeneration. *J Mech Behav Biomed Mater* **2020**, *109*, 103822.
1055 https://doi.org/10.1016/j.jmbbm.2020.103822.

1056 (23) Qasim, S. B.; Delaine-Smith, R. M.; Fey, T.; Rawlinson, A.; Rehman, I. U. Freeze Gelated Porous
1057 Membranes for Periodontal Tissue Regeneration. *Acta Biomater* **2015**, *23*, 317–328.
1058 https://doi.org/10.1016/J.ACTBIO.2015.05.001.

1059 (24) Zareidoost, A.; Yousefpour, M.; Ghasemi, B.; Amanzadeh, A. The Relationship of Surface
1060 Roughness and Cell Response of Chemical Surface Modification of Titanium. *J Mater Sci*
1061 *Mater Med* **2012**, *23* (6). https://doi.org/10.1007/s10856-012-4611-9.

1062 (25) Zan, Q.; Wang, C.; Dong, L.; Cheng, P.; Tian, J. Effect of Surface Roughness of Chitosan-Based
1063 Microspheres on Cell Adhesion. *Appl Surf Sci* **2008**, *255* (2).
1064 https://doi.org/10.1016/j.apsusc.2008.06.074.

1065 (26) Tudureanu, R.; Handrea-Dragan, I. M.; Boca, S.; Botiz, I. Insight and Recent Advances into the
1066 Role of Topography on the Cell Differentiation and Proliferation on Biopolymeric Surfaces.
1067 *International Journal of Molecular Sciences*. 2022. https://doi.org/10.3390/ijms23147731.

1068 (27) Cai, S.; Wu, C.; Yang, W.; Liang, W.; Yu, H.; Liu, L. Recent Advance in Surface Modification for
1069 Regulating Cell Adhesion and Behaviors. *Nanotechnol Rev* **2020**, *9* (1).
1070 https://doi.org/10.1515/ntrev-2020-0076.

1071 (28) Gong, M.; Chi, C.; Ye, J.; Liao, M.; Xie, W.; Wu, C.; Shi, R.; Zhang, L. Icariin-Loaded Electrospun
1072 PCL/Gelatin Nanofiber Membrane as Potential Artificial Periosteum. *Colloids Surf B*
1073 *Biointerfaces* **2018**, *170*, 201–209. https://doi.org/10.1016/J.COLSURFB.2018.06.012.

1074 (29) Lam, C. X. F.; Hutmacher, D. W.; Schantz, J. T.; Woodruff, M. A.; Teoh, S. H. Evaluation of
1075 Polycaprolactone Scaffold Degradation for 6 Months in Vitro and in Vivo. *J Biomed Mater Res*
1076 *A* **2009**, *90* (3), 906–919. https://doi.org/10.1002/JBM.A.32052.

1077 (30) Savina, I. N.; Cnudde, V.; D'Hollander, S.; van Hoorebeke, L.; Mattiasson, B.; Galaev, I. Y.; du
1078 Prez, F. Cryogels from Poly(2-Hydroxyethyl Methacrylate): Macroporous, Interconnected
1079 Materials with Potential as Cell Scaffolds. *Soft Matter* **2007**, *3* (9), 1176–1184.
1080 https://doi.org/10.1039/B706654F.

1081 (31) Li, Z.; Lv, X.; Chen, S.; Wang, B.; Feng, C.; Xu, Y.; Wang, H. Improved Cell Infiltration and
1082 Vascularization of Three-Dimensional Bacterial Cellulose Nanofibrous Scaffolds by Template
1083 Biosynthesis. *RSC Adv* **2016**, *6* (48), 42229–42239. https://doi.org/10.1039/C6RA07685H.

1084 (32) Tran, P. A. Blood Clots and Tissue Regeneration of 3D Printed Dual Scale Porous Polymeric
1085 Scaffolds. *Mater Lett* **2021**, *285*, 129184. https://doi.org/10.1016/J.MATLET.2020.129184.

1086 (33) Leon Leon U, C. A. *New Perspectives in Mercury Porosimetry*; 1998.

1087 (34) Karageorgiou, V.; Kaplan, D. Porosity of 3D Biomaterial Scaffolds and Osteogenesis.
1088 *Biomaterials*. Elsevier BV 2005, pp 5474–5491.
1089 https://doi.org/10.1016/j.biomaterials.2005.02.002.

1090 (35) Ebrahimi, M. Porosity Parameters in Biomaterial Science: Definition, Impact, and Challenges
1091 in Tissue Engineering. *Frontiers of Materials Science*. Higher Education Press Limited
1092 Company September 1, 2021, pp 352–373. https://doi.org/10.1007/s11706-021-0558-4.

1093 (36) Loh, Q. L.; Choong, C. Three-Dimensional Scaffolds for Tissue Engineering Applications: Role
1094 of Porosity and Pore Size. *Tissue Engineering - Part B: Reviews*. December 1, 2013, pp 485–
1095 502. https://doi.org/10.1089/ten.teb.2012.0437.

1096 (37) Hollister, S. J. Porous Scaffold Design for Tissue Engineering. *Nat Mater* **2005**, *4* (7), 518–524.
1097 https://doi.org/10.1038/NMAT1421.

1098 (38) Pérez, R. A.; Won, J. E.; Knowles, J. C.; Kim, H. W. Naturally and Synthetic Smart Composite
1099 Biomaterials for Tissue Regeneration. *Advanced Drug Delivery Reviews*. April 2013, pp 471–
1100 496. https://doi.org/10.1016/j.addr.2012.03.009.

1101 (39) Yadav, P.; Beniwal, G.; Saxena, K. K. A Review on Pore and Porosity in Tissue Engineering. In
1102 *Materials Today: Proceedings*; Elsevier Ltd, 2021; Vol. 44, pp 2623–2628.
1103 https://doi.org/10.1016/j.matpr.2020.12.661.

1104 (40) Mandal, B. B.; Kundu, S. C. Cell Proliferation and Migration in Silk Fibroin 3D Scaffolds.
1105 *Biomaterials* **2009**, *30* (15), 2956–2965. https://doi.org/10.1016/j.biomaterials.2009.02.006.

1106 (41) Harley, B. A. C.; Kim, H.-D.; Zaman, M. H.; Yannas, I. V; Lauffenburger, D. A.; Gibson, L. J.
1107 Microarchitecture of Three-Dimensional Scaffolds Influences Cell Migration Behavior via
1108 Junction Interactions. *Biophys J* **2008**, *95* (8), 4013–4024.
1109 https://doi.org/10.1529/biophysj.107.122598.

1110 (42) Matsiko, A.; Gleeson, J. P.; O'Brien, F. J. Scaffold Mean Pore Size Influences Mesenchymal
1111 Stem Cell Chondrogenic Differentiation and Matrix Deposition. *Tissue Eng Part A* **2015**, *21* (3–
1112 4). https://doi.org/10.1089/ten.tea.2013.0545.

1113 (43) Han, Y.; Lian, M.; Wu, Q.; Qiao, Z.; Sun, B.; Dai, K. Effect of Pore Size on Cell Behavior Using
1114 Melt Electrowritten Scaffolds. *Front Bioeng Biotechnol* **2021**, *9*.
1115 https://doi.org/10.3389/fbioe.2021.629270.

1116 (44) Oh, S. H.; Kim, T. H.; Im, G. Il; Lee, J. H. Investigation of Pore Size Effect on Chondrogenic
1117 Differentiation of Adipose Stem Cells Using a Pore Size Gradient Scaffold. *Biomacromolecules*
1118 **2010**, *11* (8). https://doi.org/10.1021/bm100199m.

1119 (45) Liu, X.; Ma, P. X. *Polymeric Scaffolds for Bone Tissue Engineering*; 2004; Vol. 32.

1120 (46) Lee, J. S.; Cha, H. do; Shim, J. H.; Jung, J. W.; Kim, J. Y.; Cho, D. W. Effect of Pore Architecture
1121 and Stacking Direction on Mechanical Properties of Solid Freeform Fabrication-Based Scaffold
1122 for Bone Tissue Engineering. *J Biomed Mater Res A* **2012**, *100 A* (7), 1846–1853.
1123 https://doi.org/10.1002/jbm.a.34149.

1124 (47) Werner, M.; Blanquer, S. B. G.; Haimi, S. P.; Korus, G.; Dunlop, J. W. C.; Duda, G. N.; Grijpma,
1125 D. W.; Petersen, A. Surface Curvature Differentially Regulates Stem Cell Migration and
1126 Differentiation via Altered Attachment Morphology and Nuclear Deformation. *Advanced*
1127 *Science* **2017**, *4* (2). https://doi.org/10.1002/advs.201600347.

1128 (48) Salerno, A.; di Maio, E.; Iannace, S.; Netti, P. A. Tailoring the Pore Structure of PCL Scaffolds
1129 for Tissue Engineering Prepared via Gas Foaming of Multi-Phase Blends. *Journal of Porous*
1130 *Materials* **2012**, *2* (19), 181–188. https://doi.org/10.1007/S10934-011-9458-9.

1131 (49) Causa, F.; Netti, P. A.; Ambrosio, L. A Multi-Functional Scaffold for Tissue Regeneration: The
1132 Need to Engineer a Tissue Analogue. *Biomaterials* **2007**, *28* (34), 5093–5099.
1133 https://doi.org/10.1016/J.BIOMATERIALS.2007.07.030.

1134 (50) Murphy, C. M.; O'Brien, F. J. Understanding the Effect of Mean Pore Size on Cell Activity in
1135 Collagen-Glycosaminoglycan Scaffolds. *Cell Adhesion and Migration*. Taylor and Francis Inc.
1136 2010, pp 377–381. https://doi.org/10.4161/cam.4.3.11747.

(51) Murphy, C. M.; Haugh, M. G.; O'Brien, F. J. The Effect of Mean Pore Size on Cell Attachment, Proliferation and Migration in Collagen-Glycosaminoglycan Scaffolds for Bone Tissue Engineering. *Biomaterials* **2010**, *31* (3), 461–466. https://doi.org/10.1016/j.biomaterials.2009.09.063.

(52) Yannas, I. v. *Tissu Egeneration by Use of Glycosaminoglycan Copolymer*; 1992; Vol. 9.

(53) Oliviero, O.; Ventre, M.; Netti, P. A. Functional Porous Hydrogels to Study Angiogenesis under the Effect of Controlled Release of Vascular Endothelial Growth Factor. *Acta Biomater* **2012**, *8* (9), 3294–3301. https://doi.org/10.1016/j.actbio.2012.05.019.

(54) Artel, A.; Mehdizadeh, H.; Chiu, Y. C.; Brey, E. M.; Cinar, A. An Agent-Based Model for the Investigation of Neovascularization within Porous Scaffolds. *Tissue Eng Part A* **2011**, *17* (17–18), 2133–2141. https://doi.org/10.1089/ten.tea.2010.0571.

(55) Kuboki, Y.; Jin, Q.; Takita, H. Geometry of Carriers Controlling Phenotypic Expression in BMP-Induced Osteogenesis and Chondrogenesis. *The Journal of Bone and Joint Surgery-American Volume* **2001**, *83*, S1-105-S1-115. https://doi.org/10.2106/00004623-200100002-00005.

(56) Vaquette, C.; Saifzadeh, S.; Farag, A.; Hutmacher, D. W.; Ivanovski, S. Periodontal Tissue Engineering with a Multiphasic Construct and Cell Sheets. *J Dent Res* **2019**, *98* (6), 673–681. https://doi.org/10.1177/0022034519837967.

(57) Zhang, L.; Dong, Y.; Zhang, N.; Shi, J.; Zhang, X.; Qi, C.; Midgley, A. C.; Wang, S. Potentials of Sandwich-like Chitosan/Polycaprolactone/Gelatin Scaffolds for Guided Tissue Regeneration Membrane. *Materials Science and Engineering C* **2020**, *109*. https://doi.org/10.1016/j.msec.2019.110618.

(58) Hollister, S. J.; Maddox, R. D.; Taboas, J. M. Optimal Design and Fabrication of Scaffolds to Mimic Tissue Properties and Satisfy Biological Constraints. *Biomaterials* **2002**, *23* (20), 4095–4103. https://doi.org/10.1016/S0142-9612(02)00148-5.

(59) Dutta, S.; Gupta, S.; Roy, M. Recent Developments in Magnesium Metal-Matrix Composites for Biomedical Applications: A Review. *ACS Biomaterials Science and Engineering*. 2020. https://doi.org/10.1021/acsbiomaterials.0c00678.

(60) Woodard, J. R.; Hilldore, A. J.; Lan, S. K.; Park, C. J.; Morgan, A. W.; Eurell, J. A. C.; Clark, S. G.; Wheeler, M. B.; Jamison, R. D.; Wagoner Johnson, A. J. The Mechanical Properties and Osteoconductivity of Hydroxyapatite Bone Scaffolds with Multi-Scale Porosity. *Biomaterials* **2007**, *28* (1), 45–54. https://doi.org/10.1016/j.biomaterials.2006.08.021.

(61) Aykul, H.; Toparli, M. A Comparison of the Stress Analysis of an Unrestored and Restored Tooth with Amalgam and Composite Resin. *Mathematical and Computational Applications* **2005**. https://doi.org/10.3390/mca10010089.

(62) Choi, J. J. E.; Zwirner, J.; Ramani, R. S.; Ma, S.; Hussaini, H. M.; Waddell, J. N.; Hammer, N. Mechanical Properties of Human Oral Mucosa Tissues Are Site Dependent: A Combined Biomechanical, Histological and Ultrastructural Approach. *Clin Exp Dent Res* **2020**. https://doi.org/10.1002/cre2.305.

(63) FARAH, J. W.; CRAIG, R. G.; MEROUEH, K. A. Finite Element Analysis of Three- and Four-unit Bridges. *J Oral Rehabil* **1989**. https://doi.org/10.1111/j.1365-2842.1989.tb01384.x.

(64) Matos, F. de S.; Cunha, T. C.; Correia, A. M. de O.; Tribst, J. P. M.; Caneppele, T. M. F.; Borges, A. L. S. Impact of Different Restorative Techniques on the Stress Distribution of Endodontically-Treated Maxillary First Premolars: A 2-Dimensional Finite Element Analysis. *JOURNAL OF RESEARCH AND KNOWLEDGE SPREADING* **2020**, *1* (1). https://doi.org/10.20952/jrks1111761.

(65) Aravamudhan, A.; Ramos, D. M.; Nip, J.; Harmon, M. D.; James, R.; Deng, M.; Laurencin, C. T.; Yu, X.; Kumbar, S. G. Cellulose and Collagen Derived Micro-Nano Structured Scaffolds for Bone Tissue Engineering. *J Biomed Nanotechnol* **2013**, *9* (4), 719–731. https://doi.org/10.1166/jbn.2013.1574.

(66) Ashworth, J. C.; Mehr, M.; Buxton, P. G.; Best, S. M.; Cameron, R. E. Optimising Collagen Scaffold Architecture for Enhanced Periodontal Ligament Fibroblast Migration. *J Mater Sci Mater Med* **2018**. https://doi.org/10.1007/s10856-018-6175-9.

(67) Zhang, Y.; Cheng, X.; Wang, J.; Wang, Y.; Shi, B.; Huang, C.; Yang, X.; Liu, T. Novel Chitosan/Collagen Scaffold Containing Transforming Growth Factor-B1 DNA for Periodontal Tissue Engineering. *Biochem Biophys Res Commun* **2006**, *344* (1), 362–369. https://doi.org/10.1016/J.BBRC.2006.03.106.

(68) Peng, L.; Xiang, R. C.; Jia, W. W.; Dong, X. X.; Wang, G. E. Preparation and Evaluation of Porous Chitosan/Collagen Scaffolds for Periodontal Tissue Engineering. *http://dx.doi.org/10.1177/0883911506065100* **2016**, *21* (3), 207–220. https://doi.org/10.1177/0883911506065100.

(69) Kikuchi, M.; Koyama, Y.; Yamada, T.; Imamura, Y.; Okada, T.; Shirahama, N.; Akita, K.; Takakuda, K.; Tanaka, J. Development of Guided Bone Regeneration Membrane Composed of β-Tricalcium Phosphate and Poly (l-Lactide-Co-Glycolide-Co-ε-Caprolactone) Composites. *Biomaterials* **2004**, *25* (28), 5979–5986. https://doi.org/10.1016/J.BIOMATERIALS.2004.02.001.

(70) Ibekwe, C. A.; Oyatogun, G. M.; Esan, T. A.; Oluwasegun, K. M. Synthesis and Characterization of Chitosan/Gum Arabic Nanoparticles for Bone Regeneration. *American Journal of Materials Science and Engineering, Vol. 5, 2017, Pages 28-36* **2017**, *5* (1), 28–36. https://doi.org/10.12691/AJMSE-5-1-4.

(71) Výborný, K.; Vallová, J.; Kočí, Z.; Kekulová, K.; Jiráková, K.; Jendelová, P.; Hodan, J.; Kubinová, Š. Genipin and EDC Crosslinking of Extracellular Matrix Hydrogel Derived from Human Umbilical Cord for Neural Tissue Repair. *Sci Rep* **2019**, *9* (1), 10674. https://doi.org/10.1038/s41598-019-47059-x.

(72) Varoni, E. M.; Vijayakumar, S.; Canciani, E.; Cochis, A.; De Nardo, L.; Lodi, G.; Rimondini, L.; Cerruti, M. Chitosan-Based Trilayer Scaffold for Multitissue Periodontal Regeneration. *J Dent Res* **2018**, *97* (3), 303–311. https://doi.org/10.1177/0022034517736255.

(73) Tai, H.-Y.; Fu, E.; Cheng, L.-P.; Don, T.-M. Fabrication of Asymmetric Membranes from Polyhydroxybutyrate and Biphasic Calcium Phosphate/Chitosan for Guided Bone Regeneration. *Journal of Polymer Research* **2014**, *21* (5), 421. https://doi.org/10.1007/s10965-014-0421-8.

(74) Batool, F.; Morand, D. N.; Thomas, L.; Bugueno, I. M.; Aragon, J.; Irusta, S.; Keller, L.; Benkirane-Jessel, N.; Tenenbaum, H.; Huck, O. Synthesis of a Novel Electrospun

Polycaprolactone Scaffold Functionalized with Ibuprofen for Periodontal Regeneration: An In Vitro AndIn Vivo Study. *Materials 2018, Vol. 11, Page 580* **2018**, *11* (4), 580. https://doi.org/10.3390/MA11040580.

(75) Münchow, E. A.; Albuquerque, M. T. P.; Zero, B.; Kamocki, K.; Piva, E.; Gregory, R. L.; Bottino, M. C. Development and Characterization of Novel ZnO-Loaded Electrospun Membranes for Periodontal Regeneration. *Dental Materials* **2015**, *31* (9), 1038–1051. https://doi.org/10.1016/J.DENTAL.2015.06.004.

(76) Duailibi, M. T.; Duailibi, S. E.; Young, C. S.; Bartlett, J. D.; Vacanti, J. P.; Yelick, P. C. Bioengineered Teeth from Cultured Rat Tooth Bud Cells. *J Dent Res* **2004**, *83* (7), 523–528. https://doi.org/10.1177/154405910408300703/ASSET/IMAGES/LARGE/10.1177_154405910408300703-FIG2.JPEG.

(77) Tatullo, M.; Spagnuolo, G.; Codispoti, B.; Zamparini, F.; Zhang, A.; Esposti, M. D.; Aparicio, C.; Rengo, C.; Nuzzolese, M.; Manzoli, L.; Fava, F.; Prati, C.; Fabbri, P.; Gandolfi, M. G. PLA-Based Mineral-Doped Scaffolds Seeded with Human Periapical Cyst-Derived MSCs: A Promising Tool for Regenerative Healing in Dentistry. *Materials 2019, Vol. 12, Page 597* **2019**, *12* (4), 597. https://doi.org/10.3390/MA12040597.

(78) Yoshimoto, I.; Sasaki, J.-I.; Tsuboi, R.; Yamaguchi, S.; Kitagawa, H.; Imazato, S. Development of Layered PLGA Membranes for Periodontal Tissue Regeneration. *Dental Materials* **2018**, *34* (3), 538–550. https://doi.org/10.1016/j.dental.2017.12.011.

(79) Puppi, D.; Migone, C.; Grassi, L.; Pirosa, A.; Maisetta, G.; Batoni, G.; Chiellini, F. Integrated Three-Dimensional Fiber/Hydrogel Biphasic Scaffolds for Periodontal Bone Tissue Engineering. *Polym Int* **2016**, *65* (6), 631–640. https://doi.org/10.1002/pi.5101.

(80) Li, P.; Li, Y.; Kwok, T.; Yang, T.; Liu, C.; Li, W.; Zhang, X. A Bi-Layered Membrane with Micro-Nano Bioactive Glass for Guided Bone Regeneration. *Colloids Surf B Biointerfaces* **2021**, *205*, 111886. https://doi.org/10.1016/j.colsurfb.2021.111886.

(81) Abe, G. L.; Sasaki, J.-I.; Katata, C.; Kohno, T.; Tsuboi, R.; Kitagawa, H.; Imazato, S. Fabrication of Novel Poly(Lactic Acid/Caprolactone) Bilayer Membrane for GBR Application. *Dental Materials* **2020**, *36* (5), 626–634. https://doi.org/10.1016/j.dental.2020.03.013.

(82) Parenteau-Bareil, R.; Gauvin, R.; Berthod, F. Collagen-Based Biomaterials for Tissue Engineering Applications. *Materials* **2010**, *3* (3), 1863. https://doi.org/10.3390/MA3031863.

(83) Sharma, S.; Srivastava, D.; Grover, S.; Sharma, V. Biomaterials in Tooth Tissue Engineering: A Review. *J Clin Diagn Res* **2014**, *8* (1), 309. https://doi.org/10.7860/JCDR/2014/7609.3937.

(84) Gümüşderelioğlu, M.; Sunal, E.; Tolga Demirtaş, T.; Kiremitçi, A. S. Chitosan-Based Double-Faced Barrier Membrane Coated with Functional Nanostructures and Loaded with BMP-6. *J Mater Sci Mater Med* **2020**, *31* (1), 1–14. https://doi.org/10.1007/S10856-019-6331-X/FIGURES/8.

(85) Lakhanisky, T. Chemical Name: ε-Caprolactone 2. *CAS Number* **2004**, 502–546.

(86) Zahid, S.; Khan, A. S.; Chaudhry, A. A.; Ghafoor, S.; Ain, Q. U.; Raza, A.; Rahim, M. I.; Goerke, O.; Rehman, I. U.; Tufail, A. Fabrication, in Vitro and in Vivo Studies of Bilayer Composite Membrane for Periodontal Guided Tissue Regeneration. *J Biomater Appl* **2019**, *33* (7), 967–978. https://doi.org/10.1177/0885328218814986.

(87) Woodruff, M. A.; Hutmacher, D. W. The Return of a Forgotten Polymer - Polycaprolactone in the 21st Century. *Progress in Polymer Science (Oxford)* **2010**, *35* (10), 1217–1256. https://doi.org/10.1016/j.progpolymsci.2010.04.002.

(88) Cortez Tornello, P. R.; Caracciolo, P. C.; Igartúa Roselló, J. I.; Abraham, G. A. Electrospun Scaffolds with Enlarged Pore Size: Porosimetry Analysis. *Mater Lett* **2018**, *227*, 191–193. https://doi.org/10.1016/J.MATLET.2018.05.072.

(89) Dikici, serkan. A Sweet Way to Increase the Metabolic Activity and Migratory Response of Wound-Related Cells: Deoxy-Sugar Incorporated Natural Polymeric Fibres as a Potential Bioactive Wound Patch. *TURKISH JOURNAL OF BIOLOGY* **2021**. https://doi.org/10.3906/biy-2108-27.

(90) Mehta, P. P.; Pawar, V. S. Electrospun Nanofiber Scaffolds: Technology and Applications. *Applications of Nanocomposite Materials in Drug Delivery* **2018**, 509–573. https://doi.org/10.1016/B978-0-12-813741-3.00023-6.

(91) Xue, J.; Wu, T.; Dai, Y.; Xia, Y. Electrospinning and Electrospun Nanofibers: Methods, Materials, and Applications. *Chem Rev* **2019**, *119* (8), 5298. https://doi.org/10.1021/ACS.CHEMREV.8B00593.

(92) Bhardwaj, N.; Kundu, S. C. Electrospinning: A Fascinating Fiber Fabrication Technique. *Biotechnol Adv* **2010**, *28* (3), 325–347. https://doi.org/10.1016/J.BIOTECHADV.2010.01.004.

(93) Thomas, K.; Engler, A. J.; Meyer, G. A. Extracellular Matrix Regulation in the Muscle Satellite Cell Niche. *Connect Tissue Res* **2015**, *56* (1), 1–8. https://doi.org/10.3109/03008207.2014.947369.

(94) Wen, S. L.; Feng, S.; Tang, S. H.; Gao, J. H.; Zhang, L. H.; Tong, H.; Yan, Z. P.; Fang, D. Z. Collapsed Reticular Network and Its Possible Mechanism during the Initiation and/or Progression of Hepatic Fibrosis. *Scientific Reports 2016 6:1* **2016**, *6* (1), 1–11. https://doi.org/10.1038/srep35426.

(95) Mouw, J. K.; Ou, G.; Weaver, V. M. Extracellular Matrix Assembly: A Multiscale Deconstruction. *Nat Rev Mol Cell Biol* **2014**, *15* (12), 771–785. https://doi.org/10.1038/NRM3902.

(96) Avossa, J.; Herwig, G.; Toncelli, C.; Itel, F.; Rossi, R. M. Electrospinning Based on Benign Solvents: Current Definitions, Implications and Strategies. *Green Chemistry* **2022**, *24* (6), 2347–2375. https://doi.org/10.1039/D1GC04252A.

(97) Dahlin, R. L.; Kasper, F. K.; Mikos, A. G. Polymeric Nanofibers in Tissue Engineering. *Tissue Eng Part B Rev* **2011**, *17* (5), 349. https://doi.org/10.1089/TEN.TEB.2011.0238.

(98) Etemadi, N.; Mehdikhani, M.; Poorazizi, E.; Rafienia, M. Novel Bilayer Electrospun Poly(Caprolactone)/ Silk Fibroin/ Strontium Carbonate Fibrous Nanocomposite Membrane for Guided Bone Regeneration. *J Appl Polym Sci* **2021**, *138* (16). https://doi.org/10.1002/app.50264.

(99) Liu, J.; Zou, Q.; Wang, C.; Lin, M.; Li, Y.; Zhang, R.; Li, Y. Electrospinning and 3D Printed Hybrid Bi-Layer Scaffold for Guided Bone Regeneration. *Mater Des* **2021**, *210*. https://doi.org/10.1016/j.matdes.2021.110047.

(100) R., M. R.; D., A.; Z., E.; D., K.; A., T. Development of a Novel Functionally Graded Membrane Containing Boron-Modified Bioactive Glass Nanoparticles for Guided Bone Regeneration. *J Tissue Eng Regen Med* **2019**, *13* (8).

(101) Niu, X.; Wang, L.; Xu, M.; Qin, M.; Zhao, L.; Wei, Y.; Hu, Y.; Lian, X.; Liang, Z.; Chen, S.; Chen, W.; Huang, D. Electrospun Polyamide-6/Chitosan Nanofibers Reinforced Nano-Hydroxyapatite/Polyamide-6 Composite Bilayered Membranes for Guided Bone Regeneration. *Carbohydr Polym* **2021**, *260*. https://doi.org/10.1016/j.carbpol.2021.117769.

(102) Sundaram, M. N.; Sowmya, S.; Deepthi, S.; Bumgardener, J. D.; Jayakumar, R. Bilayered Construct for Simultaneous Regeneration of Alveolar Bone and Periodontal Ligament. *J Biomed Mater Res B Appl Biomater* **2015**, *104* (4), 761–770. https://doi.org/10.1002/jbm.b.33480.

(103) Zhong, M.; Lin, J.; He, Z.; Wu, W.; Ji, D.; Zhang, R.; Zhang, J. Bi-Layered PLGA Electrospun Membrane with Occlusive and Osteogenic Properties for Periodontal Regeneration. *J Bioact Compat Polym* **2022**, *37* (4), 284–298. https://doi.org/10.1177/08839115221095257.

(104) Fujihara, K.; Kotaki, M.; Ramakrishna, S. Guided Bone Regeneration Membrane Made of Polycaprolactone/Calcium Carbonate Composite Nano-Fibers. *Biomaterials* **2005**, *26* (19), 4139–4147. https://doi.org/10.1016/j.biomaterials.2004.09.014.

(105) Tamburaci, S.; Tihminlioglu, F. Development of Si Doped Nano Hydroxyapatite Reinforced Bilayer Chitosan Nanocomposite Barrier Membranes for Guided Bone Regeneration. *Materials Science and Engineering: C* **2021**, *128*, 112298. https://doi.org/10.1016/j.msec.2021.112298.

(106) Bachs-Herrera, A.; Yousefzade, O.; del Valle, L. J.; Puiggali, J. Melt Electrospinning of Polymers: Blends, Nanocomposites, Additives and Applications. *Applied Sciences (Switzerland)*. MDPI AG February 2, 2021, pp 1–39. https://doi.org/10.3390/app11041808.

(107) Bubakir, M. M.; Li, H.; Barhoum, A.; Yang, W. Advances in Melt Electrospinning Technique. *Handbook of Nanofibers* **2018**, 1–32. https://doi.org/10.1007/978-3-319-42789-8_8-1.

(108) Hutmacher, D. W.; Dalton, P. D. Melt Electrospinning. *Chem Asian J* **2011**, *6* (1), 44–56. https://doi.org/10.1002/asia.201000436.

(109) Costantini, M.; Colosi, C.; Święszkowski, W.; Barbetta, A. Co-Axial Wet-Spinning in 3D Bioprinting: State of the Art and Future Perspective of Microfluidic Integration. *Biofabrication* **2018**, *11* (1), 012001. https://doi.org/10.1088/1758-5090/aae605.

(110) Vaquette, C.; Mitchell, J.; Fernandez-Medina, T.; Kumar, S.; Ivanovski, S. Resorbable Additively Manufactured Scaffold Imparts Dimensional Stability to Extraskeletally Regenerated Bone. *Biomaterials* **2021**, *269*, 120671. https://doi.org/10.1016/j.biomaterials.2021.120671.

(111) DeFrates, K. G.; Moore, R.; Borgesi, J.; Lin, G.; Mulderig, T.; Beachley, V.; Hu, X. Protein-Based Fiber Materials in Medicine: A Review. *Nanomaterials*. MDPI AG July 1, 2018. https://doi.org/10.3390/nano8070457.

(112) Ozipek, B.; Karakas, H. Wet Spinning of Synthetic Polymer Fibers. In *Advances in Filament Yarn Spinning of Textiles and Polymers*; Elsevier Ltd., 2014; pp 174–186. https://doi.org/10.1533/9780857099174.2.174.

(113) Requicha, J. F.; Viegas, C. A.; Hede, S.; Leonor, I. B.; Reis, R. L.; Gomes, M. E. Design and Characterization of a Biodegradable Double-Layer Scaffold Aimed at Periodontal Tissue-Engineering Applications. *J Tissue Eng Regen Med* **2016**, *10* (5), 392–403. https://doi.org/10.1002/term.1816.

(114) Requicha, J. F.; Viegas, C. A.; Muñoz, F.; Azevedo, J. M.; Leonor, I. B.; Reis, R. L.; Gomes, M. E. A Tissue Engineering Approach for Periodontal Regeneration Based on a Biodegradable Double-Layer Scaffold and Adipose-Derived Stem Cells. *Tissue Eng Part A* **2014**, *20* (17–18), 2483–2492. https://doi.org/10.1089/ten.tea.2013.0360.

(115) Taherkhani, S.; Moztarzadeh, F. Fabrication of a Poly(ε-Caprolactone)/Starch Nanocomposite Scaffold with a Solvent-Casting/Salt-Leaching Technique for Bone Tissue Engineering Applications. *J Appl Polym Sci* **2016**, *133* (23). https://doi.org/10.1002/APP.43523.

(116) Mikos, A. G.; Temenoff, J. S. Formation of Highly Porous Biodegradable Scaffolds for Tissue Engineering. *Electronic Journal of Biotechnology* **2000**, *3* (2), 114–119. https://doi.org/10.2225/VOL3-ISSUE2-FULLTEXT-5.

(117) Murphy, W. L.; Dennis, R. G.; Kileny, J. L.; Mooney, D. J. Salt Fusion: An Approach to Improve Pore Interconnectivity within Tissue Engineering Scaffolds. *Tissue Eng* **2002**, *8* (1), 43–52. https://doi.org/10.1089/107632702753503045.

(118) Stevens, B.; Yang, Y.; Mohandas, A.; Stucker, B.; Nguyen, K. T. A Review of Materials, Fabrication Methods, and Strategies Used to Enhance Bone Regeneration in Engineered Bone Tissues. *J Biomed Mater Res B Appl Biomater* **2008**, *85B* (2), 573–582. https://doi.org/10.1002/jbm.b.30962.

(119) S, L. M.; A, P. S.; J, T. Z.; I, D. J. Polymer Based Wafer Technology : A Review. *International Journal of Pharmaceutical & Biological Archives* **2013**.

(120) Jamuna-Thevi, K.; Saarani, N. N.; Abdul Kadir, M. R.; Hermawan, H. Triple-Layered PLGA/Nanoapatite/Lauric Acid Graded Composite Membrane for Periodontal Guided Bone Regeneration. *Materials Science and Engineering: C* **2014**, *43*, 253–263. https://doi.org/10.1016/j.msec.2014.07.028.

(121) Aldemir Dikici, B.; Reilly, G. C.; Claeyssens, F. Boosting the Osteogenic and Angiogenic Performance of Multiscale Porous Polycaprolactone Scaffolds by *In Vitro* Generated Extracellular Matrix Decoration. *ACS Applied Materials & Interfaces* **2020**, *12* (11), 12510–12524. https://doi.org/10.1021/acsami.9b23100.

(122) Cameron, N. R.; Krajnc, P.; Silverstein, M. S. Colloidal Templating. *Porous Polymers* **2010**, 119–172. https://doi.org/10.1002/9780470929445.ch4.

(123) Aldemir Dikici, B.; Claeyssens, F. Basic Principles of Emulsion Templating and Its Use as an Emerging Manufacturing Method of Tissue Engineering Scaffolds. *Front Bioeng Biotechnol* **2020**, *8*. https://doi.org/10.3389/fbioe.2020.00875.

(124) Christenson, E. M.; Soofi, W.; Holm, J. L.; Cameron, N. R.; Mikos, A. G. Biodegradable Fumarate-Based PolyHIPEs as Tissue Engineering Scaffolds. *Biomacromolecules* **2007**, *8* (12), 3806–3814. https://doi.org/10.1021/bm7007235.

(125) Johnson, D. W.; Langford, C. R.; Didsbury, M. P.; Lipp, B.; Przyborski, S. A.; Cameron, N. R. Fully Biodegradable and Biocompatible Emulsion Templated Polymer Scaffolds by Thiol-

Acrylate Polymerization of Polycaprolactone Macromonomers. *Polym Chem* **2015**, *6* (41), 7256–7263. https://doi.org/10.1039/c5py00721f.

(126) Sušec, M.; Liska, R.; Russmüller, G.; Kotek, J.; Krajnc, P. Microcellular Open Porous Monoliths for Cell Growth by Thiol-Ene Polymerization of Low-Toxicity Monomers in High Internal Phase Emulsions. *Macromol Biosci* **2015**, *15* (2), 253–261. https://doi.org/10.1002/mabi.201400219.

(127) Bokhari, M. A.; Akay, G.; Zhang, S.; Birch, M. A. The Enhancement of Osteoblast Growth and Differentiation in Vitro on a Peptide Hydrogel - PolyHIPE Polymer Hybrid Material. *Biomaterials* **2005**, *26* (25), 5198–5208. https://doi.org/10.1016/j.biomaterials.2005.01.040.

(128) Robinson, J. L.; McEnery, M. A. P.; Pearce, H.; Whitely, M. E.; Munoz-Pinto, D. J.; Hahn, M. S.; Li, H.; Sears, N. A.; Cosgriff-Hernandez, E. Osteoinductive PolyHIPE Foams as Injectable Bone Grafts. *Tissue Eng Part A* **2016**, *22* (5–6), 403–414. https://doi.org/10.1089/ten.tea.2015.0370.

(129) Owen, R.; Sherborne, C.; Paterson, T.; Green, N. H.; Reilly, G. C.; Claeyssens, F. Emulsion Templated Scaffolds with Tunable Mechanical Properties for Bone Tissue Engineering. *J Mech Behav Biomed Mater* **2016**, *54* (2016), 159–172. https://doi.org/10.1016/j.jmbbm.2015.09.019.

(130) Sherborne, C.; Owen, R.; Reilly, G. C.; Claeyssens, F. Light-Based Additive Manufacturing of PolyHIPEs: Controlling the Surface Porosity for 3D Cell Culture Applications. *Mater Des* **2018**, *156* (2018), 494–503. https://doi.org/10.1016/j.matdes.2018.06.061.

(131) Severn, C. E.; Eissa, A. M.; Langford, C. R.; Parker, A.; Walker, M.; Dobbe, J. G. G.; Streekstra, G. J.; Cameron, N. R.; Toye, A. M. Ex Vivo Culture of Adult CD34+ Stem Cells Using Functional Highly Porous Polymer Scaffolds to Establish Biomimicry of the Bone Marrow Niche. *Biomaterials* **2019**, *225*. https://doi.org/10.1016/j.biomaterials.2019.119533.

(132) Owen, R.; Sherborne, C.; Evans, R.; C. Reilly, G.; Claeyssens, F. Combined Porogen Leaching and Emulsion Templating to Produce Bone Tissue Engineering Scaffolds. *Int J Bioprint* **2020**, *6* (2), 265. https://doi.org/10.18063/ijb.v6i2.265.

(133) Dikici, S.; Aldemir Dikici, B.; Bhaloo, S. I.; Balcells, M.; Edelman, E. R.; MacNeil, S.; Reilly, G. C.; Sherborne, C.; Claeyssens, F. Assessment of the Angiogenic Potential of 2-Deoxy-D-Ribose Using a Novel in Vitro 3D Dynamic Model in Comparison With Established in Vitro Assays. *Front Bioeng Biotechnol* **2020**, *7*. https://doi.org/10.3389/fbioe.2019.00451.

(134) Aldemir Dikici, B.; Sherborne, C.; Reilly, G. C.; Claeyssens, F. Emulsion Templated Scaffolds Manufactured from Photocurable Polycaprolactone. *Polymer (Guildf)* **2019**, *175*, 243–254. https://doi.org/10.1016/j.polymer.2019.05.023.

(135) Richez, A.; Deleuze, H.; Vedrenne, P.; Collier, R. Preparation of Ultra-Low-Density Microcellular Materials. *J Appl Polym Sci* **2005**, *96* (6), 2053–2063. https://doi.org/10.1002/app.21668.

(136) Dhavalikar, P.; Shenoi, J.; Salhadar, K.; Chwatko, M.; Rodriguez-Rivera, G.; Cheshire, J.; Foudazi, R.; Cosgriff-Hernandez, E. Engineering Toolbox for Systematic Design of Polyhipe Architecture. *Polymers (Basel)* **2021**, *13* (9). https://doi.org/10.3390/polym13091479.

(137) Paterson, T. E.; Gigliobianco, G.; Sherborne, C.; Green, N. H.; Dugan, J. M.; MacNeil, S.; Reilly, G. C.; Claeyssens, F. Porous Microspheres Support Mesenchymal Progenitor Cell Ingrowth

and Stimulate Angiogenesis. *APL Bioeng* **2018**, *2* (2), 026103. https://doi.org/10.1063/1.5008556.

(138) Oh, B. H. L.; Bismarck, A.; Chan-Park, M. B. Injectable, Interconnected, High-Porosity Macroporous Biocompatible Gelatin Scaffolds Made by Surfactant-Free Emulsion Templating. *Macromol Rapid Commun* **2015**, *36* (4), 364–372. https://doi.org/10.1002/marc.201400524.

(139) Aldemir Dikici, B.; Dikici, S.; Claeyssens, F. Synergistic Effect of Type and Concentration of Surfactant and Diluting Solvent on the Morphology of Highly Porous Emulsion Templated Tissue Engineering Scaffolds. *Colloids Surf B Biointerfaces* **2022**.

(140) Durgut, E.; Sherborne, C.; Aldemir Dikici, B.; Reilly, G. C.; Claeyssens, F. Preparation of Interconnected Pickering Polymerized High Internal Phase Emulsions by Arrested Coalescence. *Langmuir* **2022**, *38* (36). https://doi.org/10.1021/acs.langmuir.2c01243.

(141) Durgut, E.; Zhou, M.; Dikici, B. A.; Foudazi, R.; Claeyssens, F. Modifying Pickering Polymerized High Internal Phase Emulsion Morphology by Adjusting Particle Hydrophilicity. *Colloids Surf A Physicochem Eng Asp* **2024**, *680*, 132629. https://doi.org/10.1016/j.colsurfa.2023.132629.

(142) Malayeri, A.; Sherborne, C.; Paterson, T.; Mittar, S.; Asencio, I. O.; Hatton, P. V.; Claeyssens, F. Osteosarcoma Growth on Trabecular Bone Mimicking Structures Manufactured via Laser Direct Write. *Int J Bioprint* **2016**, *2* (2), 67–77. https://doi.org/10.18063/IJB.2016.02.005.

(143) Samanta, A.; Nandan, B.; Srivastava, R. K. Morphology of Electrospun Fibers Derived from High Internal Phase Emulsions. *J Colloid Interface Sci* **2016**, *471*, 29–36. https://doi.org/10.1016/j.jcis.2016.03.012.

(144) Naranda, J.; Sušec, M.; Maver, U.; Gradišnik, L.; Gorenjak, M.; Vukasović, A.; Ivković, A.; Rupnik, M. S.; Vogrin, M.; Krajnc, P. Polyester Type PolyHIPE Scaffolds with an Interconnected Porous Structure for Cartilage Regeneration. *Sci Rep* **2016**, *6* (1), 28695. https://doi.org/10.1038/srep28695.

(145) Dikici, S.; Aldemir Dikici, B.; MacNeil, S.; Claeyssens, F. Decellularised Extracellular Matrix Decorated PCL PolyHIPE Scaffolds for Enhanced Cellular Activity, Integration and Angiogenesis. *Biomater Sci* **2021**, *9* (21), 7297–7310. https://doi.org/10.1039/D1BM01262B.

(146) DİKİCİ, S. Ascorbic Acid Enhances the Metabolic Activity, Growth and Collagen Production of Human Dermal Fibroblasts Growing in Three-Dimensional (3D) Culture. *GAZI UNIVERSITY JOURNAL OF SCIENCE* **2022**. https://doi.org/10.35378/gujs.1040277.

(147) Robinson, J. L.; Moglia, R. S.; Stuebben, M. C.; Mcenery, M. A. P.; Cosgriff-Hernandez, E. Achieving Interconnected Pore Architecture in Injectable PolyHIPEs for Bone Tissue Engineering. *Tissue Eng Part A* **2014**, *20* (5–6), 1103–1112. https://doi.org/10.1089/ten.tea.2013.0319.

(148) Moglia, R. S.; Holm, J. L.; Sears, N. A.; Wilson, C. J.; Harrison, D. M.; Cosgriff-Hernandez, E. Injectable PolyHIPEs as High-Porosity Bone Grafts. *Biomacromolecules* **2011**, *12* (10), 3621–3628. https://doi.org/10.1021/bm2008839.

(149) Aldemir Dikici, B.; Malayeri, A.; Sherborne, C.; Dikici, S.; Paterson, T.; Dew, L.; Hatton, P.; Ortega Asencio, I.; Macneil, S.; Langford, C.; Cameron, N. R.; Claeyssens, F. Thiolene- And Polycaprolactone Methacrylate-Based Polymerized High Internal Phase Emulsion (PolyHIPE)

Scaffolds for Tissue Engineering. *Biomacromolecules* **2021**. https://doi.org/10.1021/acs.biomac.1c01129.

(150) Wang, A.; Paterson, T.; Owen, R.; Sherborne, C.; Dugan, J.; Li, J.; Claeyssens, F. Photocurable High Internal Phase Emulsions (HIPEs) Containing Hydroxyapatite for Additive Manufacture of Tissue Engineering Scaffolds with Multi-Scale Porosity. *Materials Science and Engineering: C* **2016**, *67* (2016), 51–58. https://doi.org/10.1016/j.msec.2016.04.087.

(151) Akay, G.; Birch, M. A.; Bokhari, M. A. Microcellular PolyHIPE Polymer Supports Osteoblast Growth and Bone Formation in Vitro. *Biomaterials* **2004**, *25* (18), 3991–4000. https://doi.org/10.1016/j.biomaterials.2003.10.086.

(152) Aldemir Dikici, B.; Chen, M.-C.; Dikici, S.; Chiu, H.-C.; Claeyssens, F. In Vivo Bone Regeneration Capacity of Multiscale Porous Polycaprolactone-Based High Internal Phase Emulsion (PolyHIPE) Scaffolds in a Rat Calvarial Defect Model. *ACS Appl Mater Interfaces* **2023**, *15* (23), 27696–27705. https://doi.org/10.1021/acsami.3c04362.

(153) Mangir, N.; Dikici, S.; Claeyssens, F.; Macneil, S. Using Ex Ovo Chick Chorioallantoic Membrane (CAM) Assay to Evaluate the Biocompatibility and Angiogenic Response to Biomaterials. *ACS Biomater Sci Eng* **2019**, *5* (7), 3190–3200. https://doi.org/10.1021/acsbiomaterials.9b00172.

(154) Dikici, S.; Claeyssens, F.; MacNeil, S. Decellularised Baby Spinach Leaves and Their Potential Use in Tissue Engineering Applications: Studying and Promoting Neovascularisation. *J Biomater Appl* **2019**, *34* (4), 546–559. https://doi.org/10.1177/0885328219863115.

(155) Dikici, S.; Claeyssens, F.; MacNeil, S. Pre-Seeding of Simple Electrospun Scaffolds with a Combination of Endothelial Cells and Fibroblasts Strongly Promotes Angiogenesis. *Tissue Eng Regen Med* **2020**, *17* (4), 445–458. https://doi.org/10.1007/s13770-020-00263-7.

(156) Dikici, S.; Claeyssens, F.; MacNeil, S. Bioengineering Vascular Networks to Study Angiogenesis and Vascularization of Physiologically Relevant Tissue Models in Vitro. *ACS Biomater Sci Eng* **2020**, *6* (6), 3513–3528. https://doi.org/10.1021/acsbiomaterials.0c00191.

(157) Collins, M. N.; Ren, G.; Young, K.; Pina, S.; Reis, R. L.; Oliveira, J. M. Scaffold Fabrication Technologies and Structure/Function Properties in Bone Tissue Engineering. *Advanced Functional Materials*. 2021. https://doi.org/10.1002/adfm.202010609.

(158) Preethi Soundarya, S.; Haritha Menon, A.; Viji Chandran, S.; Selvamurugan, N. Bone Tissue Engineering: Scaffold Preparation Using Chitosan and Other Biomaterials with Different Design and Fabrication Techniques. *International Journal of Biological Macromolecules*. 2018. https://doi.org/10.1016/j.ijbiomac.2018.08.056.

(159) Fereshteh, Z. Freeze-Drying Technologies for 3D Scaffold Engineering. In *Functional 3D Tissue Engineering Scaffolds*; Elsevier, 2018; pp 151–174. https://doi.org/10.1016/B978-0-08-100979-6.00007-0.

(160) Liapis, A. I.; Bruttini, R. A Theory for the Primary and Secondary Drying Stages of the Freeze-Drying of Pharmaceutical Crystalline and Amorphous Solutes: Comparison between Experimental Data and Theory. *Separations Technology* **1994**, *4* (3), 144–155. https://doi.org/10.1016/0956-9618(94)80017-0.

(161) Parivatphun, T.; Sangkert, S.; Kokoo, R.; Khangkhamano, M.; Meesane, J. Biphasic Scaffolds of Polyvinyl Alcohol with Silk Fibroin for Oral and Maxillofacial Surgery Based on Mimicking Materials Design: Fabrication, Characterization, Properties. *J Mater Sci* **2022**, *57* (3), 2131–2148. https://doi.org/10.1007/S10853-021-06718-Z/FIGURES/10.

(162) Mishra, R.; Kumar, A. Inorganic/Organic Biocomposite Cryogels for Regeneration of Bony Tissues. *http://dx.doi.org/10.1163/092050610X534230* **2012**, *22* (16), 2107–2126. https://doi.org/10.1163/092050610X534230.

(163) Hixon, K. R.; Lu, T.; Sell, S. A. A Comprehensive Review of Cryogels and Their Roles in Tissue Engineering Applications. *Acta Biomaterialia*. 2017. https://doi.org/10.1016/j.actbio.2017.08.033.

(164) Kao, H.-H.; Kuo, C.-Y.; Chen, K.-S.; Chen, J.-P. Preparation of Gelatin and Gelatin/Hyaluronic Acid Cryogel Scaffolds for the 3D Culture of Mesothelial Cells and Mesothelium Tissue Regeneration. *Int J Mol Sci* **2019**, *20* (18), 4527. https://doi.org/10.3390/ijms20184527.

(165) Huang, R. Y.; Tai, W. C.; Ho, M. H.; Chang, P. C. Combination of a Biomolecule-Aided Biphasic Cryogel Scaffold with a Barrier Membrane Adhering PDGF-Encapsulated Nanofibers to Promote Periodontal Regeneration. *J Periodontal Res* **2020**, *55* (4), 529–538. https://doi.org/10.1111/JRE.12740.

(166) An, J.; Teoh, J. E. M.; Suntornnond, R.; Chua, C. K. Design and 3D Printing of Scaffolds and Tissues. *Engineering* **2015**, *1* (2), 261–268. https://doi.org/10.15302/J-ENG-2015061.

(167) Bittner, S. M.; Guo, J. L.; Melchiorri, A.; Mikos, A. G. Three-Dimensional Printing of Multilayered Tissue Engineering Scaffolds. *Materials Today*. Elsevier B.V. October 1, 2018, pp 861–874. https://doi.org/10.1016/j.mattod.2018.02.006.

(168) Thompson, M. K.; Moroni, G.; Vaneker, T.; Fadel, G.; Campbell, R. I.; Gibson, I.; Bernard, A.; Schulz, J.; Graf, P.; Ahuja, B.; Martina, F. Design for Additive Manufacturing: Trends, Opportunities, Considerations, and Constraints. *CIRP Ann Manuf Technol* **2016**, *65* (2), 737–760. https://doi.org/10.1016/j.cirp.2016.05.004.

(169) Chung, J. J.; Im, H.; Kim, S. H.; Park, J. W.; Jung, Y. Toward Biomimetic Scaffolds for Tissue Engineering: 3D Printing Techniques in Regenerative Medicine. *Frontiers in Bioengineering and Biotechnology*. Frontiers Media S.A. November 4, 2020. https://doi.org/10.3389/fbioe.2020.586406.

(170) Poomathi, N.; Singh, S.; Prakash, C.; Subramanian, A.; Sahay, R.; Cinappan, A.; Ramakrishna, S. 3D Printing in Tissue Engineering: A State of the Art Review of Technologies and Biomaterials. *Rapid Prototyping Journal*. Emerald Group Holdings Ltd. July 23, 2020, pp 1313–1334. https://doi.org/10.1108/RPJ-08-2018-0217.

(171) Sears, N. A.; Seshadri, D. R.; Dhavalikar, P. S.; Cosgriff-Hernandez, E. A Review of Three-Dimensional Printing in Tissue Engineering. *Tissue Engineering - Part B: Reviews*. Mary Ann Liebert Inc. August 1, 2016, pp 298–310. https://doi.org/10.1089/ten.teb.2015.0464.

(172) Nesic, D.; Schaefer, B. M.; Sun, Y.; Saulacic, N.; Sailer, I. 3D Printing Approach in Dentistry: The Future for Personalized Oral Soft Tissue Regeneration. *Journal of Clinical Medicine*. MDPI July 1, 2020, pp 1–21. https://doi.org/10.3390/jcm9072238.

(173) Pavan Kalyan, B.; Kumar, L. 3D Printing: Applications in Tissue Engineering, Medical Devices, and Drug Delivery. *AAPS PharmSciTech*. Springer Science and Business Media Deutschland GmbH May 1, 2022. https://doi.org/10.1208/s12249-022-02242-8.

(174) Subia, B.; Kundu, J.; Kundu, S. C. *Biomaterial Scaffold Fabrication Techniques for Potential Tissue Engineering Applications 141 X Biomaterial Scaffold Fabrication Techniques for Potential Tissue Engineering Applications*. www.intechopen.com.

(175) Turnbull, G.; Clarke, J.; Picard, F.; Riches, P.; Jia, L.; Han, F.; Li, B.; Shu, W. 3D Bioactive Composite Scaffolds for Bone Tissue Engineering. *Bioactive Materials*. KeAi Communications Co. September 1, 2018, pp 278–314. https://doi.org/10.1016/j.bioactmat.2017.10.001.

(176) *https://www.upnano.at/nanoone/*.

(177) Lee, C. H.; Hajibandeh, J.; Suzuki, T.; Fan, A.; Shang, P.; Mao, J. J. Three-Dimensional Printed Multiphase Scaffolds for Regeneration of Periodontium Complex. *Tissue Eng Part A* **2014**, *20* (7–8), 1342–1351. https://doi.org/10.1089/ten.tea.2013.0386.

(178) Park, C. H.; Rios, H. F.; Jin, Q.; Bland, M. E.; Flanagan, C. L.; Hollister, S. J.; Giannobile, W. V. Biomimetic Hybrid Scaffolds for Engineering Human Tooth-Ligament Interfaces. *Biomaterials* **2010**, *31* (23), 5945–5952. https://doi.org/10.1016/j.biomaterials.2010.04.027.

(179) Haraguchi, Y.; Shimizu, T.; Yamato, M.; Okano, T. Scaffold-Free Tissue Engineering Using Cell Sheet Technology. *RSC Adv* **2012**, *2* (6), 2184–2190. https://doi.org/10.1039/C2RA00704E.

(180) Hasegawa, M.; Yamato, M.; Kikuchi, A.; Okano, T.; Ishikawa, I. Human Periodontal Ligament Cell Sheets Can Regenerate Periodontal Ligament Tissue in an Athymic Rat Model. *Tissue Eng* **2005**, *11* (3–4), 469–478. https://doi.org/10.1089/TEN.2005.11.469.

(181) Dan, H.; Vaquette, C.; Fisher, A. G.; Hamlet, S. M.; Xiao, Y.; Hutmacher, D. W.; Ivanovski, S. The Influence of Cellular Source on Periodontal Regeneration Using Calcium Phosphate Coated Polycaprolactone Scaffold Supported Cell Sheets. *Biomaterials* **2014**, *35* (1), 113–122. https://doi.org/10.1016/J.BIOMATERIALS.2013.09.074.

(182) Akizuki, T.; Oda, S.; Komaki, M.; Tsuchioka, H.; Kawakatsu, N.; Kikuchi, A.; Yamato, M.; Okano, T.; Ishikawa, I. Application of Periodontal Ligament Cell Sheet for Periodontal Regeneration: A Pilot Study in Beagle Dogs. *J Periodontal Res* **2005**, *40* (3), 245–251. https://doi.org/10.1111/J.1600-0765.2005.00799.X.

(183) Dikici, S.; Çavdaroğlu, Ç. Development of Pro-Angiogenic Wound Dressings from 2-Deoxy-D-Ribose (2dDR)-Loaded Decellularized Plant Leaves. *J Mater Sci* **2023**, *58* (42), 16428–16444. https://doi.org/10.1007/s10853-023-09064-4.

(184) Cevik, M.; Dikici, S. Development of Tissue-Engineered Vascular Grafts from Decellularized Parsley Stems. *Soft Matter* **2023**. https://doi.org/10.1039/D3SM01236K.

(185) Gilpin, A.; Yang, Y. Decellularization Strategies for Regenerative Medicine: From Processing Techniques to Applications. *Biomed Res Int* **2017**, *2017*. https://doi.org/10.1155/2017/9831534.

(186) Crapo, P. M.; Gilbert, T. W.; Badylak, S. F. An Overview of Tissue and Whole Organ Decellularization Processes. *Biomaterials* **2011**, *32* (12), 3233–3243. https://doi.org/10.1016/J.BIOMATERIALS.2011.01.057.

(187) Lu, H.; Hoshiba, T.; Kawazoe, N.; Chen, G. Comparison of Decellularization Techniques for Preparation of Extracellular Matrix Scaffolds Derived from Three-Dimensional Cell Culture. *J Biomed Mater Res A* **2012**, *100A* (9), 2507–2516. https://doi.org/10.1002/JBM.A.34150.

(188) Son, H.; Jeon, M.; Choi, H. J.; Lee, H. S.; Kim, I. H.; Kang, C. M.; Song, J. S. Decellularized Human Periodontal Ligament for Periodontium Regeneration. *PLoS One* **2019**, *14* (8), e0221236. https://doi.org/10.1371/JOURNAL.PONE.0221236.

(189) dos Santos, D. M.; de Annunzio, S. R.; Carmello, J. C.; Pavarina, A. C.; Fontana, C. R.; Correa, D. S. Combining Coaxial Electrospinning and 3D Printing: Design of Biodegradable Bilayered Membranes with Dual Drug Delivery Capability for Periodontitis Treatment. *ACS Appl Bio Mater* **2021**, *5* (1), 146–159. https://doi.org/10.1021/acsabm.1c01019.

(190) Lian, M.; Han, Y.; Sun, B.; Xu, L.; Wang, X.; Ni, B.; Jiang, W.; Qiao, Z.; Dai, K.; Zhang, X. A Multifunctional Electrowritten Bi-Layered Scaffold for Guided Bone Regeneration. *Acta Biomater* **2020**, *118*. https://doi.org/10.1016/j.actbio.2020.08.017.

(191) Costa, P. F.; Vaquette, C.; Zhang, Q.; Reis, R. L.; Ivanovski, S.; Hutmacher, D. W. Advanced Tissue Engineering Scaffold Design for Regeneration of the Complex Hierarchical Periodontal Structure. *J Clin Periodontol* **2014**, *41* (3), 283–294. https://doi.org/10.1111/jcpe.12214.

(192) Rohani Shirvan, A.; Nouri, A.; Sutti, A. A Perspective on the Wet Spinning Process and Its Advancements in Biomedical Sciences. *European Polymer Journal*. 2022. https://doi.org/10.1016/j.eurpolymj.2022.111681.

(193) Rahmati, M.; Mills, D. K.; Urbanska, A. M.; Saeb, M. R.; Venugopal, J. R.; Ramakrishna, S.; Mozafari, M. Electrospinning for Tissue Engineering Applications. *Prog Mater Sci* **2021**, *117*, 100721. https://doi.org/10.1016/j.pmatsci.2020.100721.

(194) Prasad, A.; Sankar, M. R.; Katiyar, V. State of Art on Solvent Casting Particulate Leaching Method for Orthopedic ScaffoldsFabrication. *Mater Today Proc* **2017**, *4* (2), 898–907. https://doi.org/10.1016/J.MATPR.2017.01.101.

(195) Pandya, A.; Upadhaya, P.; Lohakare, S.; Srivastava, T.; Mhatre, S.; Pulakkat, S.; Patravale, V. B. Nanobiomaterials for Regenerative Medicine. *Nanotechnology in Medicine and Biology* **2022**, 141–187. https://doi.org/10.1016/B978-0-12-819469-0.00007-1.

(196) Martins, P. M.; Nunes-Pereira, J.; Lanceros-Méndez, S.; Costa, C. M. Synthetic Polymer-Based Membranes for Lithium-Ion Batteries. *Synthetic Polymeric Membranes for Advanced Water Treatment, Gas Separation, and Energy Sustainability* **2020**, 383–415. https://doi.org/10.1016/B978-0-12-818485-1.00017-4.

(197) Zhang, Y. F.; Cheng, X. R.; Chen, Y.; Shi, B.; Chen, X. H.; Xu, D. X.; Jin, K. Three-Dimensional Nanohydroxyapatite/Chitosan Scaffolds as Potential Tissue Engineered Periodontal Tissue. *J Biomater Appl* **2007**. https://doi.org/10.1177/0885328206063853.

(198) Gerçek, I.; Tiğli, R. S.; Gumusderelioglu, M. A Novel Scaffold Based on Formation and Agglomeration of PCL Microbeads by Freeze-Drying. *J Biomed Mater Res A* **2008**. https://doi.org/10.1002/jbm.a.31723.

(199) Staples, R. J.; Ivanovski, S.; Vaquette, C. Fibre Guiding Scaffolds for Periodontal Tissue Engineering. *Journal of Periodontal Research*. 2020. https://doi.org/10.1111/jre.12729.

(200) Sudhakar, C. K.; Upadhyay, N.; Jain, A.; Verma, A.; Narayana Charyulu, R.; Jain, S. Chapter 5 - Hydrogels—Promising Candidates for Tissue Engineering A2 - Thomas, Sabu. In *Nanotechnology Applications for Tissue Engineering*; 2015.

(201) Bakhshpour, M.; Idil, N.; Perçin, I.; Denizli, A. Biomedical Applications of Polymeric Cryogels. *Applied Sciences (Switzerland)*. 2019. https://doi.org/10.3390/app9030553.

(202) Bencherif, S. A.; Braschler, T. M.; Renaud, P. Advances in the Design of Macroporous Polymer Scaffolds for Potential Applications in Dentistry. *Journal of Periodontal and Implant Science*. 2013. https://doi.org/10.5051/jpis.2013.43.6.251.

(203) Zeng, W. Y.; Ning, Y.; Huang, X. Advanced Technologies in Periodontal Tissue Regeneration Based on Stem Cells: Current Status and Future Perspectives. *Journal of Dental Sciences*. Association for Dental Sciences of the Republic of China January 1, 2021, pp 501–507. https://doi.org/10.1016/j.jds.2020.07.008.

(204) Dall'Ava, L.; Hothi, H.; di Laura, A.; Henckel, J.; Hart, A. 3D Printed Acetabular Cups for Total Hip Arthroplasty: A Review Article. *Metals*. MDPI AG July 1, 2019. https://doi.org/10.3390/met9070729.

(205) Raveau, S.; Jordana, F. Tissue Engineering and Three-Dimensional Printing in Periodontal Regeneration: A Literature Review. *Journal of Clinical Medicine*. MDPI December 1, 2020, pp 1–21. https://doi.org/10.3390/jcm9124008.

(206) Vaquette, C.; Fan, W.; Xiao, Y.; Hamlet, S.; Hutmacher, D. W.; Ivanovski, S. A Biphasic Scaffold Design Combined with Cell Sheet Technology for Simultaneous Regeneration of Alveolar Bone/Periodontal Ligament Complex. *Biomaterials* **2012**, *33* (22), 5560–5573. https://doi.org/10.1016/j.biomaterials.2012.04.038.

(207) Yu, M.; Luo, D.; Qiao, J.; Guo, J.; He, D.; Jin, S.; Tang, L.; Wang, Y.; Shi, X.; Mao, J.; Cui, S.; Fu, Y.; Li, Z.; Liu, D.; Zhang, T.; Zhang, C.; Li, Z.; Zhou, Y.; Liu, Y. A Hierarchical Bilayer Architecture for Complex Tissue Regeneration. *Bioact Mater* **2022**, *10*, 93–106. https://doi.org/10.1016/j.bioactmat.2021.08.024.

(208) Sowmya, S.; Mony, U.; Jayachandran, P.; Reshma, S.; Kumar, R. A.; Arzate, H.; Nair, S. V; Jayakumar, R. Tri-Layered Nanocomposite Hydrogel Scaffold for the Concurrent Regeneration of Cementum, Periodontal Ligament, and Alveolar Bone. *Adv Healthc Mater* **2017**, *6* (7), 1601251. https://doi.org/10.1002/adhm.201601251.

(209) Prakobkarn, J.; Makeudom, A.; Jenvoraphot, T.; Supanchart, C.; Krisanaprakornkit, S.; Punyodom, W.; Daranarong, D. Biphasic Nanofibrous Scaffolds Based on Collagen and <scp>PLC</Scp> for Controlled Release <scp>LL</Scp>-37 in Guided Bone Regeneration. *J Appl Polym Sci* **2021**, *139* (7). https://doi.org/10.1002/app.51629.

(210) Gorgieva, S.; Vuherer, T.; Kokol, V. Autofluorescence-Aided Assessment of Integration and µ-Structuring in Chitosan/Gelatin Bilayer Membranes with Rapidly Mineralized Interface in Relevance to Guided Tissue Regeneration. *Materials Science and Engineering: C* **2018**, *93*, 226–241. https://doi.org/10.1016/j.msec.2018.07.077.

(211) Zhang, H.; Wang, J.; Ma, H.; Zhou, Y.; Ma, X.; Liu, J.; Huang, J.; Yu, N. Bilayered PLGA/Wool Keratin Composite Membranes Support Periodontal Regeneration in Beagle Dogs. *ACS Biomater Sci Eng* **2016**, *2* (12). https://doi.org/10.1021/acsbiomaterials.6b00357.

(212) Guo, B.; Ma, P. X. Synthetic Biodegradable Functional Polymers for Tissue Engineering: A Brief Review. *Sci China Chem* **2014**, *57* (4), 490–500. https://doi.org/10.1007/s11426-014-5086-y.

(213) Donnaloja, F.; Jacchetti, E.; Soncini, M.; Raimondi, M. T. Natural and Synthetic Polymers for Bone Scaffolds Optimization. *Polymers*. MDPI AG April 1, 2020, p 905. https://doi.org/10.3390/POLYM12040905.

(214) Satturwar, P. M.; Fulzele, S. v.; Dorle, A. K. Biodegradation and in Vivo Biocompatibility of Rosin: A Natural Film-Forming Polymer. *AAPS PharmSciTech* **2003**, *4* (4). https://doi.org/10.1208/PT040455.

(215) Liang, H.; Mirinejad, M. S.; Asefnejad, A.; Baharifar, H.; Li, X.; Saber-Samandari, S.; Toghraie, D.; Khandan, A. Fabrication of Tragacanthin Gum-Carboxymethyl Chitosan Bio-Nanocomposite Wound Dressing with Silver-Titanium Nanoparticles Using Freeze-Drying Method. *Mater Chem Phys* **2022**, *279*. https://doi.org/10.1016/j.matchemphys.2022.125770.

(216) Legeros, R. Z. *Properties of Osteoconductive Biomaterials: Calcium Phosphates List of Abbreviations Used BMP Bone Morphogenetic Protein ECM Extracellular Matrix MSC Mesenchymal Stem Cell*; 2002; Vol. 395.

(217) Gunatillake, P. A.; Adhikari, R.; Gadegaard, N. Biodegradable Synthetic Polymers for Tissue Engineering. *European Cells and Materials*. AO Research Institute Davos 2003, pp 1–16. https://doi.org/10.22203/eCM.v005a01.

(218) D'Avanzo, N.; Bruno, M. C.; Giudice, A.; Mancuso, A.; de Gaetano, F.; Cristiano, M. C.; Paolino, D.; Fresta, M. Influence of Materials Properties on Bio-Physical Features and Effectiveness of 3D-Scaffolds for Periodontal Regeneration. *Molecules 2021, Vol. 26, Page 1643* **2021**, *26* (6), 1643. https://doi.org/10.3390/MOLECULES26061643.

(219) Jiang, C. P.; Huang, J. R.; Hsieh, M. F. Fabrication of Synthesized PCL-PEG-PCL Tissue Engineering Scaffolds Using an Air Pressure-Aided Deposition System. *Rapid Prototyp J* **2011**, *17* (4), 288–297. https://doi.org/10.1108/13552541111138414/FULL/PDF.

(220) Seyednejad, H.; Ghassemi, A. H.; van Nostrum, C. F.; Vermonden, T.; Hennink, W. E. Functional Aliphatic Polyesters for Biomedical and Pharmaceutical Applications. *Journal of Controlled Release* **2011**, *152* (1), 168–176. https://doi.org/10.1016/J.JCONREL.2010.12.016.

(221) *Monocryl (poliglecaprone 25) Suture, Undyed 510(k) FDA Premarket Notification K964072 ETHICON, INC.* https://fda.report/PMN/K964072 (accessed 2022-09-02).

(222) Türkkan, S.; Pazarçeviren, A. E.; Keskin, D.; Machin, N. E.; Duygulu, Ö.; Tezcaner, A. Nanosized CaP-Silk Fibroin-PCL-PEG-PCL/PCL Based Bilayer Membranes for Guided Bone Regeneration. *Materials Science and Engineering: C* **2017**, *80*, 484–493. https://doi.org/10.1016/J.MSEC.2017.06.016.

(223) Gürbüz, S.; Demirtaş, T. T.; Yüksel, E.; Karakeçili, A.; Doğan, A.; Gümüşderelioğlu, M. Multi-Layered Functional Membranes for Periodontal Regeneration: Preparation and Characterization. *Mater Lett* **2016**, *178*, 256–259. https://doi.org/10.1016/j.matlet.2016.05.054.

(224) Nam, J. Y.; Okamoto, M.; Okamoto, H.; Nakano, M.; Usuki, A.; Matsuda, M. Morphology and Crystallization Kinetics in a Mixture of Low-Molecular Weight Aliphatic Amide and Polylactide. *Polymer (Guildf)* **2006**, *47* (4), 1340–1347. https://doi.org/10.1016/J.POLYMER.2005.12.066.

(225) Iwata, T.; Doi, Y. Morphology and Enzymatic Degradation of Poly(L-Lactic Acid) Single Crystals. *Macromolecules* **1998**, *31* (8), 2461–2467. https://doi.org/10.1021/MA980008H/ASSET/IMAGES/LARGE/MA980008HF00008.JPEG.

(226) Sawai, D.; Takahashi, K.; Imamura, T.; Nakamura, K.; Kanamoto, T.; Hyon, S. H. Preparation of Oriented β-Form Poly(L-Lactic Acid) by Solid-State Extrusion. *J Polym Sci B Polym Phys* **2002**, *40* (1), 95–104. https://doi.org/10.1002/POLB.10076.

(227) Lunt, J. Large-Scale Production, Properties and Commercial Applications of Polylactic Acid Polymers. *Polym Degrad Stab* **1998**, *59* (1–3), 145–152. https://doi.org/10.1016/S0141-3910(97)00148-1.

(228) Yu, C.; Bao, J.; Xie, Q.; Shan, G.; Bao, Y.; Pan, P. Crystallization Behavior and Crystalline Structural Changes of Poly(Glycolic Acid) Investigated via Temperature-Variable WAXD and FTIR Analysis. *CrystEngComm* **2016**, *18* (40), 7894–7902. https://doi.org/10.1039/C6CE01623E.

(229) Gentile, P.; Chiono, V.; Carmagnola, I.; Hatton, P. v. An Overview of Poly(Lactic-Co-Glycolic) Acid (PLGA)-Based Biomaterials for Bone Tissue Engineering. *International Journal of Molecular Sciences*. Molecular Diversity Preservation International February 28, 2014, pp 3640–3659. https://doi.org/10.3390/ijms15033640.

(230) Pan, Z.; Ding, J. Poly(Lactide-Co-Glycolide) Porous Scaffolds for Tissue Engineering and Regenerative Medicine. *Interface Focus*. Royal Society 2012, pp 366–377. https://doi.org/10.1098/rsfs.2011.0123.

(231) Rocha, C. V.; Gonçalves, V.; da Silva, M. C.; Bañobre-López, M.; Gallo, J. PLGA-Based Composites for Various Biomedical Applications. *International Journal of Molecular Sciences*. MDPI February 1, 2022. https://doi.org/10.3390/ijms23042034.

(232) Kaboorani, A.; Riedl, B. Mechanical Performance of Polyvinyl Acetate (PVA)-Based Biocomposites. *Biocomposites: Design and Mechanical Performance* **2015**, 347–364. https://doi.org/10.1016/B978-1-78242-373-7.00009-3.

(233) Drug-Loaded Electrospun Mats of Poly(Vinyl Alcohol) Fibres and Their Release Characteristics of Four Model Drugs. **2006**. https://doi.org/10.1088/0957-4484/17/9/041.

(234) Huang, R. Y. M.; Rhim, J. W. Modification of Poly(Vinyl Alcohol) Using Maleic Acid and Its Application to the Separation of Acetic Acid-Water Mixtures by the Pervaporation Technique. *Polym Int* **1993**, *30* (1), 129–135. https://doi.org/10.1002/PI.4990300119.

(235) *Modification of poly(vinyl alcohol) with acid chlorides and crosslinking with difunctional hardeners - Giménez - 1996 - Journal of Polymer Science Part A: Polymer Chemistry - Wiley Online Library*. https://onlinelibrary.wiley.com/doi/10.1002/(SICI)1099-0518(19960430)34:6%3C925::AID-POLA1%3E3.0.CO;2-H (accessed 2022-08-28).

(236) Krumova, M.; López, D.; Benavente, R.; Mijangos, C.; Pereña, J. M. Effect of Crosslinking on the Mechanical and Thermal Properties of Poly(Vinyl Alcohol). *Polymer (Guildf)* **2000**, *41* (26), 9265–9272. https://doi.org/10.1016/S0032-3861(00)00287-1.

(237) Chong, S. F.; Smith, A. A. A.; Zelikin, A. N. Microstructured, Functional PVA Hydrogels through Bioconjugation with Oligopeptides under Physiological Conditions. *Small* **2013**, *9* (6), 942–950. https://doi.org/10.1002/SMLL.201201774.

1746 (238) Ahsan, T.; Nerem, R. M. Bioengineered Tissues: The Science, the Technology, and the
1747 Industry. *Orthod Craniofac Res* **2005**, *8* (3), 134–140. https://doi.org/10.1111/J.1601-
1748 6343.2005.00326.X.

1749 (239) Dang, J. M.; Leong, K. W. Natural Polymers for Gene Delivery and Tissue Engineering. *Adv*
1750 *Drug Deliv Rev* **2006**, *58* (4), 487–499. https://doi.org/10.1016/J.ADDR.2006.03.001.

1751 (240) Bhatia, S. Natural Polymers vs Synthetic Polymer. *Natural Polymer Drug Delivery Systems*
1752 **2016**, 95–118. https://doi.org/10.1007/978-3-319-41129-3_3.

1753 (241) Seciu, A. M.; Craciunescu, O.; Stanciuc, A. M.; Zarnescu, O. Tailored Biomaterials for
1754 Therapeutic Strategies Applied in Periodontal Tissue Engineering.
1755 *https://home.liebertpub.com/scd* **2019**, *28* (15), 963–973.
1756 https://doi.org/10.1089/SCD.2019.0016.

1757 (242) Brinckmann, J. Collagens at a Glance. *Top Curr Chem* **2005**, *247*, 1–6.
1758 https://doi.org/10.1007/B103817/COVER.

1759 (243) Veit, G.; Kobbe, B.; Keene, D. R.; Paulsson, M.; Koch, M.; Wagener, R. Collagen XXVIII, a Novel
1760 von Willebrand Factor A Domain-Containing Protein with Many Imperfections in the
1761 Collagenous Domain. *J Biol Chem* **2006**, *281* (6), 3494–3504.
1762 https://doi.org/10.1074/JBC.M509333200.

1763 (244) Shoulders, M. D.; Raines, R. T. COLLAGEN STRUCTURE AND STABILITY. *Annu Rev Biochem*
1764 **2009**, *78*, 929. https://doi.org/10.1146/ANNUREV.BIOCHEM.77.032207.120833.

1765 (245) Rezvani Ghomi, E.; Nourbakhsh, N.; Akbari Kenari, M.; Zare, M.; Ramakrishna, S. Collagen-
1766 Based Biomaterials for Biomedical Applications. *J Biomed Mater Res B Appl Biomater* **2021**,
1767 *109* (12), 1986–1999. https://doi.org/10.1002/JBM.B.34881.

1768 (246) R, P.; G, C.; G, S.; F, N.; R, P.; G, B. Guided Tissue Regeneration Employing a Collagen
1769 Membrane in a Human Periodontal Bone Defect: A Histologic Evaluation. *Int J Periodontics*
1770 *Restorative Dent* **1997**, *17* (3), 282–291.

1771 (247) Behfarnia, P.; Khorasani, M.; Birang, R.; Abbas, F. Histological and Histomorphometric
1772 Analysis of Animal Experimental Dehiscence Defect Treated with Three Bio Absorbable GTR
1773 Collagen Membrane. *Dent Res J (Isfahan)* **2012**, *9* (5), 574. https://doi.org/10.4103/1735-
1774 3327.104876.

1775 (248) Thoma, D. S.; Halg, G. A.; Dard, M. M.; Seibl, R.; Hammerle, C. H. F.; Jung, R. E. Evaluation of a
1776 New Biodegradable Membrane to Prevent Gingival Ingrowth into Mandibular Bone Defects in
1777 Minipigs. *Clin Oral Implants Res* **2009**, *20* (1), 7–16. https://doi.org/10.1111/J.1600-
1778 0501.2008.01604.X.

1779 (249) Zhou, T.; Chen, S.; Ding, X.; Hu, Z.; Cen, L.; Zhang, X. Fabrication and Characterization of
1780 Collagen/PVA Dual-Layer Membranes for Periodontal Bone Regeneration. *Front Bioeng*
1781 *Biotechnol* **2021**, *9* (empty), 0–0. https://doi.org/10.3389/FBIOE.2021.630977/READER.

1782 (250) Tang, Y.; Chen, L.; Zhao, K.; Wu, Z.; Wang, Y.; Tan, Q. Fabrication of PLGA/HA (Core)-
1783 Collagen/Amoxicillin (Shell) Nanofiber Membranes through Coaxial Electrospinning for
1784 Guided Tissue Regeneration. *Compos Sci Technol* **2016**, *125*, 100–107.
1785 https://doi.org/10.1016/j.compscitech.2016.02.005.

1786 (251) Li, S.; Xie, Q.; Mo, A. A Biphasic Material Combined with Injectable Platelet-Rich Fibrin for the
1787 Potential Regeneration of Oral Soft and Hard Tissues. *J Mater Sci* **2022**, *57* (16), 7923–7940.
1788 https://doi.org/10.1007/S10853-022-07163-2/FIGURES/7.

1789 (252) Jayakumar, R.; Chennazhi, K. P.; Srinivasan, S.; Nair, S. V.; Furuike, T.; Tamura, H. Chitin
1790 Scaffolds in Tissue Engineering. *Int J Mol Sci* **2011**, *12* (3), 1876.
1791 https://doi.org/10.3390/IJMS12031876.

1792 (253) Wake, M. C.; Patrick, C. W.; Mikos, A. G. Pore Morphology Effects on the Fibrovascular Tissue
1793 Growth in Porous Polymer Substrates. *Cell Transplant* **1994**, *3* (4), 339–343.
1794 https://doi.org/10.1177/096368979400300411.

1795 (254) Ebhodaghe, S. O. Natural Polymeric Scaffolds for Tissue Engineering Applications. *J Biomater*
1796 *Sci Polym Ed* **2021**, *32* (16), 2144–2194. https://doi.org/10.1080/09205063.2021.1958185.

1797 (255) Sukpaita, T.; Chirachanchai, S.; Pimkhaokham, A.; Ampornaramveth, R. S. Chitosan-Based
1798 Scaffold for Mineralized Tissues Regeneration. *Mar Drugs* **2021**, *19* (10).
1799 https://doi.org/10.3390/MD19100551.

1800 (256) Osman, Z. F.; Ahmad, A.; Noordin, K. B. A. A. Naturally Derived Scaffolds for Dental Pulp
1801 Regeneration: A Review. *Gulhane Medical Journal* **2019**, *61* (2), 81–88.
1802 https://doi.org/10.26657/GULHANE.00060.

1803 (257) Shen, Z. Sen; Cui, X.; Hou, R. X.; Li, Q.; Deng, H. X.; Fu, J. Tough Biodegradable Chitosan–
1804 Gelatin Hydrogels via in Situ Precipitation for Potential Cartilage Tissue Engineering. *RSC Adv*
1805 **2015**, *5* (69), 55640–55647. https://doi.org/10.1039/C5RA06835E.

1806 (258) Lou, C. W.; Wen, S. P.; Lin, J. H. Chitosan/Gelatin Porous Bone Scaffolds Made by Crosslinking
1807 Treatment and Freeze-Drying Technology: Effects of Crosslinking Durations on the Porous
1808 Structure, Compressive Strength, and in Vitro Cytotoxicity. *J Appl Polym Sci* **2015**, *132* (17).
1809 https://doi.org/10.1002/APP.41851.

1810 (259) Shah, A. T.; Zahid, S.; Ikram, F.; Maqbool, M.; Chaudhry, A. A.; Rahim, M. I.; Schmidt, F.;
1811 Goerke, O.; Khan, A. S.; Rehman, I. ur. Tri-Layered Functionally Graded Membrane for
1812 Potential Application in Periodontal Regeneration. *Materials Science and Engineering: C* **2019**,
1813 *103*, 109812. https://doi.org/10.1016/J.MSEC.2019.109812.

1814 (260) *(PDF) Gelatin Based Scaffolds For Tissue Engineering – A review*.
1815 https://www.researchgate.net/publication/272748016_Gelatin_Based_Scaffolds_For_Tissue
1816 _Engineering_-_A_review (accessed 2022-08-24).

1817 (261) Bello, A. B.; Kim, D.; Kim, D.; Park, H.; Lee, S. H. Engineering and Functionalization of Gelatin
1818 Biomaterials: From Cell Culture to Medical Applications. *Tissue Eng Part B Rev* **2020**, *26* (2),
1819 164–180. https://doi.org/10.1089/TEN.TEB.2019.0256.

1820 (262) Echave, M. C.; Sánchez, P.; Pedraz, J. L.; Orive, G. Progress of Gelatin-Based 3D Approaches
1821 for Bone Regeneration. *J Drug Deliv Sci Technol* **2017**, *42*, 63–74.
1822 https://doi.org/10.1016/J.JDDST.2017.04.012.

1823 (263) Chuang, C. H.; Lin, R. Z.; Melero-Martin, J. M.; Chen, Y. C. Comparison of Covalently and
1824 Physically Cross-Linked Collagen Hydrogels on Mediating Vascular Network Formation for
1825 Engineering Adipose Tissue. *Artif Cells Nanomed Biotechnol* **2018**, *46* (sup3).
1826 https://doi.org/10.1080/21691401.2018.1499660.

(264) Yu, Y.; Xu, S.; Li, S.; Pan, H. Genipin-Cross-Linked Hydrogels Based on Biomaterials for Drug Delivery: A Review. *Biomaterials Science*. 2021. https://doi.org/10.1039/d0bm01403f.

(265) Yue, K.; Trujillo-de Santiago, G.; Alvarez, M. M.; Tamayol, A.; Annabi, N.; Khademhosseini, A. Synthesis, Properties, and Biomedical Applications of Gelatin Methacryloyl (GelMA) Hydrogels. *Biomaterials* **2015**, *73*, 254–271. https://doi.org/10.1016/J.BIOMATERIALS.2015.08.045.

(266) Mũnoz, Z.; Shih, H.; Lin, C. C. Gelatin Hydrogels Formed by Orthogonal Thiol-Norbornene Photochemistry for Cell Encapsulation. *Biomater Sci* **2014**, *2* (8). https://doi.org/10.1039/c4bm00070f.

(267) Göckler, T.; Haase, S.; Kempter, X.; Pfister, R.; Maciel, B. R.; Grimm, A.; Molitor, T.; Willenbacher, N.; Schepers, U. Tuning Superfast Curing Thiol-Norbornene-Functionalized Gelatin Hydrogels for 3D Bioprinting. *Adv Healthc Mater* **2021**, *10* (14). https://doi.org/10.1002/adhm.202100206.

(268) Burchak, V.; Koch, F.; Siebler, L.; Haase, S.; Horner, V. K.; Kempter, X.; Stark, G. B.; Schepers, U.; Grimm, A.; Zimmermann, S.; Koltay, P.; Strassburg, S.; Finkenzeller, G.; Simunovic, F.; Lampert, F. Evaluation of a Novel Thiol–Norbornene-Functionalized Gelatin Hydrogel for Bioprinting of Mesenchymal Stem Cells. *Int J Mol Sci* **2022**, *23* (14). https://doi.org/10.3390/ijms23147939.

(269) Rahali, K.; Ben Messaoud, G.; Kahn, C. J. F.; Sanchez-Gonzalez, L.; Kaci, M.; Cleymand, F.; Fleutot, S.; Linder, M.; Desobry, S.; Arab-Tehrany, E. Synthesis and Characterization of Nanofunctionalized Gelatin Methacrylate Hydrogels. *International Journal of Molecular Sciences 2017, Vol. 18, Page 2675* **2017**, *18* (12), 2675. https://doi.org/10.3390/IJMS18122675.

(270) Hang, Z. S.; Tan, L. H.; Cao, X. M.; Ju, F. Y.; Ying, S. J.; Xu, F. M. Preparation of Melamine Microfibers by Reaction Electrospinning. *Mater Lett* **2011**, *65* (7), 1079–1081. https://doi.org/10.1016/J.MATLET.2011.01.010.

(271) Lai, T. C.; Yu, J.; Tsai, W. B. Gelatin Methacrylate/Carboxybetaine Methacrylate Hydrogels with Tunable Crosslinking for Controlled Drug Release. *J Mater Chem B* **2016**, *4* (13), 2304–2313. https://doi.org/10.1039/C5TB02518D.

(272) Akilbekova, D.; Shaimerdenova, M.; Adilov, S.; Berillo, D. Biocompatible Scaffolds Based on Natural Polymers for Regenerative Medicine. *Int J Biol Macromol* **2018**, *114*, 324–333. https://doi.org/10.1016/J.IJBIOMAC.2018.03.116.

(273) Pan, J.; Deng, J.; Yu, L.; Wang, Y.; Zhang, W.; Han, X.; Camargo, P. H. C.; Wang, J.; Liu, Y. Investigating the Repair of Alveolar Bone Defects by Gelatin Methacrylate Hydrogels-Encapsulated Human Periodontal Ligament Stem Cells. *J Mater Sci Mater Med* **2020**, *31* (1). https://doi.org/10.1007/S10856-019-6333-8.

(274) Wang, Y.; Ma, M.; Zhang, L.; Gao, Y.; Zhang, B.; Guo, Y. Fabrication of Bi-Layer Photocrosslinked GelMA/PEGDA Fibrous Membrane for Guided Bone Regeneration Materials. *Mater Lett* **2019**, *249*. https://doi.org/10.1016/j.matlet.2019.04.076.

(275) Tandon, S.; Kandasubramanian, B.; Ibrahim, S. M. Silk-Based Composite Scaffolds for Tissue Engineering Applications. *Ind Eng Chem Res* **2020**, *59* (40), 17593–17611. https://doi.org/10.1021/ACS.IECR.0C02195/ASSET/IMAGES/LARGE/IE0C02195_0012.JPEG.

(276) Willerth, S. M.; Sakiyama-Elbert, S. E. Combining Stem Cells and Biomaterial Scaffolds for Constructing Tissues and Cell Delivery. *Stembook* **2008**. https://doi.org/10.3824/STEMBOOK.1.1.1.

(277) Brif, A.; Laity, P.; Claeyssens, F.; Holland, C. Dynamic Photo-Cross-Linking of Native Silk Enables Macroscale Patterning at a Microscale Resolution. *ACS Biomater Sci Eng* **2020**, *6* (1). https://doi.org/10.1021/acsbiomaterials.9b00993.

(278) Sun, W.; Zhang, Y.; Gregory, D. A.; Jimenez-Franco, A.; Tomeh, M. A.; Lv, S.; Wang, J.; Haycock, J. W.; Lu, J. R.; Zhao, X. Patterning the Neuronal Cells via Inkjet Printing of Self-Assembled Peptides on Silk Scaffolds. *Progress in Natural Science: Materials International* **2020**, *30* (5), 686–696. https://doi.org/10.1016/J.PNSC.2020.09.007.

(279) Melke, J.; Midha, S.; Ghosh, S.; Ito, K.; Hofmann, S. Silk Fibroin as Biomaterial for Bone Tissue Engineering. *Acta Biomater* **2016**, *31*, 1–16. https://doi.org/10.1016/J.ACTBIO.2015.09.005.

(280) Song, W.; Muthana, M.; Mukherjee, J.; Falconer, R. J.; Biggs, C. A.; Zhao, X. Magnetic-Silk Core-Shell Nanoparticles as Potential Carriers for Targeted Delivery of Curcumin into Human Breast Cancer Cells. *ACS Biomater Sci Eng* **2017**, *3* (6), 1027–1038. https://doi.org/10.1021/ACSBIOMATERIALS.7B00153.

(281) Zhang, C.; Zhang, Y.; Shao, H.; Hu, X. Hybrid Silk Fibers Dry-Spun from Regenerated Silk Fibroin/Graphene Oxide Aqueous Solutions. *ACS Appl Mater Interfaces* **2016**, *8* (5), 3349–3358. https://doi.org/10.1021/ACSAMI.5B11245.

(282) Virlan, M. J. R.; Calenic, B.; Zaharia, C.; Greabu, M. Silk Fibroin and Potential Uses in Regenerative Dentistry - a Systematic Review. *STOMATOLOGY EDU JOURNAL* **2014**, *1* (2), 108–114. https://doi.org/10.25241/STOMAEDUJ.2014.1(2).ART.5.

(283) Arango, M. C.; Montoya, Y.; Peresin, M. S.; Bustamante, J.; Álvarez-López, C. Silk Sericin as a Biomaterial for Tissue Engineering: A Review. *https://doi.org/10.1080/00914037.2020.1785454* **2020**, *70* (16), 1115–1129. https://doi.org/10.1080/00914037.2020.1785454.

(284) Cai, Y.; Mei, D.; Jiang, T.; Yao, J. Synthesis of Oriented Hydroxyapatite Crystals: Effect of Reaction Conditions in the Presence or Absence of Silk Sericin. *Mater Lett* **2010**, *64* (24), 2676–2678. https://doi.org/10.1016/J.MATLET.2010.08.071.

(285) Guo, Y.; Jiang, X.; Pan, P.; Liu, X.; Huang, L.; Li, M.; Liu, Y. Preparation of SF/SF-NHA Double-Layer Scaffolds for Periodental Tissue Regeneration. *International Journal of Polymeric Materials and Polymeric Biomaterials* **2022**. https://doi.org/10.1080/00914037.2022.2100375.

(286) Sarkar, R.; Banerjee, G. *Ceramic Based Bio-Medical Implants Nano Carbon Containing Refractory View Project Sol-Gel Bonded High Pure Alumina Castable View Project*. https://www.researchgate.net/publication/286690829.

(287) Thein-Han, W.; Xu, H. H. K. Collagen-Calcium Phosphate Cement Scaffolds Seeded with Umbilical Cord Stem Cells for Bone Tissue Engineering. *Tissue Eng Part A* **2011**, *17* (23–24), 2943–2954. https://doi.org/10.1089/ten.tea.2010.0674.

(288) Amin, A. M. M.; Ewais, E. M. M. Bioceramic Scaffolds. In *Scaffolds in Tissue Engineering - Materials, Technologies and Clinical Applications*; InTech, 2017. https://doi.org/10.5772/intechopen.70194.

(289) Kim, H.-W.; Lee, E.-J.; Jun, I.-K.; Kim, H.-E.; Knowles, J. C. Degradation and Drug Release of Phosphate Glass/Polycaprolactone Biological Composites for Hard-Tissue Regeneration. *J Biomed Mater Res B Appl Biomater* **2005**, *75B* (1), 34–41. https://doi.org/10.1002/jbm.b.30223.

(290) Tevlin, R.; McArdle, A.; Atashroo, D.; Walmsley, G. G.; Senarath-Yapa, K.; Zielins, E. R.; Paik, K. J.; Longaker, M. T.; Wan, D. C. Biomaterials for Craniofacial Bone Engineering. *J Dent Res* **2014**, *93* (12), 1187–1195. https://doi.org/10.1177/0022034514547271.

(291) Hench, L. L. *Bioceramics: From Concept to Clinic*.

(292) Zhang, Y.; Wu, C. Bioactive Inorganic and Organic Composite Materials for Bone Regeneration and Gene Delivery. In *Advanced Bioactive Inorganic Materials for Bone Regeneration and Drug Delivery*; CRC Press, 2013; pp 177–212. https://doi.org/10.1201/b13926-8.

(293) Huang, J.; Best, S. M.; Bonfield, W.; Brooks, R. A.; Rushton, N.; Jayasinghe, S. N.; Edirisinghe, M. J. *A L S I N M E D I C I N E 1 5 (2 0 0 4) 4 4 1 ± 4 4 5 In Vitro Assessment of the Biological Response to Nano-Sized Hydroxyapatite*.

(294) Szpalski, C.; Barr, J.; Wetterau, M.; Saadeh, P. B.; Warren, S. M. Cranial Bone Defects: Current and Future Strategies. *Neurosurg Focus* **2010**, *29* (6), 1–11. https://doi.org/10.3171/2010.9.FOCUS10201.

(295) Zhao, J.; Liu, Y.; Sun, W. bin; Zhang, H. Amorphous Calcium Phosphate and Its Application in Dentistry. *Chemistry Central Journal*. July 8, 2011. https://doi.org/10.1186/1752-153X-5-40.

(296) Johnson, K. D.; Frierson, K. E.; Keller, T. S.; Cook, C.; Scheinberg, R.; Zerwekh, J.; Meyers, L.; Sciadini, M. F. Porous Ceramics as Bone Graft Substitutes in Long Bone Defects: A Biomechanical, Histological, and Radiographic Analysis. *Journal of Orthopaedic Research* **1996**, *14* (3), 351–369. https://doi.org/10.1002/jor.1100140304.

(297) Kutikov, A. B.; Gurijala, A.; Song, J. Rapid Prototyping Amphiphilic Polymer/Hydroxyapatite Composite Scaffolds with Hydration-Induced Self-Fixation Behavior. *Tissue Eng Part C Methods* **2015**, *21* (3), 229–241. https://doi.org/10.1089/ten.tec.2014.0213.

(298) Oryan, A.; Alidadi, S.; Moshiri, A.; Maffulli, N. Bone Regenerative Medicine: Classic Options, Novel Strategies, and Future Directions. *J Orthop Surg Res* **2014**, *9* (1), 18. https://doi.org/10.1186/1749-799X-9-18.

(299) Nery, E. B.; Lee, K. K.; Czajkowski, S.; Dooner, J. J.; Duggan, M.; Ellinger, R. F.; Henkin, J. M.; Hines, R.; Miller, M.; Olson, J. W.; Rafferty, M.; Sullivan, T.; Walters, P.; Welch, D.; Williams, A. A Veterans Administration Cooperative Study of Biphasic Calcium Phosphate Ceramic in Periodontal Osseous Defects. *J Periodontol* **1990**, *61* (12), 737–744. https://doi.org/10.1902/jop.1990.61.12.737.

(300) Ramay, H. R. R.; Zhang, M. Biphasic Calcium Phosphate Nanocomposite Porous Scaffolds for Load-Bearing Bone Tissue Engineering. *Biomaterials* **2004**, *25* (21), 5171–5180. https://doi.org/10.1016/j.biomaterials.2003.12.023.

(301) Petrovic, V.; Zivkovic, P.; Petrovic, D.; Stefanovic, V. Craniofacial Bone Tissue Engineering. *Oral Surg Oral Med Oral Pathol Oral Radiol* **2012**, *114* (3), e1–e9. https://doi.org/10.1016/j.oooo.2012.02.030.

(302) Pilipchuk, S. P.; Plonka, A. B.; Monje, A.; Taut, A. D.; Lanis, A.; Kang, B.; Giannobile, W. v. Tissue Engineering for Bone Regeneration and Osseointegration in the Oral Cavity. *Dental Materials* **2015**, *31* (4), 317–338. https://doi.org/10.1016/j.dental.2015.01.006.

(303) Karimi, M.; Asefnejad, A.; Aflaki, D.; Surendar, A.; Baharifar, H.; Saber-Samandari, S.; Khandan, A.; Khan, A.; Toghraie, D. Fabrication of Shapeless Scaffolds Reinforced with Baghdadite-Magnetite Nanoparticles Using a 3D Printer and Freeze-Drying Technique. *Journal of Materials Research and Technology* **2021**, *14*. https://doi.org/10.1016/j.jmrt.2021.08.084.

(304) Hench, L. L. The Story of Bioglass®. *J Mater Sci Mater Med* **2006**, *17* (11), 967–978. https://doi.org/10.1007/s10856-006-0432-z.

(305) Janvikul, W.; Uppanan, P.; Thavornyutikarn, B.; Kosorn, W.; Kaewkong, P. Effects of Surface Topography, Hydrophilicity and Chemistry of Surface-Treated PCL Scaffolds on Chondrocyte Infiltration and ECM Production. *Procedia Eng* **2013**, *59*, 158–165. https://doi.org/10.1016/J.PROENG.2013.05.106.

(306) van Tienen, T. G.; Heijkants, R. G. J. C.; Buma, P.; de Groot, J. H.; Pennings, A. J.; Veth, R. P. H. Tissue Ingrowth and Degradation of Two Biodegradable Porous Polymers with Different Porosities and Pore Sizes. *Biomaterials* **2002**, *23* (8), 1731–1738. https://doi.org/10.1016/S0142-9612(01)00280-0.

(307) Achilli, M.; Mantovani, D. Tailoring Mechanical Properties of Collagen-Based Scaffolds for Vascular Tissue Engineering: The Effects of PH, Temperature and Ionic Strength on Gelation. *Polymers 2010, Vol. 2, Pages 664-680* **2010**, *2* (4), 664–680. https://doi.org/10.3390/POLYM2040664.

(308) Liu, X.; Won, Y.; Ma, P. X. Surface Modification of Interconnected Porous Scaffolds. *J Biomed Mater Res A* **2005**, *74A* (1), 84–91. https://doi.org/10.1002/JBM.A.30367.

(309) Yang, K.; Lee, J. S.; Kim, J.; Lee, Y. bin; Shin, H.; Um, S. H.; Kim, J. B.; Park, K. I.; Lee, H.; Cho, S. W. Polydopamine-Mediated Surface Modification of Scaffold Materials for Human Neural Stem Cell Engineering. *Biomaterials* **2012**, *33* (29), 6952–6964. https://doi.org/10.1016/J.BIOMATERIALS.2012.06.067.

(310) Park, K.; Ju, Y. M.; Son, J. S.; Ahn, K. D.; Han, D. K. Surface Modification of Biodegradable Electrospun Nanofiber Scaffolds and Their Interaction with Fibroblasts. *http://dx.doi.org/10.1163/156856207780424997* **2012**, *18* (4), 369–382. https://doi.org/10.1163/156856207780424997.

(311) Yang, J.; Wan, Y.; Tu, C.; Cai, Q.; Bei, J.; Wang, S. Enhancing the Cell Affinity of Macroporous Poly(L-Lactide) Cell Scaffold by a Convenient Surface Modification Method. *Polym Int* **2003**, *52* (12), 1892–1899. https://doi.org/10.1002/PI.1272.

(312) Desai, N. P.; Hubbell, J. A. Surface Physical Interpenetrating Networks of Poly(Ethylene Terephthalate) and Poly(Ethylene Oxide) with Biomedical Applications. *Macromolecules* **1992**, *25* (1), 226–232. https://doi.org/10.1021/MA00027A038/ASSET/MA00027A038.FP.PNG_V03.

(313) Wan, Y.; Qu, X.; Lu, J.; Zhu, C.; Wan, L.; Yang, J.; Bei, J.; Wang, S. Characterization of Surface Property of Poly(Lactide-Co-Glycolide) after Oxygen Plasma Treatment. *Biomaterials* **2004**, *25* (19), 4777–4783. https://doi.org/10.1016/J.BIOMATERIALS.2003.11.051.

(314) Kubies, D.; Machová, L.; Brynda, E.; Lukáš, J.; Rypáček, F. Functionalized Surfaces of Polylactide Modified by Langmuir–Blodgett Films of Amphiphilic Block Copolymers. *Journal of Materials Science: Materials in Medicine 2003 14:2* **2003**, *14* (2), 143–149. https://doi.org/10.1023/A:1022019813078.

(315) Kang, S.; Haider, A.; Gupta, K. C.; Kim, H.; Kang, I. Chemical Bonding of Biomolecules to the Surface of Nano-Hydroxyapatite to Enhance Its Bioactivity. *Coatings 2022, Vol. 12, Page 999* **2022**, *12* (7), 999. https://doi.org/10.3390/COATINGS12070999.

(316) Park, J.; Park, S.; Kim, J. E.; Jang, K.-J.; Seonwoo, H.; Chung, J. H. Enhanced Osteogenic Differentiation of Periodontal Ligament Stem Cells Using a Graphene Oxide-Coated Poly(ε-Caprolactone) Scaffold. *Polymers (Basel)* **2021**, *13* (5), 797. https://doi.org/10.3390/polym13050797.

(317) Pilipchuk, S. P.; Monje, A.; Jiao, Y.; Hao, J.; Kruger, L.; Flanagan, C. L.; Hollister, S. J.; Giannobile, W. V. Integration of 3D Printed and Micropatterned Polycaprolactone Scaffolds for Guidance of Oriented Collagenous Tissue Formation In Vivo. *Adv Healthc Mater* **2016**, *5* (6), 676–687. https://doi.org/10.1002/adhm.201500758.

(318) Pilipchuk, S. P.; Fretwurst, T.; Yu, N.; Larsson, L.; Kavanagh, N. M.; Asa'ad, F.; Cheng, K. C. K.; Lahann, J.; Giannobile, W. V. Micropatterned Scaffolds with Immobilized Growth Factor Genes Regenerate Bone and Periodontal Ligament-Like Tissues. *Adv Healthc Mater* **2018**, *7* (22), 1800750. https://doi.org/10.1002/adhm.201800750.

(319) Rojo, J.; Sousa-Herves, A.; Mascaraque, A. Perspectives of Carbohydrates in Drug Discovery. *Comprehensive Medicinal Chemistry III* **2017**, *1–8*, 577–610. https://doi.org/10.1016/B978-0-12-409547-2.12311-X.

(320) Prabaharan, M. Characterization of Tissue Scaffolds Drug Release Profiles. *Characterisation and Design of Tissue Scaffolds* **2016**, 149–168. https://doi.org/10.1016/B978-1-78242-087-3.00007-9.

(321) Calori, I. R.; Braga, G.; de Jesus, P. da C. C.; Bi, H.; Tedesco, A. C. Polymer Scaffolds as Drug Delivery Systems. *European Polymer Journal*. 2020. https://doi.org/10.1016/j.eurpolymj.2020.109621.

(322) Mo, X.; Zhang, D.; Liu, K.; Zhao, X.; Li, X.; Wang, W. Nano-Hydroxyapatite Composite Scaffolds Loaded with Bioactive Factors and Drugs for Bone Tissue Engineering. *International Journal of Molecular Sciences*. 2023. https://doi.org/10.3390/ijms24021291.

(323) Bacelar, A. H.; Cengiz, I. F.; Silva-Correia, J.; Sousa, R. A.; Oliveira, J. M.; Reisa, R. L. *"Smart" Hydrogels in Tissue Engineering and Regenerative Medicine Applications Biological Relevance of Hyaluronic Acid: High-Throughput Platforms for Molecular and Biological Studies View Project Football Medicine View Project*; Handb. Intell. Scaffolds Tissue Eng. Regen. Med, 2017.

(324) Cam, M. E.; Yildiz, S.; Alenezi, H.; Cesur, S.; Ozcan, G. S.; Erdemir, G.; Edirisinghe, U.; Akakin, D.; Kuruca, D. S.; Kabasakal, L.; Gunduz, O.; Edirisinghe, M. Evaluation of Burst Release and Sustained Release of Pioglitazone-Loaded Fibrous Mats on Diabetic Wound Healing: An in

Vitro and in Vivo Comparison Study. *J R Soc Interface* **2020**, *17* (162). https://doi.org/10.1098/RSIF.2019.0712.

(325) Moioli, E. K.; Clark, P. A.; Xin, X.; Lal, S.; Mao, J. J. Matrices and Scaffolds for Drug Delivery in Dental, Oral and Craniofacial Tissue Engineering. *Adv Drug Deliv Rev* **2007**, *59* (0), 308. https://doi.org/10.1016/J.ADDR.2007.03.019.

(326) Bascones-Martínez, A.; Figuero-Ruiz, E. Periodontal Diseases as Bacterial Infection. *Med Oral Patol Oral Cir Bucal* **2004**, *9 Suppl*. https://doi.org/10.4321/S1699-65852005000300002.

(327) Pragati S; Ashok S; Kuldeep S. Recent Advances in Periodontal Drug Delivery Systems. *International Journal of Drug Delivery* **2009**, *1*, 1–14. https://doi.org/10.5138/ijdd.2009.0975.0215.01001.

(328) Garg, T.; Arora, S.; S Rayasa, M. R.; Singh, O.; Murthy, R. Scaffold: A Novel Carrier for Cell and Drug Delivery Create New Project "Analytical Method Development and Validation " View Project Book Chapters View Project Scaffold: A Novel Carrier for Cell and Drug Delivery. *Crit Rev Ther Drug Carrier Syst* **2012**, *29* (1), 1–63. https://doi.org/10.1615/CritRevTherDrugCarrierSyst.v29.i1.10.

(329) Woo, H. N.; Cho, Y. J.; Tarafder, S.; Lee, C. H. The Recent Advances in Scaffolds for Integrated Periodontal Regeneration. *Bioact Mater* **2021**, *6* (10), 3328. https://doi.org/10.1016/J.BIOACTMAT.2021.03.012.

(330) Zamani, M.; Morshed, M.; Varshosaz, J.; Jannesari, M. Controlled Release of Metronidazole Benzoate from Poly ε-Caprolactone Electrospun Nanofibers for Periodontal Diseases. *European Journal of Pharmaceutics and Biopharmaceutics* **2010**, *75* (2), 179–185. https://doi.org/10.1016/J.EJPB.2010.02.002.

(331) Dyke, T. E. Van. The Management of Inflammation in Periodontal Disease. *J Periodontol* **2008**, *79* (8 Suppl), 1601. https://doi.org/10.1902/JOP.2008.080173.

(332) Andreu, V.; Mendoza, G.; Arruebo, M.; Irusta, S. Smart Dressings Based on Nanostructured Fibers Containing Natural Origin Antimicrobial, Anti-Inflammatory, and Regenerative Compounds. *Materials* **2015**, *8* (8), 5154. https://doi.org/10.3390/MA8085154.

(333) Hu, Z.; Ma, C.; Rong, X.; Zou, S.; Liu, X. Immunomodulatory ECM-like Microspheres for Accelerated Bone Regeneration in Diabetes Mellitus. *ACS Appl Mater Interfaces* **2018**, *10* (3), 2377. https://doi.org/10.1021/ACSAMI.7B18458.

(334) Danhier, F.; Ansorena, E.; Silva, J. M.; Coco, R.; Le Breton, A.; Préat, V. PLGA-Based Nanoparticles: An Overview of Biomedical Applications. *J Control Release* **2012**, *161* (2), 505–522. https://doi.org/10.1016/J.JCONREL.2012.01.043.

(335) Meissner, Y.; Pellequer, Y.; Lamprecht, A. Nanoparticles in Inflammatory Bowel Disease: Particle Targeting versus PH-Sensitive Delivery. *Int J Pharm* **2006**, *316* (1–2), 138–143. https://doi.org/10.1016/j.ijpharm.2006.01.032.

(336) Bae, S. E.; Son, J. S.; Park, K.; Han, D. K. Fabrication of Covered Porous PLGA Microspheres Using Hydrogen Peroxide for Controlled Drug Delivery and Regenerative Medicine. *J Control Release* **2009**, *133* (1), 37–43. https://doi.org/10.1016/J.JCONREL.2008.09.006.

(337) Murua, A.; Herran, E.; Orive, G.; Igartua, M.; Blanco, F. J.; Pedraz, J. L.; Hernández, R. M. Design of a Composite Drug Delivery System to Prolong Functionality of Cell-Based Scaffolds. *Int J Pharm* **2011**, *407* (1–2), 142–150. https://doi.org/10.1016/J.IJPHARM.2010.11.022.

(338) Cantón, I.; Mckean, R.; Charnley, M.; Blackwood, K. A.; Fiorica, C.; Ryan, A. J.; MacNeil, S. Development of an Ibuprofen-Releasing Biodegradable PLA/PGA Electrospun Scaffold for Tissue Regeneration. *Biotechnol Bioeng* **2010**, *105* (2), 396–408. https://doi.org/10.1002/BIT.22530.

(339) Umrath, F.; Pfeifer, A.; Cen, W.; Danalache, M.; Reinert, S.; Alexander, D.; Naros, A. How Osteogenic Is Dexamethasone?—Effect of the Corticosteroid on the Osteogenesis, Extracellular Matrix, and Secretion of Osteoclastogenic Factors of Jaw Periosteum-Derived Mesenchymal Stem/Stromal Cells. *Front Cell Dev Biol* **2022**, *10*. https://doi.org/10.3389/fcell.2022.953516.

(340) Lian, M.; Sun, B.; Qiao, Z.; Zhao, K.; Zhou, X.; Zhang, Q.; Zou, D.; He, C.; Zhang, X. Bi-Layered Electrospun Nanofibrous Membrane with Osteogenic and Antibacterial Properties for Guided Bone Regeneration. *Colloids Surf B Biointerfaces* **2019**, *176*, 219–229. https://doi.org/10.1016/J.COLSURFB.2018.12.071.

(341) Schliephake, H. Bone Growth Factors in Maxillofacial Skeletal Reconstruction. *Int J Oral Maxillofac Surg* **2002**, *31* (5), 469–484. https://doi.org/10.1054/IJOM.2002.0244.

(342) Agulnik, M.; Siu, L. L. An Update on the Systemic Therapy of Malignant Salivary Gland Cancers: Role of Chemotherapy and Molecular Targeted Agents. *Curr Med Chem Anticancer Agents* **2004**, *4* (6), 543–551. https://doi.org/10.2174/1568011043352641.

(343) Tziafas, D. The Future Role of a Molecular Approach to Pulp-Dentinal Regeneration. *Caries Res* **2004**, *38* (3), 314–320. https://doi.org/10.1159/000077771.

(344) Simon, S. R.; Berdal, A.; Cooper, P. R.; Lumley, P. J.; Tomson, P. L.; Smith, A. J. Dentin-Pulp Complex Regeneration: From Lab to Clinic. *Adv Dent Res* **2011**, *23* (3), 340–345. https://doi.org/10.1177/0022034511405327.

(345) Nakashima, M.; Tachibana, K.; Iohara, K.; Ito, M.; Ishikawa, M.; Akamine, A. Induction of Reparative Dentin Formation by Ultrasound-Mediated Gene Delivery of Growth/Differentiation Factor 11. *Hum Gene Ther* **2003**, *14* (6), 591–597. https://doi.org/10.1089/104303403764539369.

(346) *Growth factors in periodontal regeneration: A review | International Journal of Current Research*. https://www.journalcra.com/article/growth-factors-periodontal-regeneration-review (accessed 2022-08-12).

(347) Lee, K.; Silva, E. A.; Mooney, D. J. Growth Factor Delivery-Based Tissue Engineering: General Approaches and a Review of Recent Developments. *J R Soc Interface* **2011**, *8* (55), 153. https://doi.org/10.1098/RSIF.2010.0223.

(348) Jamnezhad, S.; Asefnejad, A.; Motififard, M.; Yazdekhasti, H.; Kolooshani, A.; Saber-Samandari, S.; Khandan, A. Development and Investigation of Novel Alginate-Hyaluronic Acid Bone Fillers Using Freeze Drying Technique for Orthopedic Field. *Nanomedicine Research Journal* **2020**, *5* (4). https://doi.org/10.22034/NMRJ.2020.04.001.

(349) Li, F.; Liu, X.; Zhao, S.; Wu, H.; Xu, H. H. K. Porous Chitosan Bilayer Membrane Containing TGF-B1 Loaded Microspheres for Pulp Capping and Reparative Dentin Formation in a Dog Model. *Dental Materials* **2014**, *30* (2), 172–181. https://doi.org/10.1016/J.DENTAL.2013.11.005.

(350) Kaigler, D.; Cirelli, J. A.; Giannobile, W. V. Growth Factor Delivery for Oral and Periodontal Tissue Engineering. *Expert Opin Drug Deliv* **2006**, *3* (5), 647. https://doi.org/10.1517/17425247.3.5.647.

(351) Bessa, P. C.; Casal, M.; Reis, R. L. Bone Morphogenetic Proteins in Tissue Engineering: The Road from Laboratory to Clinic, Part II (BMP Delivery). *Journal of Tissue Engineering and Regenerative Medicine*. 2008. https://doi.org/10.1002/term.74.

(352) Bessa, P. C.; Casal, M.; Reis, R. L. Bone Morphogenetic Proteins in Tissue Engineering: The Road from the Laboratory to the Clinic, Part I (Basic Concepts). *Journal of Tissue Engineering and Regenerative Medicine*. 2008. https://doi.org/10.1002/term.63.

(353) Tevlek, A.; Hosseinian, P.; Ogutcu, C.; Turk, M.; Aydin, H. M. Bi-Layered Constructs of Poly(Glycerol-Sebacate)-β-Tricalcium Phosphate for Bone-Soft Tissue Interface Applications. *Materials Science and Engineering: C* **2017**, *72*, 316–324. https://doi.org/10.1016/j.msec.2016.11.082.

(354) Boyne, P. J.; Lilly, L. C.; Marx, R. E.; Moy, P. K.; Nevins, M.; Spagnoli, D. B.; Triplett, R. G. De Novo Bone Induction by Recombinant Human Bone Morphogenetic Protein-2 (RhBMP-2) in Maxillary Sinus Floor Augmentation. *J Oral Maxillofac Surg* **2005**, *63* (12), 1693–1707. https://doi.org/10.1016/J.JOMS.2005.08.018.

(355) Giannobile, W. V.; Ryan, S.; Shih, M.-S.; Su, D. L.; Kaplan, P. L.; Chan, T. C. K. Recombinant Human Osteogenic Protein-1 (OP-1) Stimulates Periodontal Wound Healing in Class III Furcation Defects. *J Periodontol* **1998**, *69* (2), 129–137. https://doi.org/10.1902/JOP.1998.69.2.129.

(356) Viswanathan, H. L.; Berry, J. E.; Foster, B. L.; Gibson, C. W.; Li, Y.; Kulkarni, A. B.; Snead, M. L.; Somerman, M. J. Amelogenin: A Potential Regulator of Cementum-Associated Genes. *J Periodontol* **2003**, *74* (10), 1423–1431. https://doi.org/10.1902/JOP.2003.74.10.1423.

(357) Bottino, M. C.; Thomas, V.; Janowski, G. M. A Novel Spatially Designed and Functionally Graded Electrospun Membrane for Periodontal Regeneration. *Acta Biomater* **2011**, *7* (1), 216–224. https://doi.org/10.1016/J.ACTBIO.2010.08.019.

(358) Tayebi, M.; Parham, S.; Abbastabbar Ahangar, H.; Zargar Kharazi, A. Preparation and Evaluation of Bioactive Bilayer Composite Membrane PHB/β-TCP with Ciprofloxacin and Vitamin D3 Delivery for Regenerative Damaged Tissue in Periodontal Disease. *J Appl Polym Sci* **2022**, *139* (3), 51507. https://doi.org/10.1002/APP.51507.

(359) Rasperini, G.; Pilipchuk, S. P.; Flanagan, C. L.; Park, C. H.; Pagni, G.; Hollister, S. J.; Giannobile, W. V. 3D-Printed Bioresorbable Scaffold for Periodontal Repair. *J Dent Res* **2015**, *94* (9 Suppl), 153S-157S. https://doi.org/10.1177/0022034515588303.

(360) Sudheesh Kumar, P. T.; Hashimi, S.; Saifzadeh, S.; Ivanovski, S.; Vaquette, C. Additively Manufactured Biphasic Construct Loaded with BMP-2 for Vertical Bone Regeneration: A Pilot Study in Rabbit. *Materials Science and Engineering C* **2018**, *92*. https://doi.org/10.1016/j.msec.2018.06.071.

2150